SECURITY CLASSIFICATION OF THIS PAGE (When Data Entered)

REPORT DOCUMENTATION PAGE

READ INSTRUCTIONS BEFORE COMPLETING FORM

1. REPORT NUMBER: AFIT/CI/NR 88- 56
2. GOVT ACCESSION NO.
3. RECIPIENT'S CATALOG NUMBER

4. TITLE (and Subtitle): DIGITAL SIGNAL DESIGN FOR METEOR-SCATTER COMMUNICATIONS
5. TYPE OF REPORT & PERIOD COVERED: MS THESIS
6. PERFORMING ORG. REPORT NUMBER

7. AUTHOR(s): JAY MICHAEL JACOBSMEYER
8. CONTRACT OR GRANT NUMBER(s)

9. PERFORMING ORGANIZATION NAME AND ADDRESS: AFIT STUDENT AT: CORNELL UNIVERSITY
10. PROGRAM ELEMENT, PROJECT, TASK AREA & WORK UNIT NUMBERS

11. CONTROLLING OFFICE NAME AND ADDRESS
12. REPORT DATE: 1988
13. NUMBER OF PAGES: 132

14. MONITORING AGENCY NAME & ADDRESS (if different from Controlling Office): AFIT/NR, Wright-Patterson AFB OH 45433-6583
15. SECURITY CLASS. (of this report): UNCLASSIFIED
15a. DECLASSIFICATION/DOWNGRADING SCHEDULE

16. DISTRIBUTION STATEMENT (of this Report): DISTRIBUTED UNLIMITED: APPROVED FOR PUBLIC RELEASE

17. DISTRIBUTION STATEMENT (of the abstract entered in Block 20, if different from Report): SAME AS REPORT

18. SUPPLEMENTARY NOTES: Approved for Public Release: IAW AFR 190-1
LYNN E. WOLAVER
Dean for Research and Professional Development
Air Force Institute of Technology
Wright-Patterson AFB OH 45433-6583
19 July 88

19. KEY WORDS (Continue on reverse side if necessary and identify by block number)

20. ABSTRACT (Continue on reverse side if necessary and identify by block number): ATTACHED

DD FORM 1 JAN 73 1473 EDITION OF 1 NOV 65 IS OBSOLETE

SECURITY CLASSIFICATION OF THIS PAGE (When Data Entered)

Title: Digital Signal Design for Meteor-Scatter Communications

Author: Captain Jay M. Jacobsmeyer, USAF

Date: 1987

Number of Pages: 132

Degree Awarded: Master of Science in Electrical Engineering

Institution: Cornell University, Ithaca, New York

Abstract. This thesis is concerned with the efficient design of digital modulation and error-control schemes for point-to-point meteor-scatter communication systems. The methods introduced exploit the unique properties of the meteor-scatter channel.

A channel model is derived based on the work of other researchers. The channel model includes expressions for meteor arrival rate, burst duration, and received power. Meteor arrivals are modeled as a Poisson random process and the properties of the Poisson process are used extensively. Channel noise is modeled as additive, white, and Gaussian distributed. The multipath structure of the channel is evaluated only to the extent that it affects channel bandwidth.

New expressions for long run average bit rate and mean message waiting time are derived. Performance of the fixed-rate and adaptive-symbol-rate modem is evaluated in terms of average bit rate and mean waiting time. Bounds on the improvement in mean waiting time over the fixed-rate modem are derived.

M-ary modulation methods are investigated to find the optimal modulation for the fixed-rate modem and adaptive-symbol-rate modem. It is shown that the adaptive-symbol-rate modem is not optimal on a bandwidth-limited channel. An alternative scheme, called adaptive quadrature amplitude modulation (QAM) is evaluated and shown to outperform adaptive-symbol-rate modulation on a bandwidth-limited channel. A suggested implementation of adaptive QAM is presented to include a modem block diagram and signal constellation. This implementation appears to be more practical than the proposed implementation of adaptive-symbol-rate.

DIGITAL SIGNAL DESIGN
FOR
METEOR-SCATTER COMMUNICATIONS

A Thesis
Presented to the Faculty of the Graduate School
of Cornell University
in Partial Fulfillment of the Requirements for the Degree of
Master of Science

by
Jay Michael Jacobsmeyer
August, 1987

Abstract

This thesis is concerned with the efficient design of digital modulation and error-control schemes for point-to-point meteor-scatter communication systems. The methods introduced exploit the unique properties of the meteor-scatter channel.

A channel model is derived based on the work of other researchers. The channel model includes expressions for meteor arrival rate, burst duration, and received power. Meteor arrivals are modeled as a Poisson random process and the properties of the Poisson process are used extensively. Channel noise is modeled as additive, white, and Gaussian distributed. The multipath structure of the channel is evaluated only to the extent that it affects channel bandwidth.

New expressions for long run average bit rate and mean message waiting time are derived. Performance of the fixed-rate and adaptive-symbol-rate modem is evaluated in terms of average bit rate and mean waiting time. Bounds on the improvement in mean waiting time over the fixed-rate modem are derived.

M-ary modulation methods are investigated to find the optimal modulation for the fixed-rate modem and adaptive-symbol-rate modem. It is shown that the adaptive-symbol-rate modem is not optimal on a bandwidth-limited channel. An alternative scheme, called adaptive quadrature amplitude modulation (QAM) is evaluated and shown to out-perform adaptive-symbol-rate on a bandwidth-limited channel. A suggested implementation of adaptive QAM is presented to include a modem block diagram and signal constellation. This implementation appears to be more practical than the proposed implementation of adaptive-symbol-rate.

The use of Reed-Solomon codes in forward-error-correction is investigated. An appropriate figure of merit for coding schemes used on the meteor-scatter channel is derived. The performance of Reed-Solomon codes is evaluated in terms of improvement in average bit rate or mean waiting time. The optimal code rate is found to be about 4/5. A lower bound on the optimal code rate is derived as a function of block length. This lower bound applies to any maximum distance separable (MDS) code operating with M-ary phase shift keying (PSK), M-ary QAM or binary frequency shift keying (FSK).

Topics of further research are suggested, especially the use of adaptive trellis coded modulation (TCM) on the meteor-scatter channel.

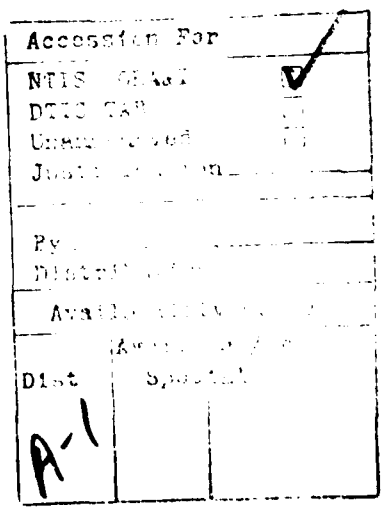

Biographical Sketch

PII Redacted

Jay Michael Jacobsmeyer [redacted], the son of John and Patricia Jacobsmeyer of Portsmouth, New Hampshire. He graduated magna cum laude from Virginia Polytechnic Institute and State University in June, 1981 with a Bachelor of Science degree in Electrical Engineering. He was commissioned a Second Lieutenant in the United States Air Force on June 5, 1981 and is currently serving on active duty with the rank of Captain. Captain Jacobsmeyer was stationed in the Federal Republic of Germany for three years where he designed and supervised the installation of Air Force tactical communication systems. In 1984 he was selected by the commander of Air Force Communications Command to enter the graduate Electrical Engineering program at Cornell University. He attended Cornell University from August, 1985 to August, 1987 with support from a U. S. Air Force scholarship. Upon graduation, Captain Jacobsmeyer was transferred to Headquarters, Air Force Space Command in Colorado Springs, Colorado. Captain Jacobsmeyer is married to the former Joyce Ann Deem of Annandale, Virginia. They have one daughter, Abigail Ann, age two years.

Dedication

To my wife, Joyce, whose respect and devotion have inspired me to do great things.

Acknowledgments

Over the course of this research project I have had the pleasure of working with several outstanding faculty members. This space serves to acknowledge their contribution.

Professor James Thorp, who offered free use of the Kettering Laboratory computing resources, which I used to the fullest.

Professor Chris Heegard, for his insight on coding theory and its application to meteor-scatter communications.

Professor Terrence Fine, my chairman, who always gave excellent advice concerning the direction of my academic program at Cornell.

And finally, Dr. Richard E. Blahut, who unselfishly served as thesis advisor despite handling a full load at IBM, authoring two books, and teaching a graduate course at Cornell.

Table of Contents

Biographical Sketch iii
Dedication iv
Acknowledgments v
Table of Contents vi
List of Tables x
List of Figures xi

Chapter 1 - Introduction 1

1.1 Basic Concepts 1
1.2 Adaptive Modulation Methods 2
1.3 Objectives 3

Chapter 2 - Channel Model 6

2.1 Properties of Meteor Arrivals 6
2.2 Types of Meteor Trails 7
2.3 Received Power Models 8
2.4 Meteor Statistics 11
2.4.1 Electron line density 11
2.4.2 Burst duration 11
2.3.3 Meteor arrival rate 13
2.5 Noise 14
2.6 Multipath 15
2.7 Bandwidth 16
2.8 Link parameters 16
2.9 Summary 17

Chapter 3 - Performance Measures 18

3.1 Long Run Average Symbol Rate, R_{avg} 19
3.1.1 Fixed symbol rate modem 22
3.1.2 Adaptive symbol rate modem 23
3.1.3 Constrained channel 24
3.1.4 Improvement factor 26
3.2 Mean Message Waiting Time, T_{avg} 28
3.2.1 Fixed-rate modem 30
3.2.2 Optimal symbol rate for fixed-rate modem 33
3.2.3 Adaptive-symbol-rate modem 36
3.2.4 Improvement factor 41

Chapter 4 - Modulation Methods 43

4.1 M-ary Modulation Techniques 44
4.1.1 M-ary QAM 45
4.1.2 M-ary FSK 53
4.2 Optimal Waveform Modulation For Fixed-Rate 58
4.2.1 Maximizing long run average bit rate, R_b 59
4.2.2 Minimizing mean message waiting time, T_{avg} 63
4.3 Optimal Waveform Modulation For Adaptive-Symbol-Rate 64
4.3.1 Maximizing long run average bit rate, R_b 64
4.3.2 Minimizing mean message waiting time, T_{avg} 66
4.4 Adaptive QAM 67
4.4.1 Average bit rate, R_{avg} 71
4.4.2 Mean waiting time, T_{avg} 73
4.4.3 Optimal symbol rate 80
4.4.4 Constellation mapping 81
4.4.5 Modem block diagram 85

Chapter 5 - Error-Control Codes 88

5.1 Properties of Reed-Solomon Codes 89
5.2 Figure of Merit 91
5.2.1 Figure of merit for R_{avg} 92
5.2.2 Figure of merit for T_{avg} 92
5.3 Optimal Code Rates 93
5.4 Performance Estimates 96

Chapter 6 - Conclusion 101

6.1 Summary of Findings 101
6.1.1 Channel model 101
6.1.2 Long run average bit rate 102
6.1.3 Mean message waiting time 103
6.1.4 Optimal M-ary modulation 104
6.1.5 Adaptive QAM 104
6.1.6 Reed-Solomon codes 105
6.2 Recommendations for Further Research 106
6.2.1 Experimental confirmation of findings 106
6.2.2 Signal detection and estimation 106
6.2.3 Variable rate codes 106
6.2.4 Trellis codes for digital modulation 106

Appendix A - Expressions For Long Run Average Symbol Rate 107

A.1 Fixed-Symbol-Rate Modem 107
A.1.1 Underdense trails 109
A.1.2 Overdense trails 110
A.2 Adaptive-Symbol-Rate Modem 113
A.2.1 Underdense trails 113

A.2.2 Overdense trails 114

Appendix B - Mean Waiting Time For Adaptive QAM 116

B.1 CDF For Bits per Burst, W 116
B.2 Exponential Approximation 124
B.3 Mean Waiting Time 127

References 130

List of Tables

Chapter 2 - Channel Model

Table 2.1 Link parameters 16

Chapter 3 - Performance Measures

Table 3.1 Average symbol rate in Hz for fixed-rate modem 22
Table 3.2 Average symbol rate in Hz for adaptive-symbol-rate modem on bandwidth-limited channel ($R(t) \leq R_{max}$) .....
Table 3.3 Typical values of mean message waiting time, T_{avg} 33
Table 3.4 Typical values of optimal symbol rate, R_{sopt}, in Hz 35

Chapter 4 - Modulation Methods

Table 4.1 Improvement factor for M-ary QAM 50
Table 4.2 $(E_b/N_0)_{req}$ in dB for several values of P_b for M-ary QAM 52
Table 4.3 $(E_b/N_0)_{req}$ in dB for M-ary FSK with coherent demodulation 54
Table 4.4 $(E_b/N_0)_{req}$ in dB for M-ary FSK with noncoherent demodulation 55
Table 4.5 Maximum bit rate for M-ary QAM and M-ary FSK 61
Table 4.6 $(E_s/N_0)_{req}$ in dB for several values of P_b for M-ary QAM 69
Table 4.7 Average bit rate in bits/s for adaptive QAM 72
Table 4.8 Improvement in waiting time for adaptive QAM over fixed-rate 79
Table 4.9 Average transmitter power in watts for adaptive QAM constellation 83

Appendix B - Mean Waiting Time for Adaptive QAM

Table B.1 $(E_s/N_0)_{req}$ in dB for several values of P_b for M-ary QAM 117

List of Figures

Chapter 2 - Channel Model

Figure 2.1 Received power from an underdense trail 9
Figure 2.2 Received power from an overdense trail 10

Chapter 3 - Performance Measures

Figure 3.1 Average symbol rate as a function of instantaneous symbol rate 23
Figure 3.2 Improvement factor, adaptive-symbol-rate over fixed-rate for a strictly power-limited channel 27
Figure 3.3 Improvement factor, adaptive-symbol-rate over fixed-rate for a bandwidth-limited channel 28
Figure 3.4 Upper and lower bounds on mean waiting time for adaptive-symbol-rate modem 41

Chapter 4 - Modulation Methods

Figure 4.1 Modulator and demodulator sections for a quadrature amplitude modulation modem 46
Figure 4.2 Rectangular signal constellations 48
Figure 4.3 Probability of bit error for M-ary QAM with Gray coding 51
Figure 4.4 Probability of bit error for coherent demodulation of M-ary FSK signals 55
Figure 4.5 Probability of bit error for noncoherent demodulation of M-ary FSK signals 56
Figure 4.6 Average bit rate for M-ary modulation on the fixed-rate modem 62
Figure 4.7 Bandwidth efficiency/power efficiency for underdense trails .. 63
Figure 4.8 Average bit rate for M-ary modulation on the adaptive-symbol-rate modem 66
Figure 4.9 Instantaneous symbol rate, R(t), for an overdense trail 67
Figure 4.10 Operation of adaptive QAM on an underdense trail 70
Figure 4.11 Operation of adaptive QAM on an overdense trail 70

Figure 4.12 Improvement in average bit rate for adaptive QAM over adaptive-symbol-rate 72
Figure 4.13 Average bit rate as a function of symbol rate for adaptive QAM 74
Figure 4.14 Approximate CDF for adaptive QAM 75
Figure 4.15 Cumulative distribution functions for three meteor-scatter modulation methods 77
Figure 4.16 Improvement in mean waiting time for adaptive QAM over fixed-rate 80
Figure 4.17 Average bit rate as a function of symbol rate for adaptive QAM..... 81
Figure 4.18 Signal constellation for adaptive QAM 84
Figure 4.19 Block diagram for adaptive QAM modem 86

Chapter 5 - Error-Control Coding

Figure 5.1 Coding gain for a (31,23) Reed-Solomon code with 32-FSK modulation 91
Figure 5.2 (31, k) Reed-Solomon codes with BPSK 98
Figure 5.3 (31, k) Reed-Solomon codes with 32-ary FSK 99
Figure 5.4 (63, k) Reed-Solomon codes with 64-ary FSK 99

Appendix A - Expressions for Long Run Average Symbol Rate

Figure A.1 Piecewise linear approximation to R(t) for overdense trails ... 111

Appendix B - Mean Waiting Time for Adaptive QAM

Figure B.1 Operation of adaptive QAM on an underdense trail 118
Figure B.2 Cumulative distribution function for bits per burst, W, for adaptive QAM 124
Figure B.3 Approximate CDF for adaptive QAM 126
Figure B.4 Mean waiting time for adaptive QAM 129

Chapter 1 - Introduction

The Earth sweeps up billions of tiny meteors each day. As these meteors enter the Earth's atmosphere, they create short-lived ionization trails. These trails of ionized electrons reflect radio signals in the frequency range 40 – 100 Mhz. A digital radio communication system that uses these trails is called a *meteor-scatter* or *meteor-burst* system. Meteor-scatter communication systems operate over distances from 400 to 2000 km. Such systems are highly reliable and since the "foot print" for a particular reflection is quite small, there is an inherent privacy feature. This thesis is concerned with efficient digital *signal design* of a point-to-point meteor-scatter communication system. The term signal design for digital radio refers to the integration of modulation and coding to produce an effective communication system.

The meteor-scatter channel has several unique properties that should be exploited in signal design. A brief description of these properties is given in the following section.

1.1 Basic Concepts. With the exception of meteor showers, meteor arrivals are considered random, isolated events. The mass of each arriving meteor is also random with a probability distribution roughly proportional to the inverse of the meteor mass. The large meteors that cause visible trails ("shooting stars") arrive infrequently and contribute little to channel capacity. Meteor trails occur in the altitude range 80 - 120 km with typical trails having length 25 km. The mean time between observed trails on a point-to-point link is about 10 seconds. Because meteor trails diffuse rapidly after formation, typical burst durations are on the order of 0.5 seconds. An effective communication system must therefore acquire the signal quickly and transmit information efficiently before the burst termination.

Each meteor trail is characterized by its capacity in bits. Trail capacity is a function of meteor mass, so large meteors leave trails with large capacities. Since the mass of arriving meteors is random, the corresponding trail capacity is also random. The role of the system designer for any communication system is to achieve a large fraction of *channel* capacity. For meteor-scatter, attempting to achieve channel capacity normally involves a trade-off: maximizing trail capacity in bits causes the observed number of trails per second to decrease. Essentially, this trade-off between trail capacity in bits versus arrival rate in trails per second is the overriding concern of the system designer.

Conventional meteor-scatter systems operate at constant bit rates in the range 5-15 k bits/s. Because of the burst characteristics of the channel, long run average bit rates for these systems are typically 100 - 200 bits/s. These rates are quite low compared to modern day satellite and terrestrial microwave systems. Thus, one of the goals of this thesis is to find ways to increase long run average bit rate. Long run performance is important in some applications, but another consideration is the waiting time to transmit short messages. This topic will be investigated also.

1.2 Adaptive Modulation Methods. There are two modulation methods proposed for use on the meteor-scatter channel: *fixed information rate* and *adaptive information rate*. One important property of meteor trails is that the received power as a function of time is predictable once the trail is formed. For most meteor trails, the received power decays exponentially from the inception of the trail. Therefore, the potential information rate at the beginning of the burst is greater than at the end. An adaptive modem varies the information rate to match the time-varying signal-to-noise ratio (SNR) at the receiver. The fixed-rate modem, on the other hand, operates at a constant information rate for the entire burst.

For meteor-scatter channels with unlimited bandwidth, the optimal adaptive scheme is one in which the channel symbol rate adapts to match the SNR. For bandwidth-limited channels, this scheme is not optimal and the author proposes a new scheme, called *adaptive QAM*. A third approach to adaptive information rate is to use error-control codes. During periods of high SNR, codes with high code rates and relatively weak coding gain would be used. During periods of low SNR, codes with low code rates and strong coding gain would be used. Thus, the information rate would vary with SNR. Adaptive coding is beyond the scope of this thesis, but adaptive modulation with traditional coding will be discussed.

1.3 Objectives. The two main drawbacks of conventional meteor-scatter communication systems are the low average bit rates (also called throughput) and long message waiting times. This thesis attempts to improve average bit rate and message waiting time through the use of digital modulation and error-control coding techniques. The digital modulation methods discussed in this thesis involve the use of M-ary quadrature amplitude modulation (QAM) and M-ary frequency shift keying (FSK) in adaptive and fixed-rate schemes. The analysis of error-control coding is restricted to the use of Reed-Solomon codes in forward-error correction.

The objectives of this thesis can be stated as follows:

1) Derive expressions for two measures of performance for digital communication systems on the meteor-scatter channel: long run average bit rate, R_{bavg}, and mean message waiting time, T_{avg}.

2) Evaluate the performance of the fixed-rate and adaptive-symbol-rate modems in terms of the performance measures, R_{bavg} and T_{avg}.

3) Design an adaptive modulation scheme called adaptive QAM that approaches optimality for bandwidth-limited channels.

4) Evaluate the performance of adaptive QAM in terms of the two performance measures.

5) Evaluate the performance of Reed-Solomon codes used for forward-error correction.

6) Derive a lower bound on the optimal code rate for Reed-Solomon codes.

A brief summary of the main results follows.

Expressions for average bit rate and mean waiting time are derived because the expressions found in the literature are narrowly defined and usually apply only to packet communication systems. The expressions derived in this thesis are quite general in nature and have wide application. The expression for average bit rate is an approximation since it assumes that all meteor trails occur at a fixed point in the sky and that the electron line density is upper-bounded by 10^{17} e/m. On the other hand, the expression for mean waiting time for a fixed-rate modem is exact and a natural extension of earlier work by Oetting (1980). Bounds on mean waiting time are derived for the general case and an expression for the Laplace transform of the mean waiting time in the general case is also derived as a special application of earlier work by Cox (1962).

The two performance measures serve as figures of merit for evaluating the performance of the fixed-rate modem and adaptive-symbol-rate modem. The adaptive-symbol-rate modem out-performs the fixed-rate modem by a

significant amount in terms of average bit rate. The improvement in mean waiting time is upper-bounded by a factor of 2.0.

On a bandwidth-limited channel, the adaptive QAM scheme developed by the author can out-perform the adaptive-symbol-rate scheme by a 3 to 1 margin in terms of average bit rate. In terms of mean waiting time, the adaptive-symbol-rate modem out-performs adaptive QAM.

Reed-Solomon codes used for forward-error correction offer modest gains in average bit rate and decreases in mean waiting time.

The remaining chapters are concerned with the derivations and designs that lead to the results summarized above. In Chapter 2, a channel model is derived. This channel model is based on the work of other researchers and includes models for meteor arrivals, burst duration, received power, noise, and multipath effects. Chapter 3 is concerned with the derivation of the two performance measures and evaluation of the performance of the fixed-rate modem and adaptive-symbol-rate modem in terms of these two performance measures. Chapter 4 deals with optimal use of waveform modulation for meteor-scatter communication. Optimal M-ary modulation techniques are found for the fixed-rate and adaptive-symbol-rate modems. The adaptive QAM modem is designed and the performance evaluated. In Chapter 5, Reed-Solomon codes for forward-error-correction are evaluated. Chapter 6 summarizes the main results and provides suggestions for further research in this field.

Chapter 2 - Channel Model

In this chapter we shall derive a model for the meteor-scatter channel. This model will serve as the foundation for the results derived in Chapters 3, 4, and 5. Skywave propagation in the frequency band 30-100 MHz is primarily a meteor-scatter phenomenon, but experiments conducted by the U.S. Air Force in Greenland indicate that returns are also caused by sporadic E layers and "unidentified scatter returns" (Ostergaard et al., 1985). This channel model will only consider returns from ionized meteor trails.

2.1 Properties of Meteor Arrivals. With the exception of meteor showers, meteor arrivals are considered random events and experimental evidence indicates that meteors arrive according to a Poisson random process with rate λ (Oetting, 1980 and Weitzen, 1983). Since the arrival rate, λ, is a function of the time of day and season, a more appropriate model for meteor arrivals would be a *nonstationary* Poisson process with rate $\lambda(t)$ (Ross, 1985). However, the arrival rate changes slowly, so for short periods of time (less than 30 minutes), the process can be considered stationary (Weitzen, 1983). For long periods (several days or more), one can approximate the process as stationary with rate λ equal to the mean value of $\lambda(t)$ over time. In the next chapter we shall derive expressions for the mean message waiting time and long run average symbol rate. These two performance measures fall into the short and long periods, respectively. Hence, for our purposes, we treat λ as a constant, independent of time. The following properties of the Poisson process will prove useful (Ross, 1985):

- **Stationarity**. The Poisson process possesses *stationary increments,* meaning that the distribution of the number of events that occur in any interval of time depends only on the length of the interval.

• **Independence**. The Poisson process possesses *independent increments*, meaning that the number of events that occur in disjoint time intervals are independent.

• **Number of Arrivals**. The number of arrivals in time t is a Poisson random variable with probability mass function

$$p_X(i) = P(X = i) = e^{-\lambda t} \frac{(\lambda t)^i}{i!} \quad i = 0, 1, 2, \ldots \tag{2.1}$$

The mean number of arrivals in time t is λt.

• **Interarrival time.** The time between arrivals, T, is an exponential random variable with probability density function

$$f_T(t) = \lambda e^{-\lambda t} \qquad t > 0 \tag{2.2}$$

The mean time between arrivals is $1/\lambda$.

• **Waiting time until m^{th} arrival.** Let S_m equal the arrival time of the m^{th} event, $m > 0$. S_m has a Gamma distribution with parameters m and λ . The probability density for S_m is given by

$$f_{S_m}(t) = \lambda e^{-\lambda t} \frac{(\lambda t)^{m-1}}{(m-1)!}, \qquad t \geq 0 \tag{2.3}$$

The random variable S_m has mean m/λ .

2.2 Types of Meteor Trails. Meteor trails are normally categorized as underdense or overdense, according to the electron line density of the trail. Most meteor-scatter channel models ignore overdense trails, but we shall

demonstrate their importance. Ostergaard et al., (1985) propose a third type of trail, called "tiny," to explain short duration returns that do not exhibit the exponential decay of underdense trails. Most meteor-scatter communication systems employ acquisition times on the order of 0.1 sec (Kokjer, 1986) and since "tiny" trails have typical durations of less than 0.1 sec, their contribution to the performance of a meteor-scatter system is negligible and we shall ignore them. If the electron line density of the meteor trail is less than 10^{14} electrons/meter (e/m), then each electron reflects independently of all others and the trail is labeled *underdense*. If the electron line density exceeds 10^{14} e/m, then an incident wave cannot penetrate the cloud of electrons and the trail is modeled as a metallic cylinder. The incident wave is reflected from the surface of the trail and such a trail is labeled *overdense*. Overdense trails are infrequent, but Weitzen (1983) and Ostergaard et al. (1985) have shown that overdense trails contribute the majority of channel capacity when long run performance is considered. For example, data from the experimental link in Greenland show that although overdense trails account for only 5% of returns, these trails contribute over 60% of the throughput when adaptive signaling is used. We can conclude that theoretical models for the long run performance of meteor-scatter systems should include overdense trails.

2.3 Received Power Models. The power received due to reflection from an underdense trail is given by Eshlemann (1955) as

$$P_r(t) = \frac{P_T\, G_T\, G_r\, \sigma_e\, \lambda^3\, q^2 \exp\left[-\dfrac{32\,\pi^2 Dt + 8\,\pi^2\, r_0{}^2}{\lambda^2 \sec^2\phi}\right]}{(4\pi)^3\, R_{CT}\, R_{CR}\, (R_{CT} + R_{CR})\, (1 - \sin^2\phi\, \cos^2\beta)}, \quad q \le 10^{14} \text{ e/m} \qquad (2.4)$$

where P_T is the transmitter power

G_R is the receiver antenna gain

G_T is the transmitter antenna gain

λ	is the wavelength of the carrier
q	is the electron line density of the trail
D	is the diffusion coefficient of the atmosphere (~ 5 - 10 m^2/s)
ϕ	is the angle of incidence of the transmitted plane wave
β	is the angle between the trail and the great circle path from the receiver to the transmitter
R_{CR}	is the distance from the receiver to the trail
R_{CT}	is the distance from the transmitter to the trail
r_0	is the nominal radius of a trail (0.65 m)
σ_e	is the effective echoing area of the electron (~ 10^{-28} m^2)

Note that λ represents wavelength as well as meteor arrival rate. Usage will be clear from the context. Equation 2.4 is plotted as a function of time in Figure 2.1. Note that the received power decays exponentially with time.

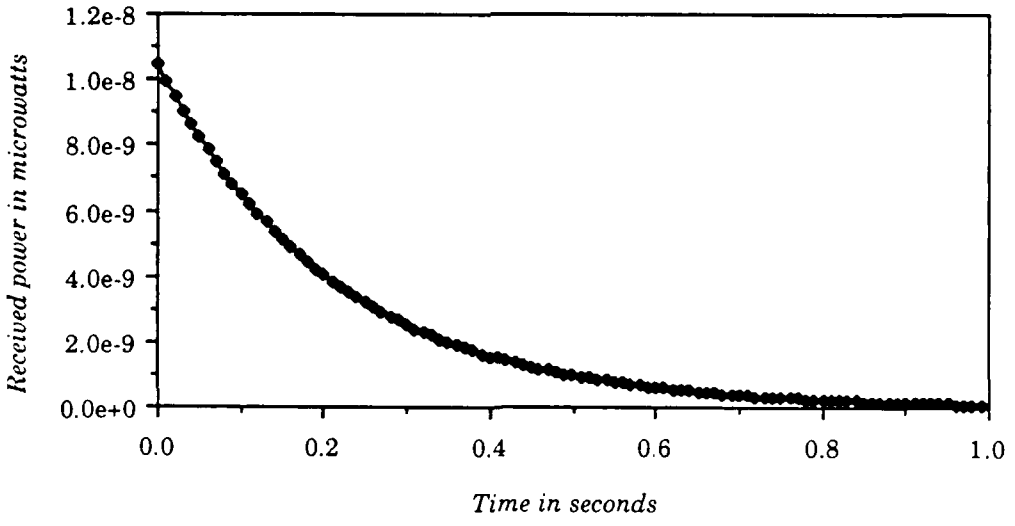

Figure 2.1 $P_r(t)$ for underdense trail (P_T = 2000 watts, q = 10^{13} e/m)

Equation 2.4 is a theoretical result that is obtained using the tools of classical antenna theory. For the overdense trail model, Hines and Forsythe (1957)

found the solution more difficult and resorted to an approximate expression. The received power for an overdense trail is approximated by Hines and Forsythe as

$$P_r(t) = \frac{P_T G_T G_R \lambda^2 \left[\frac{(4Dt + r_0^2)}{\sec^2 \phi} \ln\left(\frac{r_e \, q \, \lambda^2 \sec^2 \phi}{\pi^2 (4Dt + r_0^2)} \right) \right]^{1/2}}{32 \pi^2 R_{CR} R_{CT} (R_{CR} + R_{CT}) (1 - \cos^2 \beta \sin^2 \phi)}, \quad 10^{14} < q \leq 10^{17} \qquad (2.5)$$

where r_e (~3 x 10-15 m) is the classical radius of the electron. This model holds provided the argument of the logarithm is greater than unity. For an in-depth treatment of the derivations of (2.4) and (2.5), the reader should consult Weitzen's Ph.D. thesis (1983). Weitzen (1983) points out that due to the physics of particle reentry, meteor trails with electron line densities greater than 10^{17} e/m rarely exist. Thus our model holds for $q \leq 10^{17}$ e/m. Equation 2.5 is plotted as a function *of time* in Figure 2.2.

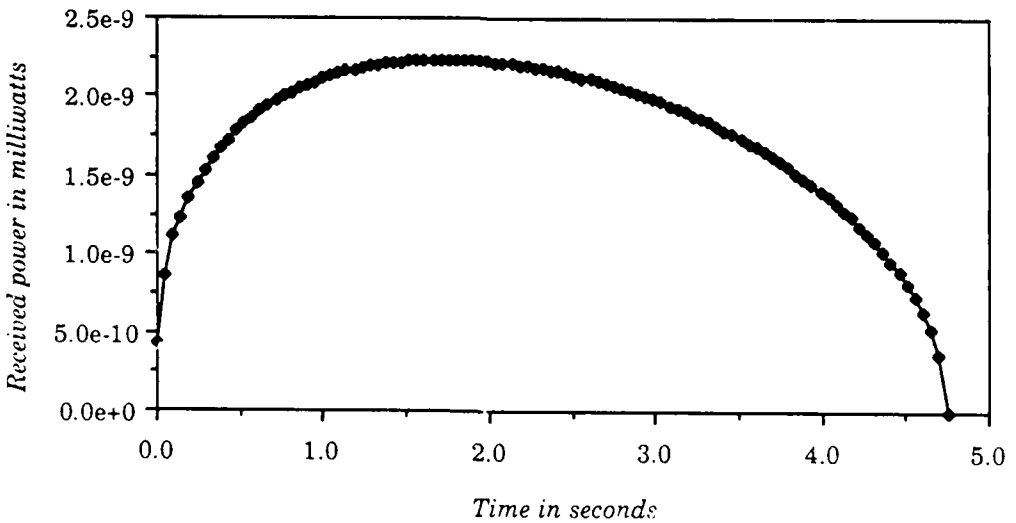

Figure 2.2 $P_r(t)$ for overdense trail (P_T = 2000 watts, q = 10^{15} e/m)

From Figure 2.2 we note that overdense trails do not decay exponentially with time. In fact, the received power from these trails actually increases at first, reaching a peak value before decaying.

2.4 Meteor Statistics. In this section we shall derive probability distributions for electron line density and burst duration. In addition, we shall derive an expression for the arrival rate, λ, in terms of the link parameters.

2.4.1 Electron line density. The meteors that are useful for communications have masses that are roughly distributed in numbers proportional to the reciprocal of their mass (Kokjer and Roberts, 1986). Assuming that the electron line density, q, is directly proportional to the meteor mass, then the cumulative distribution function (CDF) for the random variable Q is given by

$$F_Q(q) = P(Q \le q) = 1 - \frac{q_0}{q}, \quad q \ge q_0 \tag{2.6}$$

If we define (2.6) as the distribution for *observable* meteor trails, then q_0 is the electron line density of the smallest observable meteor. We emphasize that this distribution is approximate and is least accurate for large values of q. Since we know that electron line densities greater than 10^{17} e/m are almost nonexistent, then a better distribution for electron line density is the following

$$F_Q(q) = P(Q \le q) = 1 - \frac{q_0}{q} + \frac{q_0}{10^{17}}, \quad q_0 \le q \le 10^{17} \tag{2.7}$$

We can now use (2.6) to derive the distribution for burst duration.

2.4.2 Burst Duration. Assume for the moment that all trails are

underdense. The received power for an underdense trail is given by (2.4) and can be written as

$$P_r(t, q) = P_r(0,1)\ q^2\ \exp\left[\frac{-2t}{t_c}\right] \tag{2.8}$$

where

$$P_r(0,1) = \frac{P_T\ G_T\ G_r\ \sigma_e\ \lambda^3\ \exp\left[-\frac{8\pi^2 r_0^2}{\lambda^2 \sec^2\phi}\right]}{(4\pi)^3\ R_{CT}\ R_{CR}\ (R_{CT} + R_{CR})\ (1 - \sin^2\phi\cos^2\beta)}$$

$$t_c = \frac{\lambda^2\ \sec^2\phi}{16\pi^2 D}$$

Note that $P_r(0,1)$ is defined as the received power at time $t = 0$ when $q = 1$ e/m. Let T_d = burst duration in seconds, a random variable. The termination of a burst is defined as the time when the received power has decayed to a threshold value, $P_r(T_d, q) = P_r(0, q_0)$. Substituting into (2.8) and solving for t yields

$$T_d = \frac{t_c}{2}\ \ln\left[\frac{P_r(0,1)\ Q^2}{P_r(0, q_0)}\right] = t_c \ln\left[\frac{Q}{q_0}\right]$$

The CDF for burst duration, T_d, is then given by

$$F_{T_d}(t) = P(T_d \le t) = P\left(t_c \ln\left[\frac{Q}{q_0}\right] \le t\right)$$

$$= P\left(Q \le q_0 \exp\left[\frac{t}{t_c}\right]\right)$$

Using (2.6) results in

$$F_{T_d}(t) = 1 - e^{-t/\tau}, \qquad t \geq 0 \tag{2.9}$$

where $\tau = t_c$. Therefore, the burst duration is exponentially distributed with mean τ. The exponential distribution is almost universally accepted as the proper distribution for burst duration when all trails are assumed underdense. See Campbell and Hines (1957), Nes (1985), Oetting (1980), and Milstein et al. (1987). Havens (1976) prefers a *sectional logarithmic* distribution for burst duration, but his distribution does not have a strong following. Havens suggests a mean burst duration of 0.58 s, independent of season, time of day, and system sensitivity. He notes that results of experiments conducted from 1958 to 1968 support this conclusion. If the mean burst duration is indeed constant, and the modulation scheme is fixed, then all variations in throughput are attributable to λ, the meteor arrival rate.

2.4.3 Meteor arrival rate. Weitzen (1983) and others have shown that the number of observable trails per second is proportional to the inverse of the electron line density, q. Assuming that all trails are underdense, then one can show that the mean number of trails per second, λ, is proportional to the square root of the transmitter power. For meteor-scatter systems operating at a fixed rate, experiments have shown (Brown, 1969) that the throughput (average bit rate) is proportional to $P_T^{0.6}$. One can reason that the difference between the experimental results and the theoretical claim (exponent of 0.6 versus 0.5) is due to overdense trails. The difference of 0.1 in exponent will not change our results significantly, so we will assume a $P_T^{0.5}$ behavior. The dependence of throughput on frequency is more complex. Oetting (1980) points out that a simple theoretical analysis indicates that the throughput should vary as $f^{-2.4}$, where f is the RF carrier frequency. Assuming that the

throughput varies as $P_T^{0.5}$, and as $f^{-2.4}$, then we write the following expression for the mean number of trails/s (Oetting, 1980)

$$\lambda = \lambda^{(C)} \left[\frac{G_T}{G_T^{(C)}} \frac{R_s^{(C)}}{R_s} \frac{G_R}{G_R^{(C)}} \frac{P_T}{P_T^{(C)}} \frac{(E_s/N_0)_{req}^{(C)}}{(E_s/N_0)_{req}} \right]^{0.5} \left(\frac{f}{f^{(C)}} \right)^{-2.4} \qquad (2.10)$$

where the superscript (C) denotes the COMET values.[1] For the COMET system, $\lambda = 0.1$ trails/s, $G_T = G_R = 10$ dB, $P_T = 200$ W, $R_s = 2000$ symbols/s, and $f = 37.5$ MHz. $(E_s/N_0)_{req}$ is the minimum required signal-to-noise ratio per channel symbol to maintain reliable communications. For the COMET system, we assume noncoherent FSK and a bit-error rate (BER) of 10^{-4}. The corresponding value of $(E_s/N_0)_{req}$ is 17.0 (12.3 dB). Substituting these values into (2.10) yields the following empirical formula

$$\lambda = 0.1 \left[\frac{1.7\, G_T\, G_R\, P_T}{R_s\, (E_s/N_0)_{req}} \right]^{0.5} \left(\frac{f}{37.5} \right)^{-2.4} \qquad (2.11)$$

The reader should note that (2.11) will prove useful by showing the dependence of the meteor arrival rate as a function of the link parameters, symbol rate, and $(E_s/N_0)_{req}$. The actual value of λ has little importance except to give realistic values for performance measures.

2.5 Noise. Excluding man-made noise, the predominant noise source in the range 30-100 MHz for meteor-scatter systems is galactic noise. Careful antenna siting is required to avoid other noise sources. Galactic noise is Gaussian distributed and assumed white. Hence, the noise power spectral density is constant and is given by

$$N_0 = k\, T_a$$

[1] The COMET system became operational in the 1960's. It is probably the most studied meteor-burst communication system. See Bartholome and Vogt (1968).

where k is Boltzman's constant, (1.38 x 10^{-23} J/°K) and T_a is the antenna noise temperature. For galactic noise in the frequency range 30-100 MHz, Villard et al. (1956) approximate T_a as

$$T_a = \left(\frac{\lambda}{\lambda_0} \right)^{2.3} T_0 \qquad (2.12)$$

where λ_0 (= 1.8 m) is a constant and T_0 = 290 K. This expression assumes a receiver noise Figure of 0 dB. We can conclude that the meteor-scatter channel is an additive white Gaussian noise (AWGN) channel.

2.6 Multipath. Conventional meteor-scatter communication systems are fixed-symbol-rate systems with symbol rates on the order of 5 to 15 kHz (Weitzen et al., Jan., 1984). In Chapter 3, we shall show that to maximize the long run average symbol rate, the meteor-scatter system should employ symbol rates on the order of 1 to 10 MHz. In order to implement such a system, the multipath structure of the channel must be known. Multipath propagation degrades channel performance in two ways:

- Multipath fading
- Intersymbol interference

The causes of multipath propagation on the meteor-scatter channel are many. Included are the following (Weitzen et al., Jan.,1984): wind induced warping of long duration trails, multiple trails in the common volume of the antenna pattern, "sporadic E" layer anomalies, and fragmentation of meteoric particles upon entry into the earth's atmosphere. Weitzen's experimental research indicates that multipath spreads rarely exceed 1 μs and therefore systems with symbol rates on the order of 500 kHz should, in general, be able to operate free of intersymbol interference. To operate at higher symbol rates, adaptive correction of intersymbol interference is required.

2.7 Bandwidth. Radio channels are often categorized as either bandwidth-limited or power-limited. Since conventional meteor-scatter systems operate at low symbol rates (5 - 15 kHz), bandwidth has received little attention. Future systems operating at higher symbol rates will encounter bandwidth restrictions from the following sources:

- Multipath-induced intersymbol interference
- Regulatory agencies (to prevent adjacent channel interference)
- Hardware constraints.

For our purposes, the only bandwidth constraint is that imposed by intersymbol interference.

2.8 Link Parameters. When actual values of link parameters are needed for illustration, the values in table 2.1 will be used. These link parameters are typical for existing meteor-scatter communication systems.

Table 2.1 Link parameters

P_T	=	Transmitter power = 2000 W
$G_T = G_R$	=	Antenna gain = 13 dB
d	=	Path distance = 1000 km
f	=	Radio frequency = 50 MHz
ϕ	=	Angle of incidence = 1.37 rads
β	=	Angle between trail and great circle path = $\pi/6$ rads
h	=	Meteor trail height = 100 km
D	=	Diffusion coefficient of the atmosphere = 10 m^2/s
$(BER)_{max}$	=	Maximum acceptable bit error rate = 10^{-4}

The angles ϕ and β are actually random variables, but in Chapter 3 the channel model will be simplified by assuming that all trails arrive at a fixed point in the h–plane. Furthermore, unless stated otherwise, we shall

assume binary phase shift keying (BPSK) for waveform modulation. The minimum required signal-to-noise ratio per channel symbol for BPSK is $(E_s/N_0)_{req}$ = 8.4 dB for a bit-error rate (BER) of 10^{-4} (Lee, 1986).

2.9 Summary. Following is a brief summary of the important characteristics of the meteor-scatter channel according to the model derived in this chapter.

- Meteors arrive according to a Poisson process with rate λ.
- Received power from a meteor trail is given by (2.4) or (2.5), according to electron line density.
- Assuming all trails are underdense, burst duration has an exponential distribution with mean τ. The mean burst duration is constant, independent of system sensitivity.
- Variations in throughput are attributed to the arrival rate, λ, given by (2.11).
- The channel noise is additive white Gaussian noise (AWGN).
- Intersymbol interference caused by multipath propagation limits the maximum channel symbol rate to ~ 500 kHz.
- The channel is bandwidth limited. The only bandwidth constraint is the coherent bandwidth, determined by the multipath structure of the channel.

Chapter 3 - Performance Measures

Historically, the performance of a meteor-scatter communications system is measured in terms of either information throughput or message waiting time (Milstein et al., 1987). Definitions of throughput vary, but we shall define throughput as the long run average bit rate, R_{bavg}. An appropriate measure of message waiting time is the expected value, or mean. Therefore, we are interested in the following two performance measures:

- Long run average bit rate, R_{bavg}
- Mean message waiting time, T_{avg}

The nature of the message traffic determines which performance measure has priority. For example, a point-to-point link that transmits thousands of messages per day should be designed to maximize long run average bit rate. On the other hand, the user may want to transmit a single message as quickly as possible. In this case, one should minimize the mean message waiting time (or simply waiting time). This chapter is devoted to the derivation of expressions for long run average *symbol* rate, denoted by R_{avg}, and mean waiting time. The corresponding bit rate depends on the modulation scheme and will be discussed in Chapter 4. The fixed-symbol-rate (or simply fixed-rate) modem and adaptive-symbol-rate modem are considered. For the adaptive case, we assume that a noiseless feedback path with zero delay is present. Weitzen (1983) discusses the effects of path delay, a noisy feedback channel, and rate quantization for the adaptive-symbol-rate modem. Treatment of these subjects is beyond the scope of this thesis. The two performance measures, R_{bavg} and T_{avg}, will serve as figures of merit when comparing the performance of various modulation and coding schemes. We begin by deriving an expression for the long run average

symbol rate.

3.1 Long Run Average Symbol Rate, R_{avg}. Recall from Chapter 2 that meteors arrive according to a Poisson process with rate λ. Most messages will be long enough to require several bursts to complete transmission. We assume that the message can be partitioned at arbitrary points without loss of information. On the average, the capacity of a single burst is many thousand channel symbols. For this reason, we can approximate the number of symbols per burst as a continuous (rather than discrete) random variable, W. We shall consider the general case, and thus we ignore any packet structure or message protocols. Let the total number of symbols transmitted by time t be W(t). Given the above arguments, we can model the stochastic process $\{W(t), t > 0\}$ as a *compound Poisson process* where a compound Poisson process is defined as follows (Ross, 1985):

Definition 3.1. *Consider a Poisson process $\{N(t), t > 0\}$ having interarrival times T_m $m \geq 1$. Suppose that when an arrival occurs we receive a reward. Denote by W_m the reward earned at the time of the mth arrival. Assume that the W_m, $m = 1, 2, 3, \ldots$ are independent, identically distributed (iid) random variables that are also independent of $\{N(t), t > 0\}$. Let*

$$W(t) = \sum_{m=1}^{N(t)} W_m \tag{3.1}$$

Then W(t) represents the total reward earned by time t. $\{W(t), t > 0\}$ is said to be a compound Poisson process.

Clearly, the process of transmitting messages on the meteor-scatter channel is a compound Poisson process where W_m represents the number of symbols sent during the m^{th} burst. Since the probability of multiple (overlapping in time) trails is small ($\sim 10^{-3}$) (Weitzen, 1983), then we can assume that W_m is independent of $\{N(t), t > 0\}$. The compound Poisson process is a member of the larger family of random processes called *renewal reward processes.*

For these random processes one can show the following (Ross, 1985): If $E[W] < \infty$, and $E[T] < \infty$, then with probability 1,

$$\frac{W(t)}{t} \rightarrow \frac{E[W]}{E[T]} \text{ as } t \rightarrow \infty \tag{3.2}$$

Thus, we can write the long run average symbol rate (as $t \rightarrow \infty$) as the following

$$R_{avg} = \lambda E[W] \tag{3.3}$$

Let's compare this expression for throughput with that obtained using the one of the most popular definitions of throughput. Oetting (1980) defines throughput as the average number of data bits (or symbols) received per unit time. Ignoring packet structure, this definition gives an expression identical to (3.3). To see why this is true, consider the following derivation. The mean number of symbols transferred in time t is simply the expected value of the compound Poisson process (Ross, 1985)

$$E[W(t)] = E[N(t)] E[W]$$

Since the expected value of N(t) is just λt, then we have

$$E[W(t)] = \lambda t \; E[W]$$

Dividing both sides of this equation by t gives the average number of symbols received per unit time

$$R_{avg} = \lambda E[W]$$

This expression is identical to (3.3). Therefore, the long run average symbol rate is equivalent to the "throughput" as defined in the literature. Oetting's expression for throughput differs from the expression derived in this chapter because he assumes a particular packet structure.

The number of symbols per burst, W is a function of the random variables Φ, Z, and Q where

Z = Reflection point in the h-plane ($Z \in \mathbf{R}^2$)

Φ = Angle of incidence at reflection point

Q = Electron line density of the meteor trail

We assume that Z is a uniform random variable over a large, finite region of the h-plane (Weitzen, 1983). As long as the region is large, its actual size is not important because the geometry precludes good paths from distant points in the plane. Furthermore, based on the properties of meteor arrivals, it is reasonable to assume that Φ, Z, and Q are independent. Then we can write the average symbol rate as

$$R_{avg} = \frac{\lambda}{A} \int_A \int_\Phi \int_Q W(Z, \Phi, Q)\, f_Q(q)\, f_\Phi(\phi)\, dq\, d\phi\, dA \qquad (3.4)$$

where A= the area of the finite region of the h-plane. As it stands, this expression for R_{avg} is unwieldy. Weitzen (1983) and others simplify their models by assuming that all trails arrive at a fixed point in the h-plane. Making this simplification, we get the following expression for the long run average symbol rate:

$$R_{avg} = \lambda \int_Q W(q)\, f_Q(q)\, dq \qquad (3.5)$$

We can further justify (3.5) by noting that we are interested in the relative, not absolute performance of several modulation and coding schemes. The reader should be cautioned, however, about using (3.5) to compare performance over values of path distance. For values of β (defined in Chapter 2) other than $\pi/2$, equation 3.5 is not strictly decreasing for increasing path distance.

3.1.1 Fixed-symbol-rate modem. For a fixed-rate modem the expression for long run average symbol rate is given by

$$R_{avg} = \lambda \int_Q R_s \, T_d(q) \, f_Q(q) \, dq \tag{3.6}$$

where R_s = channel symbol rate in Hz and $T_d(q)$ = the useful duration of the trail in seconds. This integral is evaluated in Appendix A. For the link parameters of Chapter 2, we get the following table of values for R_{avg}:

Table 3.1 Average symbol rate in Hz for fixed-rate modem

R_s (kHz)	underdense	overdense	Total
1	4.7	.83	5.5
5	9.5	4.2	13.6
10	12.5	8.3	20.8
50	21.1	41.3	62.4
100	24.4	81.8	106.3
500	21.3	379.1	400.4
1 000	11.5	682.8	694.3

The values of R_{avg} in Table 3.1 were calculated by scaling (3.6) by a constant. This constant was chosen to give values consistent with the results from the experimental link in Greenland (Ostergaard, et al., 1985). Note that overdense trails account for anywhere from 15% to 98% of channel capacity, depending on symbol rate. Equation 3.6 is plotted in figure 3.1. From Figure 3.1, we see that there exists an optimal symbol rate, that is one that

maximizes R_{avg}. For our link parameters, this optimal rate is found graphically from Figure 3.1 to be approximately 10 MHz.

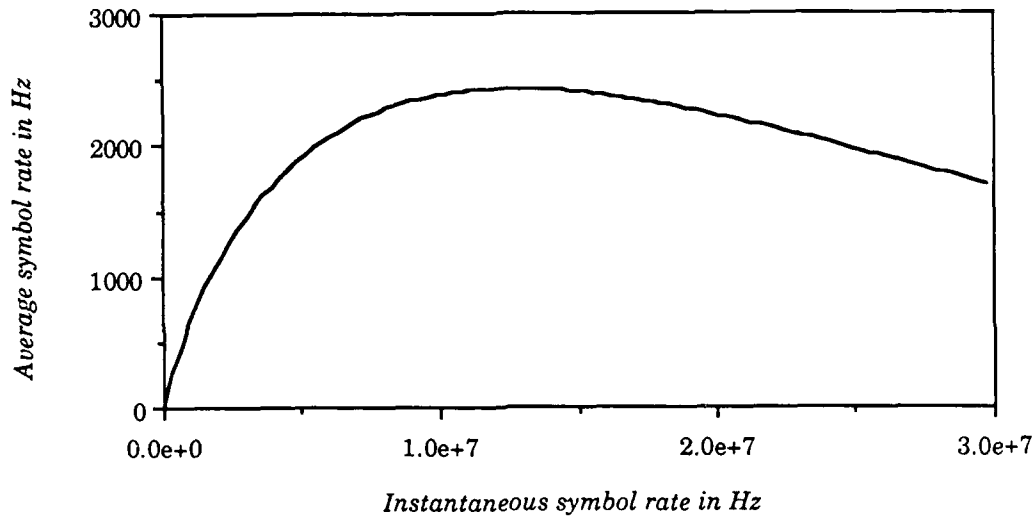

Figure 3.1 Average symbol rate as a function of instantaneous symbol rate, R_s

The author has found that for transmitter power levels as low as 200 watts, the optimal symbol rate still exceeds 1 MHz. Since the meteor-scatter channel is constrained by multipath propagation to symbol rates less than 500 kHz, we conclude that the optimal symbol rate is the maximum rate that the channel can support, i.e. ~ 500 kHz. This result agrees with Abel's conclusion (1986), although Abel did not derive an expression for R_{avg}.

3.1.2 Adaptive-symbol-rate modem: The adaptive-symbol-rate modem varies the symbol rate continuously to match the time-varying received power levels. Since the received power is equal to the product of the energy per channel symbol, E_s, and the channel symbol rate, R(t), we can write the instantaneous symbol rate as

$$R(t) = \frac{P_r(t)}{N_0 (E_s / N_0)_{req}} \tag{3.7}$$

where $(E_s / N_0)_{req}$ is the ratio of received energy per symbol to noise power spectral density required by the modem to maintain an acceptable bit error rate (BER). The number of symbols transmitted per burst is then given by

$$W = \int_0^{T_d(q)} R(t)\, dt \tag{3.8}$$

where $T_d(q)$ = the useful burst duration as a function of the electron line density, q. It follows that the long run average symbol rate for the adaptive-symbol-rate modem is given by

$$R_{avg} = \lambda \int_Q \int_0^{T_d(q)} R(t)\, f_Q(q)\, dt\, dq \tag{3.9}$$

Equation 3.9 is evaluated in Appendix A. At a transmitter power level of 2000 watts, we get an average symbol rate of 6.04 kHz, an improvement of 15.1 over fixed-rate at R_s = 500 kHz. Recall from Section 2.4.3 of Chapter 2 that the meteor arrival rate, λ, is a function of the symbol rate, R_s. For the adaptive symbol rate modem, the meteor arrival rate is a function of the minimum realizable symbol rate, R_{min} (a hardware constraint). Note that for our model, $\lambda \rightarrow \infty$ as $R_{min} \rightarrow 0$, indicating that $R_{avg} \rightarrow \infty$. This is not the case, however, because as $\lambda \rightarrow \infty$, trails start to overlap and our expression for R_{avg} is no longer valid. In practice, however, hardware constraints will confine R_{min} to values that make our model valid. The improvement factor for the adaptive-symbol-rate modem versus the fixed-rate modem is discussed in Section 3.1.4.

3.1.3 Constrained channel. In Chapter 2 we found that the meteor-

scatter channel is constrained by multipath-induced intersymbol interference to a maximum symbol rate of R_{max} ~ 500 kHz. For such a channel, the expressions for long run average symbol rate must be modified as follows:

Fixed-rate modem:

$$R_{avg} = \lambda \int_Q R_s \, T(R_s , q) \, f_Q(q) \, dq , \qquad R_s \leq R_{max} \tag{3.10}$$

Adaptive-symbol-rate modem:

$$R_{avg} = \lambda \int_Q \int_0^{T(R_{min} , q)} R(t) \, f_Q (q) \, dt \, dq \tag{3.11}$$

where $R(t) = \begin{cases} \dfrac{P_r (t)}{N_0 (E_s / N_0)_{req}} , & \dfrac{P_r (t)}{N_0 (E_s / N_0)_{req}} \leq R_{max} \\ R_{max} , & \dfrac{P_r (t)}{N_0 (E_s / N_0)_{req}} > R_{max} \end{cases}$

Because of the added complexity of this expression, we resort to numerical integration to evaluate Equation 3.11. Table 3.2 lists values of R_{avg} for several values of maximum symbol rate.

Note that at R_{max} = 500 kHz, the average symbol rate has dropped by a factor of 13.7 from the value of the previous section. We can conclude therefore that the ceiling on symbol rate has a serious effect on the long run average symbol rate. In fact, we shall show in the next section that for a bandwidth-limited channel, the adaptive-symbol-rate modem does not exceed a factor of 2.0 improvement over the fixed-rate modem, assuming that the fixed-rate

modem is operating at the maximum rate (~ 500 kHz). This result seems to contradict some recent experimental evidence. Ostergaard et al. (1985) found that very few returns would support symbol rates exceeding 1 MHz, and concluded that the channel was effectively power limited, not bandwidth limited. This author does not dispute this conclusion, but he wishes to point out that systems with higher transmitter power or antenna gain will invariably encounter these signal levels with greater frequency. Therefore, the effect of the bandwidth ceiling on the adaptive-symbol-rate modem will depend on the link parameters and the receiver sensitivity.

Table 3.2 Average symbol rate in Hz for adaptive-symbol-rate modem on bandwidth limited channel ($R(t) \leq R_{max}$)

R_{max} (kHz)	underdense	overdense	Total
50	40.4	35.2	75.6
100	58.1	70.3	128.4
250	81.4	174.3	255.7
500	97.9	343.9	441.8
1 000	109.5	668.9	778.5
2 000	113.5	1238.9	1352.4
5 000	113.5	2243.2	2356.8

3.1.4 Improvement factor. For an unconstrained channel ($R_{max} \rightarrow \infty$) the adaptive-symbol-rate modem provides a significant improvement in R_{avg} over the fixed-rate modem. Define the improvement factor as

$$I = \frac{R_{avg}\,(\text{adaptive})}{R_{avg}\,(\text{fixed})} \tag{3.12}$$

With the aid of the computer we can use the expressions derived in Appendix A to get the graph of Figure 3.2. Note the vast improvement that the adaptive modem offers on a strictly power-limited channel.

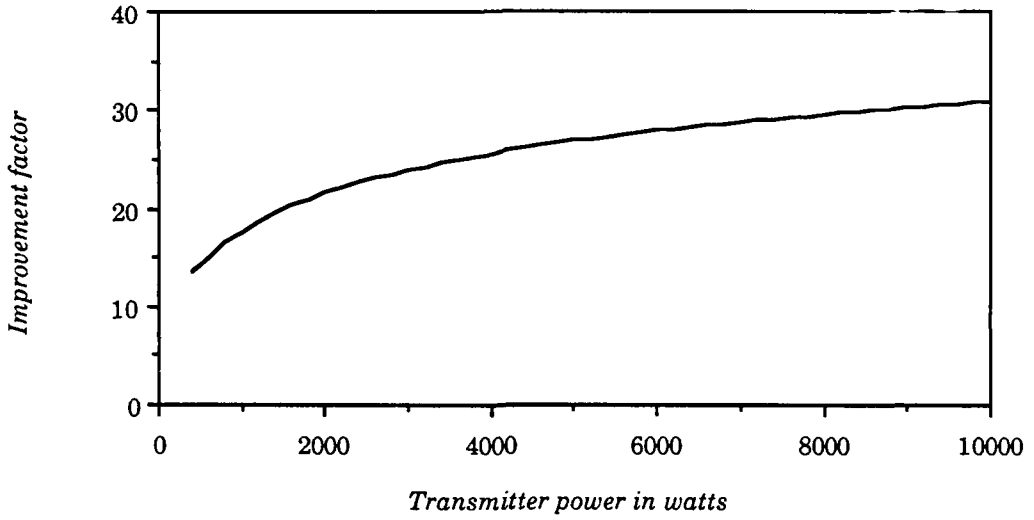

Figure 3.2 Improvement factor, adaptive-symbol-rate over fixed-rate for a strictly power-limited channel

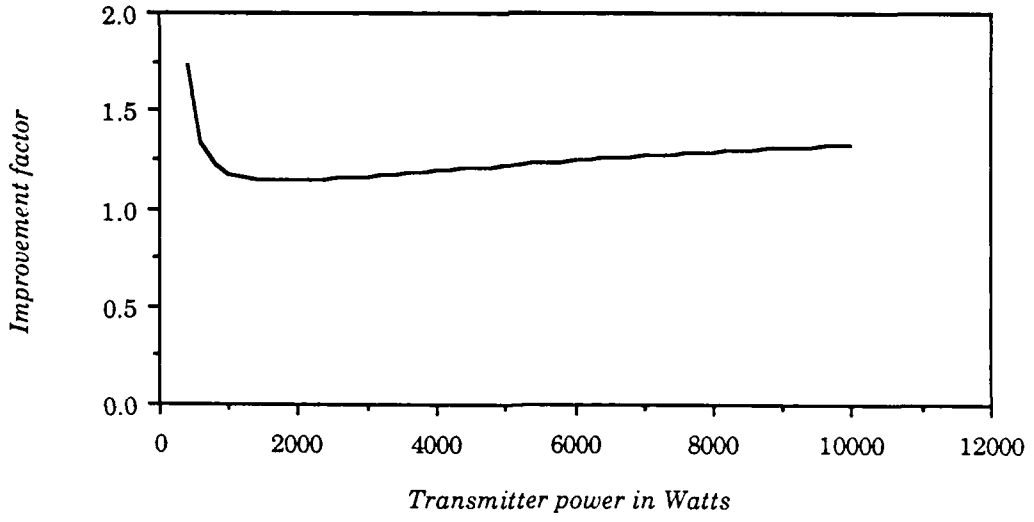

Figure 3.3 Improvement factor, adaptive-symbol-rate over fixed-rate for bandwidth-limited channel (R_{max} = 500 kHz)

The results for the bandwidth-limited channel are less remarkable. Note from Figure 3.3 (above) that the improvement factor varies from 1.25 to 1.75.

These results should encourage further research into adaptive techniques to correct intersymbol interference on the meteor-scatter channel.

3.2 Mean Message Waiting Time, T_{avg}. Long run performance on the meteor-scatter channel may not be important in some applications. Often the user would rather minimize the waiting time required to transmit a message of length N bits. In fact, much of the recent literature on meteor-scatter communications is focused on this subject. See Oetting (1980), Hampton (1985), and Milstein et al. (1987). Oetting derives an expression (in the form of an infinite sum) for the CDF of the waiting time, but does not discuss mean waiting time. Hampton and Milstein, et al. limit their discussions to packet structures.

We shall derive a closed-form expression for the mean waiting time for the fixed-rate modem, assuming no packet structure. However, we shall assume that the message can be partitioned at arbitrary points without loss of information. For the adaptive-symbol-rate modem, we derive some tight bounds on the mean waiting time. In addition, we extend a result from Cox (1962) to derive a general expression for the Laplace transform of the mean waiting time. This expression is valid for any modem, as long as the distribution for the number of symbols/burst, W, is known and the Laplace transform of the probability density function for W exists. As in Section 3.1, we assume that multiple trails are nonexistent and that the number of symbols per burst is normally quite large. Thus, we approximate the number of symbols/burst, W, as a continuous (rather than discrete) random variable. One can extend the results of this section to packet structures when the packets are small (few symbols/packet). Define message waiting time as follows:

Definition 3.2. *Consider a compound Poisson process, {W(t), t ≥ 0}. The message waiting time, T_w, is the time required to completely transmit a message of length N symbols when the message can be partitioned into arbitrary segments of size W_m.*

The mean waiting time, denoted by T_{avg}, is defined as the expected value of the message waiting time. We make the following assumptions:

- All trails are underdense
- The W_m symbols transmitted during the m^{th} burst are sent in a time $\Delta t=0$

We can justify these assumptions by noting that the waiting time for overdense trails is typically an order of magnitude greater than the waiting time for underdense trails. For example, an overdense trail with electron line density of 10^{15} e/m has a waiting time of about 15 minutes. In contrast, an underdense trail with electron line density 10^{13} e/m arrives about every 15 seconds. A single message of reasonable length is not likely to see an overdense trail. Also, the duration of a burst is typically a fraction of the time between bursts (e.g. 0.5 s vs. 10 s). The duration of the last burst for a given message will not make a significant contribution to the message waiting time.

3.2.1 Fixed-rate modem. Oetting (1980) derived an expression for the CDF of T_W for a fixed-rate modem, but the literature lacks a general closed form expression for the mean waiting time. In Section 3.2.3 we shall present a general expression for mean waiting time in terms of an inverse Laplace transform. For the fixed-rate modem, however, we can derive the mean waiting time via straightforward application of conditional expectation. We can write the mean waiting time as

$$E[T_w] = \sum_{m=1}^{\infty} E[\, T_w \mid m]\, P(m) \tag{3.13}$$

where P(m) is the probability that exactly m bursts are required to completely transmit the N-symbol message. We notice that

$$E\,[\, T_w \mid m\,] \;=\; E\,[\, S_m\,] \tag{3.14}$$

where S_m = the waiting time until the mth meteor arrival. Since S_m is a Gamma random variable with parameters (m, λ), then

$$E\,[\, T_w \mid \text{exactly m bursts required}] = E\,[S_m] = \frac{m}{\lambda} \tag{3.15}$$

The probability that exactly m bursts are required to send the message is given by

$$P(m) = P\left(\sum_{i=1}^{m-1} W_i < N \le \sum_{i=1}^{m} W_i \right)$$

$$= P\left(\sum_{i=1}^{m-1} W_i \;< N\,,\; W_m + \sum_{i=1}^{m-1} W_i \;\ge N \right)$$

if we let $X = \sum_{i=1}^{m-1} W_i$ and $Y = W_m$ then we can write

$$P(m) = P(\, X < N\,,\, X + Y \ge N\,) \tag{3.16}$$

Recall that the distribution for underdense burst duration in seconds is exponential with mean τ. It follows that the underdense burst duration in symbols is also exponential with mean $\tau_0 = R_s \tau$. Let $\lambda_0 = 1/\tau_0$. The random variable X is the sum of m-1 independent and identically distributed (iid) exponential random variables with mean τ_0. Then one can show (Ross, 1984) that X is a Gamma random variable with parameters (m-1, λ_0). The random variables X and Y are independent, so we can write (3.16) as the following:

$$P(m) = \int_0^N \int_{N-x}^{\infty} f_X(x)\, f_Y(y)\, dy\, dx \qquad (3.17)$$

where $$f_X(x) = \frac{\lambda_0 e^{-\lambda_0 x} (\lambda_0 x)^{m-2}}{\Gamma(m-1)}, \qquad x \geq 0$$

$$f_Y(y) = \lambda_0 e^{-\lambda_0 y}, \qquad y \geq 0$$

$\Gamma(s)$ is the Gamma function where $\Gamma(s) = (s-1)!$ for integer s. Evaluating (3.17), we find that P(m) is given by

$$P(m) = \frac{e^{-\lambda_0 N} (\lambda_0 N)^{m-1}}{(m-1)!} \qquad (3.18)$$

Note from (3.18) that if we let U = the number of bursts required to completely send the message, then U-1 is Poisson with mean λ_0 N. Combining (3.15) and (3.18), we find that the mean message waiting time is given by

$$E[T_W] = \sum_{m=1}^{\infty} \frac{m}{\lambda} \frac{e^{-\lambda_0 N} (\lambda_0 N)^{m-1}}{(m-1)!} \qquad (3.19)$$

Let n = m-1 and $x = \lambda_0 N$. Then we can write

$$E[T_w] = \frac{e^{-x}}{\lambda} \sum_{n=0}^{\infty} \frac{(1+n)\,x^n}{n!} \tag{3.20}$$

$$= \frac{e^{-x}}{\lambda} \left\{ \sum_{n=0}^{\infty} \frac{x^n}{n!} + \sum_{n=1}^{\infty} \frac{x^n}{(n-1)!} \right\}$$

$$= \frac{e^{-x}}{\lambda} \{ e^x + x e^x \}$$

Substituting $x = \lambda_0 N$, and simplifying, results in

$$E[T_W] = \frac{1}{\lambda} + \frac{N \lambda_0}{\lambda} \tag{3.21}$$

or equivalently,

$$E[T_W] = \frac{1}{\lambda} + \frac{N}{\lambda \tau R_s} \tag{3.22}$$

The reader should note that (3.22) is an exact result. Inspection of Equation 3.22 reveals that in the limit as N is small with respect to symbol rate, R_s, the mean waiting time is simply the mean waiting time for the first meteor burst. This result is intuitively sound. Table 3.3 gives some typical values for T_{avg} using equation 3.22 for τ = .58 sec., λ = 0.1 trails/s, and R_s = 1200 symbols/s. BPSK modulation is assumed, so N symbols = N bits.

Table 3.3 Typical values of mean message waiting time, T_{avg}

N (bits)	T_{avg} (sec.)	N (bits)	T_{avg} (sec.)
100	11.44	1 000	24.37
200	12.87	2 000	38.73
300	14.31	5 000	81.84
400	15.57	10 000	153.7
500	17.18	50 000	728.4

We can now derive an expression for the optimal symbol rate – the rate that minimizes T_{avg}.

3.2.2 Optimal symbol rate for fixed-rate modem. To minimize the waiting time on a power-limited channel, the system designer simply increases the symbol rate. Because of the burst characteristics of the meteor-scatter channel, we cannot minimize message waiting time simply by increasing the symbol rate to an arbitrarily high value. There is a penalty to be paid for any increase in bit rate. The penalty is a corresponding decrease in the number of observable trails per second, λ. This penalty applies regardless of whether the channel is modeled as bandwidth-limited or power-limited. In the past, the behavior of the message waiting time as a function of bit rate was not known precisely because a general expression for mean waiting time was not available. Now that we have derived such an expression (3.22), we can proceed to find the symbol rate that minimizes the mean waiting time. Since we made the conservative assumption that all trails are underdense, the behavior of the meteor arrival rate, λ, as a function of symbol rate is given by

$$\lambda = c\, R_s^{-1/2}$$

where $$c = 0.1 \sqrt{\frac{1.7\, G_T\, G_R\, P_T}{(E_s/N_0)_{req}}} \left(\frac{f}{37.5}\right)^{-2.4}$$

Substituting this expression into (3.22), we get

$$T_{avg} = E\,[T_w] = \frac{1}{c}\, R_s^{1/2} + \frac{N}{c\,\tau}\, R_s^{-1/2}$$

Differentiating and setting the result equal to 0,

$$\frac{\partial\, T_{avg}}{\partial\, R_s} = \frac{1}{2\,c}\, R_s^{-1/2} - \frac{N}{2\,c\,\tau}\, R_s^{-3/2} = 0$$

Solving for R_s, we get $R_s = 0$, $R_s = N/\tau$. Therefore, the optimal symbol rate is simply

$$R_{sopt} = \frac{N}{\tau} \tag{3.23}$$

A check of the second derivative confirms that this is indeed a minimum. Table 3.4 gives some typical values of R_{sopt} for $\tau = .58$ sec.

Table 3.4 Typical values of optimal symbol rate, R_{sopt}, in Hz

N (symbols)	R_{sopt} (Hz)	N (symbols)	R_{sopt} (Hz)
100	172.4	1 000	1 724
200	344.8	2 000	3 448
300	517.2	5 000	8 621
400	689.7	10 000	17 240
500	862.1	50 000	86 210

Note that even for large messages, the optimal symbol rate is only a fraction of the rate that maximizes R_{avg}. We can conclude that a fixed-rate scheme cannot be designed to maximize R_{avg} and minimize T_{avg} simultaneously. To get an expression for the minimum mean waiting time, we substitute (3.23) into (3.22) to get

$$E\,[T_w]_{opt} = \frac{2}{c}\sqrt{\frac{N}{\tau}} \tag{3.24}$$

Or in terms of the meteor arrival rate, λ,

$$E\,[T_w]_{opt} = \frac{2}{\lambda} \tag{3.25}$$

Substituting the value for c into (3.24), we get the following expression for the mean message waiting time with $R_s \approx R_{sopt}$

$$E\,[T_w]_{opt} = 20\sqrt{\frac{N(E_s/N_0)_{req}}{1.7\,G_T\,G_R\,P_T\,\tau}}\left(\frac{f}{37.5}\right)^{2.4} \tag{3.26}$$

3.2.3 Adaptive-symbol-rate modem. Recall that the expression for mean waiting time is given by (3.13):

$$E[T_W] = \sum_{m=1}^{\infty} E[\,T_W \mid m]\,P(m) \tag{3.13}$$

and that P(m) is given by

$$P(m) = P(X < N,\, X + Y \geq N)$$

For the fixed-rate case, the random variable X is the sum of m-1 iid

exponential random variables and therefore X has a Gamma probability distribution. In the adaptive case, X will not be exponential and the $(m-1)^{th}$ order convolution of the density, $f_W(t)$ will be dependent on m. Therefore, to get a general result, we must resort to other methods. Discussion of the mean waiting time for a compound Poisson process is almost nonexistent in the literature, but Cox (1962) does give an expression for the Laplace transform of the mean *first passage time*, which is equivalent to our mean waiting time. Substituting our notation into Cox's expression, we get the important result:

$$\mathcal{L}\{ E[T_w] \} = \frac{1}{\lambda}\left[\frac{1}{s} + \frac{F(s)}{s[1 - F(s)]} \right] \tag{3.27}$$

where

F(s) = Laplace transform of the density for the random variable W.

s = the argument of the Laplace transform with respect to N, the number of symbols in the message.

We can easily check that (3.27) gives an expression identical to (3.22) for the fixed-rate modem. Note that for the fixed-rate modem, the number of symbols per burst is an exponential random variable with mean $1/\lambda_0 = \tau R_s$. The Laplace transform of the probability density function, $f_W(N)$, is then given by

$$F(s) = \frac{\lambda_0}{\lambda_0 + s}$$

Substituting this expression into (3.27) and taking the inverse Laplace transform, we get our previous result:

$$E[T_W] = \frac{1}{\lambda} + \frac{N}{\lambda \tau R_s} \tag{3.22}$$

Next we consider the adaptive-symbol-rate modem. First we need the distribution for W, the number of symbols per burst. In Section 3.1 we derived the following expression for W:

$$W = \int_0^T R(t)\, dt$$

$$= \int_0^T \frac{P_r(0)\, q^2\, e^{-2t/\tau}}{(E_s/N_0)_{req}\, N_0}\, dt$$

$$= \frac{P_r(0)\, q^2\, \tau}{2\,(E_s/N_0)_{req}\, N_0}\,(1 - e^{-2T/\tau}) \qquad (3.28)$$

We can write q^2 as a function of T,

$$q^2 = \frac{(E_s/N_0)_{req}\; N_0\, R_{min}\, e^{2T/\tau}}{P_r(0)}$$

Substituting this into (3.28), we get

$$W = \frac{R_{min}\,\tau}{2}\,(e^{2T/\tau} - 1)$$

The distribution for W is then given by

$$F_W(x) = P(W \le x) = P\left(\frac{R_{min}\,\tau}{2}\,(e^{2T/\tau} - 1) \le x\right)$$

$$= P\left(T \le \frac{\tau}{2}\,\ln\left[\frac{2x}{R_{min}\,\tau} + 1\right]\right)$$

Since T is exponential with mean τ, we have the following:

$$P(W \le x) = 1 - \exp\left\{ -\frac{1}{\tau} \frac{\tau}{2} \ln\left[\frac{2x}{R_{min}\tau} + 1 \right] \right\}$$

Simplifying, we get the distribution for W for the adaptive modem:

$$P(W \le x) = 1 - \frac{1}{\sqrt{\frac{2x}{R_{min}\tau} + 1}} \tag{3.29}$$

Let $a = 2/(R_{min}\,\tau)$. Differentiating (3.29) yields the density for W:

$$f_W(N) = \frac{a}{2} (aN + 1)^{-3/2} \tag{3.30}$$

Consulting a table of Laplace transforms (Fodor, 1965), we find that the Laplace transform of $f_W(N)$ is given by

$$F(s) = 1 - \sqrt{\frac{\pi}{a}}\ \sqrt{s}\ e^{s/a}\ \mathrm{erfc}\left(\sqrt{\frac{s}{a}}\right) \tag{3.31}$$

where erfc (u) is the complementary error function, defined as

$$\mathrm{erfc}\,(u) = \frac{2}{\sqrt{\pi}} \int_u^\infty e^{-x^2}\, dx$$

Substituting (3.31) into (3.27) results in the expression for the Laplace transform of the mean waiting time for the adaptive-symbol-rate modem:

$$\mathcal{L}\{ E[T_w] \} = \frac{1}{\lambda} \left[\frac{1}{\sqrt{\frac{\pi}{a}}\ s^{3/2}\ e^{s/a}\ \mathrm{erfc}\left(\sqrt{\frac{s}{a}}\right)} \right] \tag{3.32}$$

Thus, finding the mean waiting time reduces to finding the inverse Laplace transform of (3.32). Unfortunately, this transform (3.32) is not found in any published table of Laplace transforms. In fact, the inverse Laplace transform may not exist in closed form. For this reason, we resort to finding bounds on mean waiting time for the adaptive-symbol-rate modem.

Consider the ideal modem – one that can transmit the entire message of N symbols on the very first burst. In this case the lower bound on T_{avg} is simply the mean waiting time for the first arrival, $1/\lambda$. The upper bound on T_{avg} is found by assuming the worst case – we send nothing until a burst occurs that can transmit the entire message of N symbols. Let T_b = the waiting time until such a burst occurs and let X = the number of bursts required. Then we can write the upper bound as follows:

$$E[T_w] \leq E[T_b] = \sum_{m=1}^{\infty} E[\, T_b \mid \text{no successes until } m^{th} \text{ burst}]\, P(X = m)$$

Since consecutive meteor bursts are independent trials, then X is a geometric random variable with the following probability mass function

$$p_X(m) = P(X = m) = (1-p)^{m-1}\, p$$

where $p = P(W \geq N) = 1 - F_W(N)$. The upper bound can then be written as

$$E[T_w] \leq \sum_{m=1}^{\infty} \frac{m}{\lambda}\, (1-p)^{m-1}\, p = \frac{1}{\lambda}\, E[X] = \frac{1}{\lambda\, p}$$

Where we made use of the result

$$E[\, T_b \mid \text{no successes until } m^{th} \text{ burst}] = E[S_m] = \frac{m}{\lambda}$$

Therefore, the mean waiting time for any modem, including the adaptive-symbol-rate modem, is bounded in the following way

$$\frac{1}{\lambda} \leq E[T_w] \leq \frac{1}{\lambda p} \tag{3.33}$$

Since $p = 1 - F_W(N)$, we can use (3.29) to get the following bounds for the adaptive-symbol-rate modem

$$\frac{1}{\lambda} \leq E[T_w] \leq \frac{1}{\lambda} \sqrt{\frac{2N}{R_{min}\tau} + 1} \tag{3.34}$$

Figure 3.4 demonstrates the behavior of these bounds as a function of message size, N, for R_{min} = 25 kHz, λ = 0.1 trails/s, and τ = .58 s. As expected, the mean waiting time approaches the lower bound for small N.

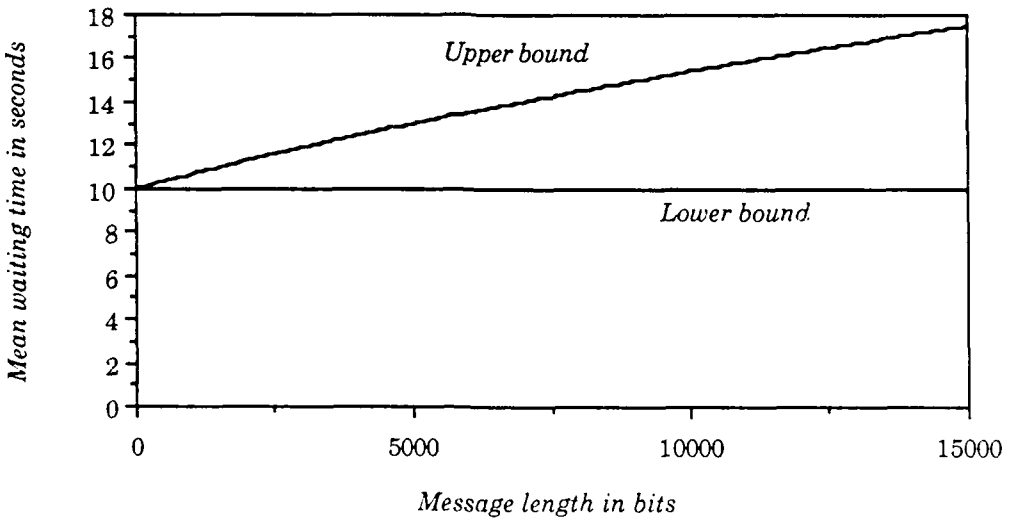

Figure 3.4 Upper and lower bounds on mean waiting time for adaptive-symbol-rate modem

3.2.4 Improvement factor. Define the improvement factor as follows:

$$I = \frac{E\,[T_w]_{fixed}}{E\,[T_w]_{adaptive}}$$

where $E\,[T_w]_{adaptive}$ is the mean message waiting time for any adaptive-information-rate modem. Before deriving the improvement factor for the adaptive-symbol-rate modem, it will prove useful to derive bounds on the improvement factor in the general case. The improvement factor is bounded as follows:

$$\frac{E\,[T_w]_{\,fixed}}{E\,[T_w]^{\,ub}_{\,adaptive}} \leq I \leq \frac{E\,[T_w]_{\,fixed}}{E\,[T_w]^{\,lb}_{\,adaptive}}$$

where the superscripts "ub" and "lb" denote upper bound and lower bound, respectively. Recall that the mean message waiting time for the fixed-rate modem operating at the optimal symbol rate is given by the following:

$$E\,[T_w]_{opt} = \frac{2}{\lambda} \tag{3.25}$$

Since any adaptive modem is bounded according to (3.33), we can write the bounds on improvement factor as the following

$$2p \leq I \leq 2 \tag{3.35}$$

where $p = P(W \geq N)$ and we have assumed that the meteor arrival rate is the same for both modems. Now consider the specific case of the adaptive-symbol-rate modem. To make a fair comparison, we assume that the fixed-rate modem is operating at the optimal symbol rate, $R_{sopt} = N/\tau$ and that the adaptive modem operates with a minimum symbol rate equal to R_{sopt}. The

meteor arrival rate, λ, is then the same for both modems and we can write the bounds on the improvement factor as follows:

$$\frac{2}{\sqrt{3}} \leq I \leq 2 \tag{3.36}$$

These bounds are remarkably tight considering the weakness of the assumptions we made to get them. Note that for an adaptive-symbol-rate modem operating with $R_{min} = R_{sopt}$, the maximum improvement is just 2.0. In fact, for any modulation scheme with this minimum symbol rate, we cannot exceed 2.0 improvement factor over fixed-rate.

Chapter 4 - Modulation Methods

In the preceding chapter, we investigated the performance of the fixed-rate modem and the adaptive-symbol-rate modem on the meteor-scatter channel. We assumed that both modems map information bits onto channel symbols (or waveforms) in the same manner, but we did not examine the details of this mapping, called *waveform modulation*. This chapter is concerned with the optimal use of waveform modulation for meteor-scatter communications.

We should now distinguish between *adaptive* modulation and *waveform* modulation. The function of the digital waveform modulator is to match the output of the encoder, which is digital, to the channel, which is analog. Adaptive modulation, on the other hand, uses one or more waveform modulation techniques to match the information rate to the time-varying signal-to-noise ratio (SNR) at the receiver. By definition, the adaptive-symbol-rate modem uses a single waveform modulation technique and varies the symbol rate to match the time-varying SNR. The author proposes a complementary scheme: fix the symbol rate and vary the number of bits per symbol. The author calls this adaptive scheme *adaptive QAM* since the scheme uses M-ary quadrature amplitude modulation (QAM). Adaptive QAM should be less difficult to implement than adaptive-symbol-rate, and on a bandwidth-limited channel, adaptive QAM will out-perform adaptive-symbol-rate.

The remainder of the chapter is divided into four sections:

- Section 4.1 is an introduction to two important families of waveform modulation: M-ary QAM and M-ary Frequency Shift Keying (FSK).

- Section 4.2 is dedicated to finding the optimal M-ary modulation technique for the fixed-rate modem.

- Section 4.3 is dedicated to finding the optimal M-ary modulation technique for the adaptive-symbol-rate modem.

- Section 4.4 investigates the performance and implementation of adaptive QAM.

4.1 M-ary Waveform Modulation Techniques. This section briefly summarizes the important properties of M-ary QAM and M-ary FSK, where $M = 2^k$, ($k = 1, 2, ...$). These two families are chosen because they have proven to be powerful modulation techniques for channels impaired by additive white Gaussian noise (AWGN). The key properties of each family are power efficiency and bandwidth efficiency. These two properties are defined below.

Definition 4.1. *Consider a M-ary modulation scheme operating on a AWGN channel with noise power spectral density N_0. Assume a user-defined specification on the maximum probability of bit error, P_b, and a minimum required energy per bit, E_b, to meet that specification. Define power efficiency as*

$$\varepsilon_P = (E_b/N_0)_{req} \tag{4.1}$$

In other words, power efficiency is the required SNR per bit to maintain reliable communication.

Definition 4.2. *Consider a M-ary modulation scheme operating at R bits/s and consuming a bandwidth W Hertz. Define the bandwidth efficiency by*

$$\varepsilon_B = \frac{R}{W} \tag{4.2}$$

Bandwidth efficiency has the units bits/second/Hertz (bits/s/Hz).

The *bandwidth expansion factor*, B_e, is defined as the reciprocal of the bandwidth efficiency. The following treatment of M-ary QAM and M-ary FSK is necessarily brief. For a complete description of these modulation schemes, see Blahut (1987) or Proakis (1983). A excellent treatment of M-ary QAM is also found in Noguchi et al. (1986).

4.1.1 M-ary QAM. Typical modulator and demodulator sections for a digital radio link are shown in Figure 4.1. The output of the modulator section is the sum of the outputs of two balanced modulators in phase quadrature, hence the name *quadrature amplitude modulation (QAM)*. The input to the digital-to-analog (D/A) converter is a sequence of binary digits (bits) traveling at a rate k/T bits/s, where $k = \log_2 M$. The D/A converter takes groups of k bits at a time and maps these k-bit symbols onto pairs of analog data values $\{a_n , b_n\}$. At the n^{th} signaling period, the value a_n is the input to the in-phase (I) channel and the value b_n is the input to the quadrature (Q) channel. Note that each signaling period has length T seconds and the channel symbol rate is $R_s = 1/T$ symbols/s (Hertz). Let p(t) be the pulse shape produced by the filtering of the low-pass filters. The modulator section output, s(t), can then be written as

$$s(t) = \left[\sum_n a_n \, p(t - nT) \cos \omega_0 t \right] - \left[\sum_n b_n \, p(t - nT) \sin \omega_0 t \right] \qquad (4.3)$$

where $\omega_0 = 2\pi f_c$ and f_c is the carrier frequency. The data value corresponding to the n^{th} signaling period can be represented by a complex number, $a_n + j\, b_n$. This data value is taken from a finite, discrete alphabet (or constellation) with M elements. The choice of alphabet determines the amplitude and phase characteristics of the resulting modulation scheme. For example, if $a_n = \cos \phi_n$ and $b_n = \sin \phi_n$, where $\phi_n \in \{0, 2\pi/M, 4\pi/M, \ldots, (M-1)2\pi/M\}$, then the modulation is M-ary PSK.

M–ary PSK has the desirable property that s(t) has constant amplitude. Certain constellations with multiple amplitudes and multiple phases have better power efficiency (lower $(E_b/N_0)_{req}$) than M-ary PSK, however, and these constellations are the popular choice for digital radio (Noguchi et al., 1986).

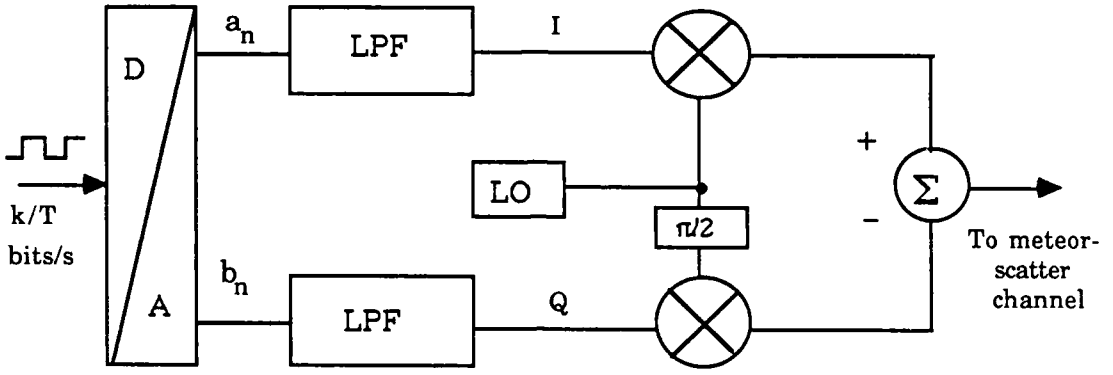

(a) Modulator section

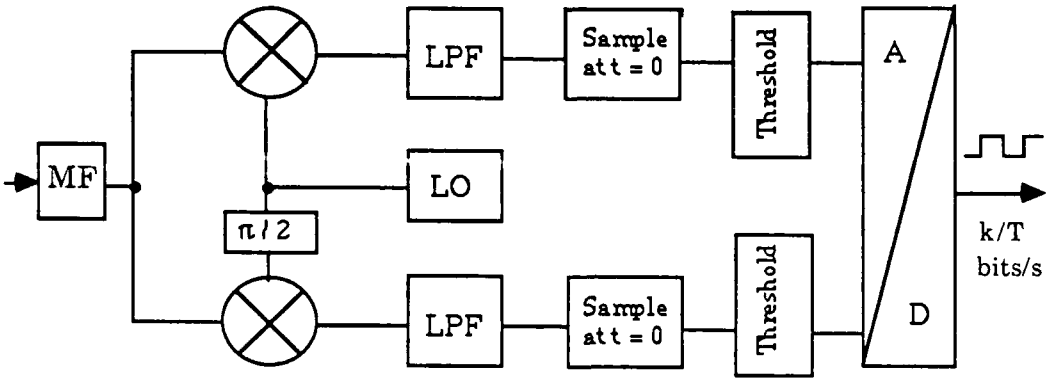

(b) Demodulator section

Figure 4.1 Modulator and demodulator sections for QAM modem

When M is a perfect square, the square constellations are usually preferred. When M is not a perfect square (i.e. k is odd), square constellations are not

possible and non-rectangular constellations often have better power efficiency. For our purposes, the rectangular constellations are preferred because these constellations lead to closed form approximations for the probability of bit error, P_b (Proakis, 1983). Examples of square and rectangular signal constellations for M = 4, 16, 32, and 64 are shown in Figure 4.2.[1] (The rectangular constellation for 8-ary QAM is purposely omitted from Figure 4.2 because it obscures the other constellations. The 8-ary QAM constellation is just one-half of the 16-ary constellation.)

Now consider the demodulator section of Figure 4.1. The received signal at the front end of the receiver is the transmitted signal, s(t), plus noise

$$r(t) = s(t) + n(t) \tag{4.5}$$

where n(t) is white Gaussian noise with noise power spectral density N_0. We wish to demodulate the signal r(t) such that the probability of correct demodulation is maximized. The optimal demodulation for M-ary QAM is *matched* filter demodulation (Blahut, 1987). The two main results from matched filter theory are the following:

- The impulse response of the matched filter is given by p*(-t) = the complex conjugate of pulse waveform evaluated at -t.

- The maximum signal-to-noise ratio at the output of the matched filter is given by

$$\frac{S}{N} = \frac{2E_p}{N_0} \tag{4.4}$$

where E_p = the energy of the pulse, p(t).

---

[1] In common usage, the QAM label is applied to those modulations for which M is a perfect square and the constellation is a square lattice. Our definition applies to all rectangular constellations.

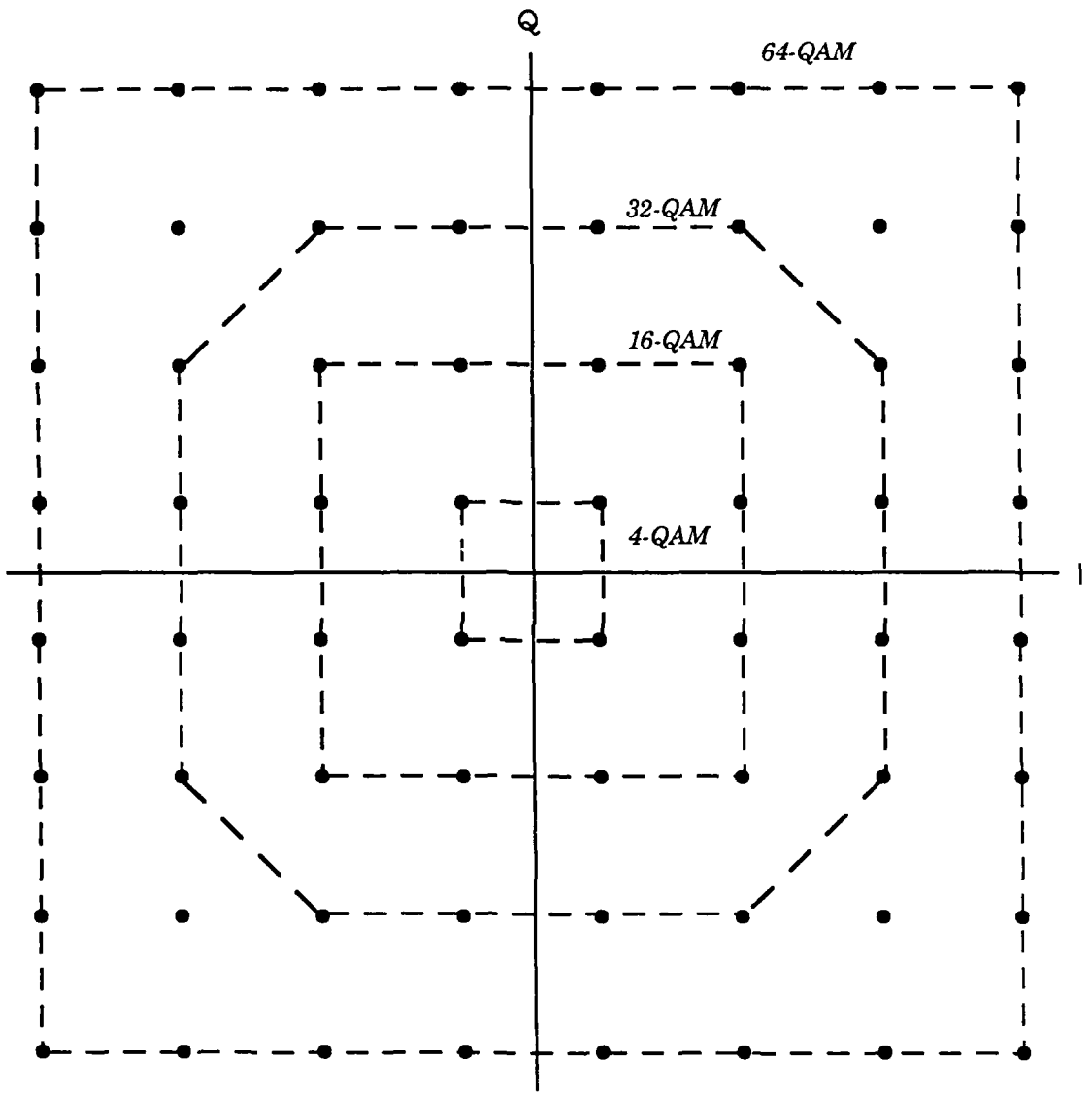

Figure 4.2 Rectangular signal constellations

Provided there are no timing errors at the sampler, the input signal to the threshold detector will achieve the SNR of (4.4). For a complete description of matched filter demodulation, the reader should consult Blahut (1987), Proakis (1983), or Haykin (1983). One can show that, in the presence of additive white Gaussian noise, the optimal decision at the threshold detector is to choose the constellation point that is nearest to the received point in terms of Euclidean distance (Blahut, 1987 and Proakis, 1983). This decision rule minimizes the probability of demodulation error and is the *maximum a posteriori probability* (MAP) rule. Thus, the threshold detectors on the I and Q channels of the demodulator choose the nearest allowed values for a_n and b_n . These values are the inputs to the analog-to-digital (A/D) converter, which performs the inverse mapping of the D/A converter of the modulator. Next, we examine the error performance of M-ary QAM by deriving an approximate expression for the probability of bit error, P_b.

The probability of symbol error for M-ary PSK can be approximated by the following expression for $M \geq 4$ (Michelson and Levesque, 1985):

$$P_M \cong \text{erfc}\left(\sqrt{\frac{E_s}{N_0}}\ \sin\frac{\pi}{M}\right) \tag{4.6}$$

where erfc(u) is the complementary error function, defined as [2]

$$\text{erfc}(u) = \frac{2}{\sqrt{\pi}} \int_u^\infty e^{-x^2}\, dx \tag{4.7}$$

---

[2] Error probabilities for coherent demodulation are often expressed in terms of the Q function, defined as

$$Q(y) = \frac{1}{\sqrt{2\pi}} \int_y^\infty e^{-\frac{x^2}{2}}\, dx$$

The Q function and the complementary error function are related by

$$\text{erfc}(u) = 2\, Q(\sqrt{2}u)$$

One can show that the average power for M-ary PSK must increase as $(M/\pi)^2$ in order to maintain the same error rate performance as M increases. On the other hand, for M-ary QAM (rectangular constellations), the power must increase as 2 (M - 1)/3 (Proakis, 1983). Therefore, the advantage of M-ary QAM over M-ary PSK is given by the ratio

$$D_m = \frac{3\,M^2}{2\,(M-1)\,\pi^2} \tag{4.8}$$

Table 4.1 lists this ratio in dB for several values of M.

Table 4.1 Improvement factor for M-ary QAM

M	$10 \log D_m$
8	1.43
16	4.14
32	7.01
64	9.95

We can combine (4.8) and (4.6) to get the following approximate expression for the probability of symbol error

$$P_M \equiv \text{erfc}\left(\sqrt{\frac{E_s}{N_0}\left(\frac{3\,M^2}{2\,(M-1)\,\pi^2}\right)\sin^2\frac{\pi}{M}}\right) \tag{4.9}$$

The equivalent bit error probability depends on the particular mapping of the k-bit symbols onto the signal constellation. The preferred mapping uses a *Gray code*. When a Gray code is used, adjacent points in the constellation differ by exactly one bit. The Gray code is used because, in the presence of additive noise, the most likely demodulation error is one that results a demodulated symbol that is adjacent to the correct symbol. If a Gray code is used, this type of symbol error will result in only one bit error.

Assuming that a Gray code is used and that all k-bit combinations are equally likely, then the equivalent bit error probability is given by

$$P_b = \frac{1}{k} P_M$$

where $k = \log_2 M$. Combining the above with (4.9) yields

$$P_b \cong \frac{1}{\log_2 M} \operatorname{erfc}\left(\sqrt{\frac{E_s}{N_0}\left(\frac{3\,M^2}{2\,(M-1)\,\pi^2}\right)\sin^2\frac{\pi}{M}}\right) \qquad (4.10)$$

In Figure 4.3, equation 4.10 is plotted as a function of E_b/N_0 for M = 4, 8, 16, 32, and 64. These curves agree closely with those published in Proakis (1983).

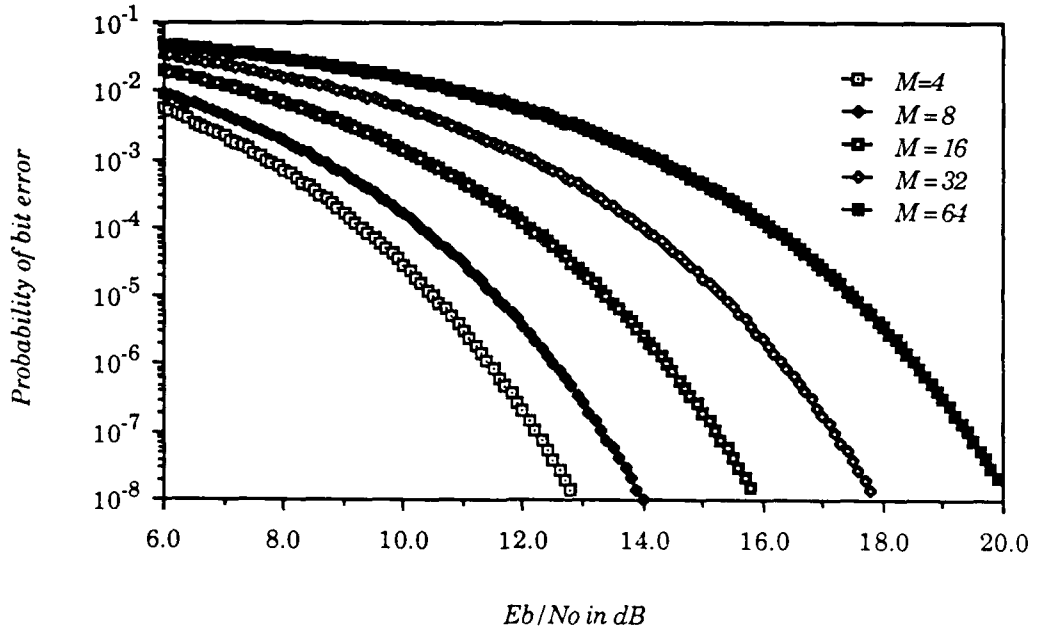

Figure 4.3 Probability of bit error for M-ary QAM with Gray coding

In later sections we shall compare modulation methods on the basis of power efficiency, $(E_b/N_0)_{req}$, and the values listed in Table 4.2 will prove useful. The data for Table 4.2 were computed using (4.10).

Table 4.2 $(E_b/N_0)_{req}$ in dB for several values of P_b for M-ary QAM

Modulation	$P_b = 10^{-3}$	$P_b = 10^{-4}$	$P_b = 10^{-5}$	$P_b = 10^{-6}$
4-QAM (QPSK)	6.6	8.4	9.6	10.5
8-QAM	8.7	10.4	11.6	12.6
16-QAM	10.3	12.1	13.4	14.3
32-QAM	12.3	14.1	15.4	16.4
64-QAM	14.4	16.2	17.6	18.6

The primary advantage of M-ary QAM over other modulation types is bandwidth efficiency. The bandwidth efficiency for M-ary QAM is determined by the spectral properties of the pulse, p(t). The maximum bandwidth efficiency is achieved when the Fourier transform of p(t), given by P(f), satisfies the following:

$$P(f) = \begin{cases} |P(f)|, & |f| \le \dfrac{1}{2T} \\ 0, & |f| > \dfrac{1}{2T} \end{cases} \tag{4.11}$$

One pulse that meets this requirement is the sinc pulse, given by

$$p(t) = \frac{\sin(\pi\, t/T)}{\pi\, t/T} \tag{4.12}$$

When such a pulse is used, the bandwidth efficiency achieves the maximum value, given by

$$\frac{R}{W} = \log_2 M \quad \text{bits/s/Hz} \tag{4.13}$$

Future discussion of M-ary QAM will assume a bandwidth efficiency given by (4.13).

4.1.2 M-ary FSK. Like the M-ary QAM modulator, the input to the D/A converter (or pulse generator) is a sequence of bits traveling at a rate k/T bits/s. Each signaling period has length T seconds, thus the channel symbol rate is $R_s = 1/T$ symbols/s. The D/A converter maps each k-bit symbol onto one of M complex *orthogonal* pulses, $p_i(t)$ (i = 0, 1, ... , M-1). Pulses $p_i(t)$ and $p_j(t)$ ($i \neq j$) are orthogonal if the following is true

$$\int_{-\infty}^{\infty} p_i(t)\ p_j^*(t)\, dt = 0$$

where * denotes complex conjugate. The real part of $p_i(t)$ is fed to the in-phase channel and the imaginary part is fed to the quadrature channel. Therefore, the output of the modulator section, s(t), for a single signaling period can be written as

$$s(t) = \mathrm{Re}[\, p_i(t)\,] \cos \omega_0 t - \mathrm{Im}[\, p_i(t)\,] \sin \omega_0 t \tag{4.14}$$

For demodulation, we have a choice of coherent demodulation or noncoherent demodulation. For coherent demodulation of M-ary FSK in AWGN, the probability of symbol error is given by (Michelson and Levesque, 1985)

$$P_M = \frac{1}{\sqrt{2\pi}} \int_{-\infty}^{\infty} \left\{ 1 - \left[1 - \frac{1}{2}\, \mathrm{erfc}\left(\frac{y}{\sqrt{2}} \right) \right]^{M-1} \right\} \exp\left[-\frac{1}{2}\left(y - \sqrt{2\, E/N_0} \right)^2 \right] dy \tag{4.15}$$

For noncoherent demodulation, the probability of symbol error is given by (Proakis, 1983)

$$P_M = \sum_{i=1}^{M-1} (-1)^{i+1} \binom{M-1}{i} \frac{1}{i+1} \exp\left[-\frac{E_s}{N_0} \left(\frac{i}{i+1} \right) \right] \tag{4.16}$$

The probability of symbol error for M-ary FSK can be converted to a bit-error probability by assuming that when a M-ary symbol is in error, each of the 2^k-1 incorrect k-bit patterns is equally likely. One can show that this assumption leads to the expression

$$P_b = \frac{2^{k-1}}{2^k - 1} P_M \tag{4.17}$$

Table 4.3 lists values of $(E_b/N_0)_{req}$ for coherent demodulation of M-ary FSK. Table 4.4 gives values of $(E_b/N_0)_{req}$ for the noncoherent case. The values for these tables were computed using equations 4.15, 4.16, and 4.17.

Table 4.3 $(E_b/N_0)_{req}$ in dB for M-ary FSK with coherent demodulation

Modulation	$P_b = 10^{-3}$	$P_b = 10^{-4}$	$P_b = 10^{-5}$	$P_b = 10^{-6}$
4-FSK	7.2	8.7	9.8	10.7
8-FSK	6.0	7.3	8.4	9.2
16-FSK	5.2	6.5	7.4	8.2
32-FSK	4.6	5.8	6.7	7.5
64-FSK	4.2	5.3	6.2	6.9

Curves of P_b versus E_b/N_0 are shown in Figure 4.4 for coherent demodulation of M-ary FSK. Curves of P_b versus E_b/N_0 are shown in Figure 4.5 for noncoherent demodulation of M-ary FSK.

Table 4.4 $(E_b/N_0)_{req}$ in dB for M-ary FSK and noncoherent demodulation

Modulation	$P_b = 10^{-3}$	$P_b = 10^{-4}$	$P_b = 10^{-5}$	$P_b = 10^{-6}$
4 FSK	8.3	9.6	10.6	11.4
8 FSK	7.0	8.2	9.2	9.9
16 FSK	6.2	7.3	8.2	8.9
32 FSK	5.5	6.6	7.4	8.1
64 FSK	4.9	5.8	6.8	7.5

A comparison of Figures 4.4 and 4.5 indicates that there is a penalty in power efficiency for noncoherent demodulation. Note also that in contrast to M-ary QAM, the curves for M-ary FSK shift to the left as M increases. In fact, for coherent M-ary FSK signaling, it can be shown that as $M \rightarrow \infty$, the channel capacity approaches the limit predicted by Shannon's capacity formula (Blahut, 1987).

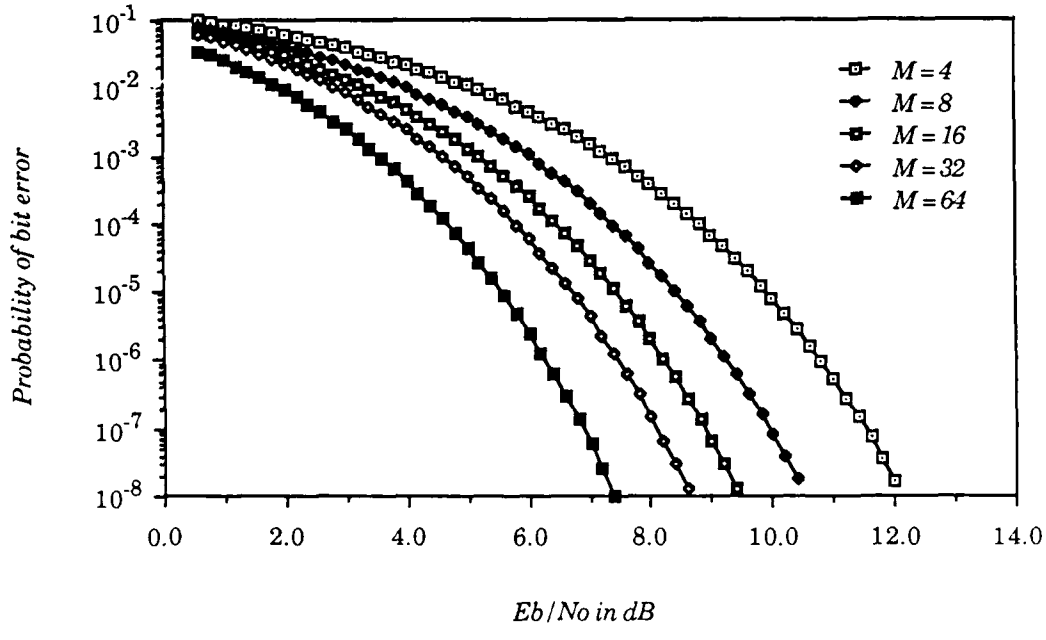

Figure 4.4 Probability of bit error for coherent demodulation of M-ary FSK signals

Unfortunately, the use of large FSK tone libraries has two serious drawbacks: (1) Coherent reception of a large number of orthogonal waveforms leads to a complex design and (2) Large tone libraries consume bandwidth. To see why (2) is true, consider the bandwidth efficiency of M-ary FSK.

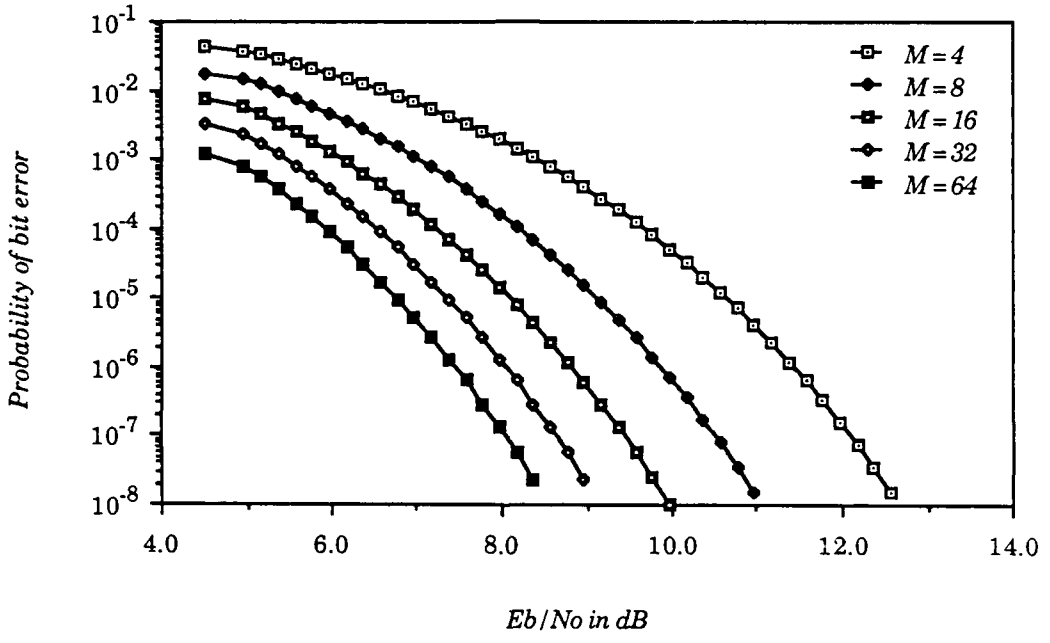

Figure 4.5 Probability of bit error for noncoherent demodulation of M-ary FSK signals

For M-ary FSK with tones spaced at 1/2T Hz, the overall required bandwidth is approximately M/2T, where T is the FSK pulse duration. The bit rate, R, is given by k/T where $k = \log_2 M$. Therefore, we see that the bandwidth efficiency is given by the following

$$\varepsilon_B = \frac{R}{W} = \frac{2 \log_2 M}{M} \tag{4.18}$$

Thus, as $M \rightarrow \infty$, the bandwidth required also goes to infinity.

From the previous discussion of M-ary QAM and M-ary FSK, we can conclude that M-ary QAM is optimal for strictly bandwidth-limited channels (unlimited power) and M-ary FSK is optimal for strictly power-limited channels (unlimited bandwidth). Because of the complexity of employing large sets of orthogonal waveforms, M-ary FSK for large M may be impractical even on channels with large bandwidths. On such channels, error-control coding can improve the power efficiency without adding the complexity of orthogonal waveforms.

The next two sections of this chapter are concerned with finding the optimal M-ary waveform modulation for the fixed-rate modem and the adaptive-symbol-rate modem. By optimal, we mean the waveform modulation that either maximizes the average bit rate, R_{bavg}, or minimizes the mean message waiting time, T_{avg}. In general, the modulation that is optimal in terms of average bit rate will not be optimal for mean waiting time. For our purposes, each modulation is completely specified by the following three parameters:

- Bits per channel symbol: $k = \log_2 M$
- Power efficiency: $\varepsilon_P = (E_b/N_0)_{req}$
- Bandwidth efficiency: $\varepsilon_B = R/W$

Noncoherent demodulation in itself has no direct effect on average bit rate or mean waiting time, but because of its widespread use in meteor-scatter communications, we shall investigate its performance also. In the discussion that follows, binary FSK and binary PSK have been purposely omitted for the following reasons: Binary FSK is always 3 dB less efficient in terms of power than BPSK (Blahut, 1987), so the only advantage of binary FSK

is noncoherent demodulation. If Gray coding is used, one can show that QPSK (4-QAM) has identical power efficiency to BPSK. Therefore, the only advantage of BPSK over QPSK is the absence of the quadrature channel and its potential crosstalk contribution.

4.2 Optimal Waveform Modulation For Fixed-Rate. Several factors govern the choice of modulation technique:

- Power efficiency
- Bandwidth efficiency
- Use of noncoherent demodulation
- Tolerance to impairments

The use of noncoherent demodulation is an important consideration on the meteor-scatter channel. Noncoherent demodulators are immune to phase errors, so acquisition of the signal is greatly simplified and acquisition time is shortened. Because acquisition time is typically a significant portion of burst duration, noncoherent demodulation is preferred. Impairments (other than noise) in digital communications are caused by the equipment and the channel. Impairments caused by equipment include linear distortion, nonlinear distortion, and synchronization errors. Those caused by the channel include interference, jamming, and multipath fading (Noguchi, et al., 1986). The factors of greatest interest to us are those that affect our two performance measures, R_{avg} and T_{avg}. These factors are power and bandwidth efficiency. Noncoherent demodulation will be a secondary consideration. The topic of tolerance to impairments is beyond the scope of this thesis.

Conventional meteor-scatter communication systems employ frequency shift keying (FSK) or binary phase shift keying (BPSK). The chief advantage of FSK is the option of noncoherent demodulation. BPSK is 3 dB better in terms

of power efficiency, but BPSK requires a coherent demodulator. Both are rather easy to implement, but there is no evidence that either technique is optimal in terms of our performance measures, R_{avg} and T_{avg}. In fact, the topic of the appropriate modulation technique for meteor-scatter is rarely discussed in the literature. Restricting the class of modulation techniques to M-ary QAM and M-ary FSK, we can find the optimal modulation technique for a given set of link parameters. In general, the optimal modulation technique will depend on which performance measure we are trying to optimize and the bandwidth constraints of the channel. Consider first the waveform modulation technique that maximizes the long run average bit rate, R_{bavg}, for a fixed-rate modem.

4.2.1 Maximizing long run average bit rate, R_{bavg}. Assume for the moment that the channel is unconstrained (unlimited bandwidth). We wish to maximize the average bit rate, R_{bavg} over the allowable waveform modulation methods: M-ary QAM and M-ary FSK. The expression for average symbol rate, R_{avg}, for the fixed-rate modem is derived in Appendix A and is given below ($q_0 << 10^{14}$ e/m)

$$R_{avg} \cong \lambda R_s t_c + \lambda R_s B q_0 \left[6.91 - \frac{2 R_s}{A 10^7} \right] \tag{4.19}$$

where $$A = \left[\frac{P_r(0)}{N_0 (E_s/N_0)_{req}} \right] \left[\frac{r_e \lambda_w^2}{\pi^2 e} \right]^{1/2}$$

$$q_0 = \sqrt{\frac{R_s N_0 (E_s/N_0)_{req}}{P_r(0,1)}}$$

$$\lambda = 0.1 \left[\frac{1.7 G_T G_R P_T}{R_s (E_s/N_0)_{req}} \right]^{1/2} \left(\frac{f}{37.5} \right)^{-2.4}$$

and all other terms are defined either in Chapter 2 or Appendix A. We can convert (4.19) into an expression for average bit rate by noting that the average bit rate is simply the product of number of bits per symbol and the average symbol rate

$$R_{bavg} = (\log_2 M)\ R_{avg} \tag{4.20}$$

Assuming a constant bit rate, R_b, for all modulation methods, we can attempt to maximize R_{bavg} as a function of M and $(E_b/N_0)_{req}$. We can write an expression for R_{bavg} in terms of these two parameters by noting that

$$R_s\,(E_s/N_0)_{req} = R_b\,(E_b/N_0)_{req}$$

Using this result leads to the following expression for average bit rate

$$R_{bavg} = C_1 \sqrt{\frac{R_b}{(E_b/N_0)_{req}}} + C_2\,R_b\left[6.91 - C_3\,R_b\,(E_b/N_0)_{req}\right] \tag{4.21}$$

where $$C_1 = 0.1\,[1.7\,G_T\,G_R\,P_T]^{0.5}\left(\frac{f}{37.5}\right)^{-2.4} t_c$$

$$C_2 = 0.1\left[\frac{1.7\,G_T\,G_R\,P_T\,N_0}{P_r(0,1)}\right]^{1/2} B$$

$$C_3 = \left[\frac{2 \times 10^{-7}\ N_0}{P_r\,(0)}\right]\left[\frac{\pi^2\,e}{r_e\,\lambda_w^2}\right]^{1/2}$$

Since (4.21) is a strictly decreasing function of $(E_b/N_0)_{req}$, the maximum is not attained and the optimal modulation is M-ary FSK, $M \to \infty$. This is the

expected result since we assumed the channel is strictly power-limited.

For a bandwidth-limited channel, we must consider the bandwidth efficiency, ε_B. Assuming a bandwidth limit of R_{max} (= maximum symbol rate), we can compute the maximum bit rate as

$$R_{bmax} = \varepsilon_B \; R_{max}$$

Values of maximum bit rate for R_{max} = 500 kHz are listed in Table 4.5 for M–ary QAM and M-ary FSK, M = 4, 8, 16, 32, and 64.

Table 4.5 Maximum Bit Rate for M-ary QAM and M-ary FSK

Modulation	ε_B	R_{bmax}
64-QAM	6	3.0 M b/s
32-QAM	5	2.5 M b/s
16-QAM	4	2.0 M b/s
8-QAM	3	1.5 M b/s
4-QAM	2	1.0 M b/s
4-FSK	1.0	500 k b/s
8-FSK	3/4	375 k b/s
16-FSK	1/2	250 k b/s
32-FSK	5/16	156 k b/s
64-FSK	3/16	93.8 k b/s

Now assume that each M-ary modulation scheme is operating at the maximum bit rate, given by Table 4.5. We wish to maximize (4.21) as a function of the allowed values of $(E_b/N_0)_{req}$, with $R_b = R_{bmax}$. The curve of Figure 4.6 demonstrates this behavior for a bit-error-rate of 10^{-4}.

From Figure 4.6 we see that 8-QAM is optimal, but there is negligible difference between 8-QAM and 4-QAM. In general, the optimal modulation is a function of transmitter power. The higher order M-ary QAM waveforms are favored for high transmitter power.

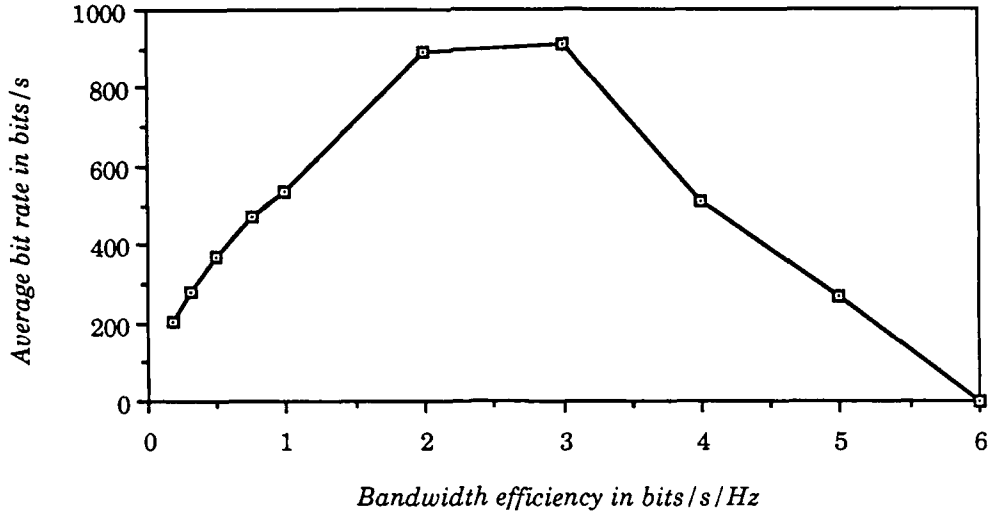

Figure 4.6 Average bit rate for M-ary modulation on fixed-rate modem

Since the overdense trail model is only an approximation, one may wish to find the optimal modulation assuming that all trails are underdense. The expression for R_{bavg} assuming all trails are underdense is given by the first term of (4.20)

$$R_{bavg} = C_1 \sqrt{\frac{R_b}{(E_b/N_0)_{req}}} \tag{4.22}$$

To maximize (4.22), we must simply maximize the square root of the bandwidth efficiency over the power efficiency

$$\sqrt{\frac{\varepsilon_B}{(E_b/N_0)_{req}}}$$

From Figure 4.7 we can see that 4-QAM (QPSK) is optimal for this case, independent of the link parameters. Next we want to consider minimizing

the mean message waiting time for the fixed-rate modem.

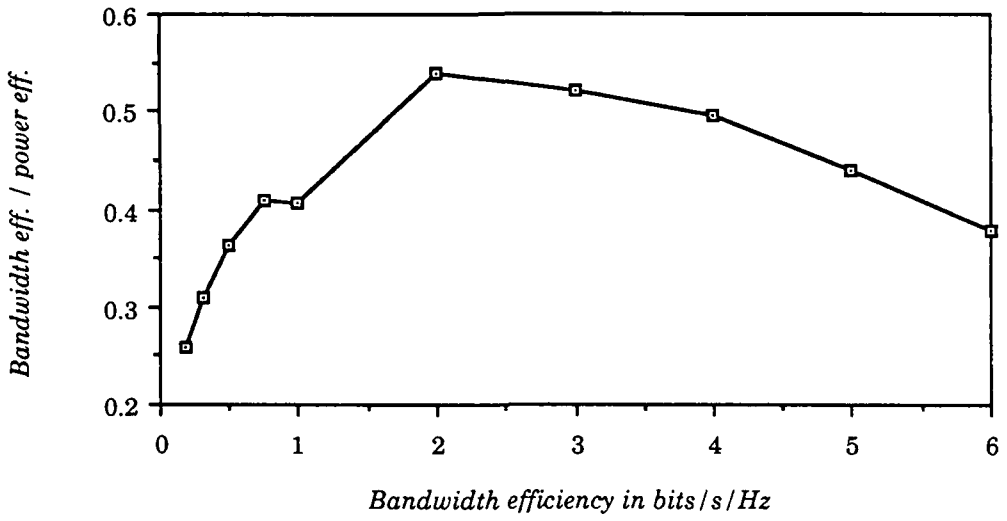

Figure 4.7 Bandwidth efficiency/power efficiency for $P_b = 10^{-4}$

4.2.2 Minimizing mean message waiting time, T_{avg}. Recall from Chapter 3 that the mean message waiting time for a fixed-rate modem is given by the following

$$E[T_w] = \frac{1}{\lambda} + \frac{N}{\lambda \tau R_s} \tag{4.23}$$

where N = the message length in symbols, τ = mean burst duration (= .58 s), and R_s is the symbol rate in Hz. It is easy to show that the following expression is equivalent to (4.23) where N is now in bits

$$E[T_w] = \frac{1}{\lambda} + \frac{N}{\lambda \tau R_b} \tag{4.24}$$

The optimal bit rate is then $R_{bopt} = N/\tau$ bits/s. Typical message lengths are on the order of 10,000 bits, so if we operate at or near the optimal bit rate we

will be operating considerably below the maximum symbol rate of the channel, except for M-ary FSK, with M very large.

The mean waiting time when operating at the optimal bit rate will be the same as that found in Chapter 3, i.e.

$$E\,[T_w]_{opt} = \frac{2}{\lambda} \tag{4.25}$$

From the previous section we know that (4.25) is a strictly increasing function of $(E_b/N_0)_{req}$. Therefore, the minimum is not attained and the optimal modulation is M-ary FSK, $M \rightarrow \infty$. This conclusion is not entirely valid because for very large M, the bandwidth may approach the bandwidth limit of 500 kHz. For example, consider a system operating at a bit rate of 5,000 bits per second. To approach the bandwidth limit, we would have to have a bandwidth expansion factor of 100. This value is not reached until M = 4096. It is highly unlikely that a system of this complexity would ever be implemented. To improve the power efficiency a system designer would incorporate some form of error-control coding. Thus, we conclude that the strictly power-limited channel model is quite good when message waiting time is the performance measure of interest.

4.3 Optimal Waveform Modulation for Adaptive-Symbol-Rate.

4.3.1 Maximizing long run average bit rate, R_{bavg}. The expression for average symbol rate for the adaptive-symbol-rate modem is derived in Appendix A and is found to be

$$R_{avg} = \lambda \frac{P_r\,(0,1)\,t_c\,q_0\,10^{14}}{2\,N_0\,(E_s/N_0)_{req}} + 3.06 \times 10^8\,\lambda\,A\,B\,q_0 \tag{4.26}$$

where all terms have been defined previously. Using the same arguments as in Subsection 4.2.1, we can convert (4.26) to the equivalent expression for average bit rate. This leads to the following

$$R_{bavg} = \frac{C_4 + C_5}{(E_b/N_0)_{req}} \tag{4.27}$$

where $$C_4 = 0.1\left[\frac{1.7\, G_T\, G_R\, P_T\, N_0}{P_r(0,1)}\right]^{1/2}\left(\frac{f}{37.5}\right)^{-2.4}\frac{P_r(0,1)\,\tau_c\,10^{14}}{2\,N_0}$$

$$C_5 = 3.06 \times 10^7\left[\frac{1.7\, G_T\, G_R\, P_T\, N_0}{P_r(0,1)}\right]^{1/2}\left(\frac{f}{37.5}\right)^{-2.4}\left[\frac{P_r(0)}{N_0}\right]\left[\frac{r_e\,\lambda_w^2}{\pi^2\, e}\right]^{1/2} B$$

Assume for the moment that the channel is strictly power-limited. Since (4.27) is a strictly decreasing function of $(E_b/N_0)_{req}$, then the optimal modulation is once again M-ary FSK, $M \to \infty$.

Now consider the bandwidth-limited case. The average bit rate is given by the following expression

$$R_{bavg} = \lambda \int_Q \int_0^{T(q)} R_b(t)\, f_Q(q)\, dt\, dq \tag{4.28}$$

where

$$R_b(t) = \begin{cases} \dfrac{P_r(t,q)}{N_0\,(E_b/N_0)_{req}}, & \dfrac{P_r(t,q)}{N_0\,(E_b/N_0)_{req}} \leq R_{bmax} \\ R_{bmax}, & \dfrac{P_r(t,q)}{N_0\,(E_b/N_0)_{req}} > R_{bmax} \end{cases}$$

and R_{bmax} is given by the values in Table 4.5. Figure 4.8 consists of a plot of (4.28) for a bit-error rate of 10^{-4}. The transmitter power is 2000 watts and all other link parameters are those of Chapter 2. The curve of Figure 4.8 indicates that the optimal modulation is 16-QAM, but the optimal modulation will in general be a function of the transmitter power. As the transmitter power increases, the percentage of time that the modem operates at $R_b(t) = R_{bmax}$ increases and the modulation with greater bandwidth efficiency is favored.

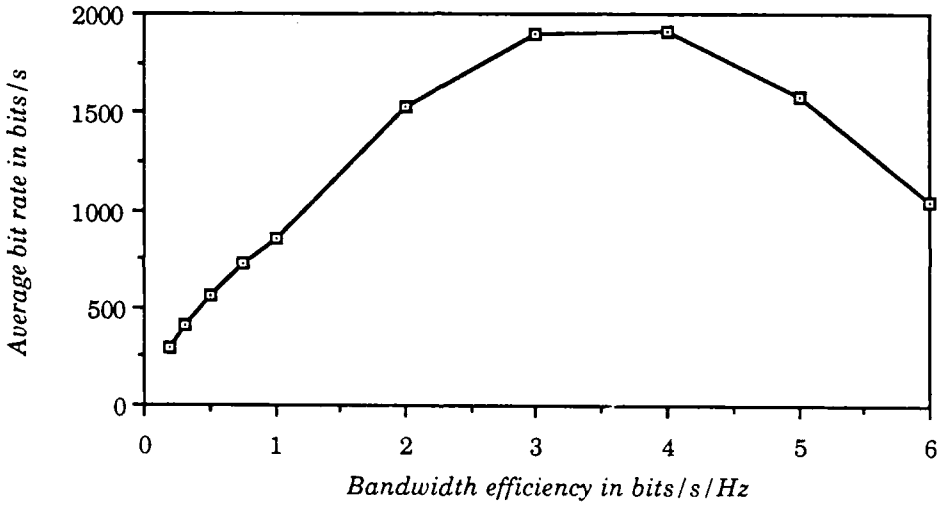

Figure 4.8 Average bit rate for M-ary modulation on adaptive-symbol-rate modem (P_T = 2 000 watts, BER = 10^{-4})

4.3.2 Minimizing mean message waiting time, T_{avg}. We do not have a closed form expression for the mean message waiting time for the adaptive-symbol-rate modem, but from equation 3.32 of Chapter 3 we know that the mean waiting time is directly proportional to the inverse of the meteor arrival rate. Therefore, we come to the same conclusion as for the fixed-rate modem: the optimal modulation is M-ary FSK with M large. This result supports the argument that error-control coding should be effective in

minimizing message waiting time. Coding can greatly improve power efficiency without the complexity of additional orthogonal waveforms.

4.4 Adaptive QAM. The discussion of adaptive techniques thus far has been restricted to the adaptive-symbol-rate modem. The adaptive-symbol-rate modem employing M-ary FSK (large M) uses the channel optimally, assuming that the channel is strictly power-limited. This assumption is valid for systems with low transmitter power levels, small antenna gains, or noisy receivers. On the other hand, systems with high transmitter power levels will encounter signal-to-noise ratios (SNR) that will support symbol rates exceeding the coherent bandwidth of the channel. For these systems, the adaptive-symbol-rate modem is not optimal. To see why, consider the plot of instantaneous symbol rate versus time found in Figure 4.9

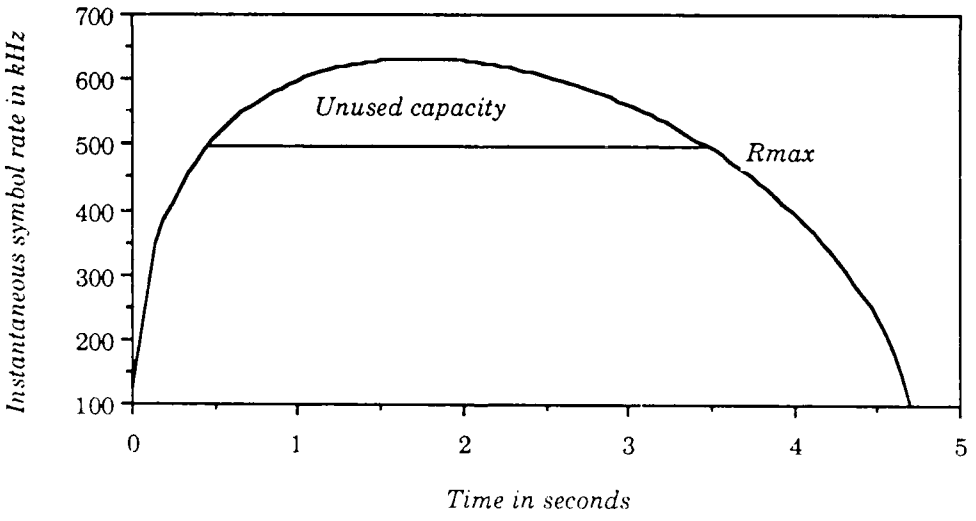

Figure 4.9 Instantaneous symbol rate R(t) for an overdense trail

When the SNR at the receiver exceeds the value corresponding to the maximum symbol rate, R_{max}, the adaptive-symbol-rate modem must operate at a fixed symbol rate *and* a fixed bit rate, R_{bmax}. (R_{max} and R_{bmax} are

related by bandwidth efficiency, see Table 4.5.) At these high received signal levels, the channel is being under-utilized, since the SNR indicates that the channel can support higher bit rates.

A better adaptive system is one that uses waveforms with high bandwidth efficiency when the SNR is high and waveforms with good power efficiency when the SNR is low. Thus, the ideal adaptive scheme on a bandwidth-limited channel would be one that operates at an adaptive (time-varying) symbol rate until such time that the SNR supports the maximum symbol rate, R_{max}. At this time, the symbol rate would stay constant at $R_s = R_{max}$ and we would employ a modulation technique with high bandwidth efficiency such as M-ary QAM. Such a hybrid system of part adaptive-symbol rate and part fixed-symbol rate would be difficult to analyze and to implement, but the author encourages further research in this direction. For the purpose of this thesis, we shall limit discussion to a fixed-symbol-rate system that adapts the bit rate to the time-varying SNR through the use of M-ary QAM waveform modulation. The author calls this adaptive scheme *adaptive QAM*.

The adaptive QAM scheme that we shall analyze employs the set of M-ary quadrature amplitude signal constellations of Figure 4.2. The reader will recall that these were the rectangular constellations for M = 4, 8, 16, 32, and 64. Larger constellations will not be used since their exclusion has little impact on performance for reasonable values of transmitter power. The operational concept for adaptive QAM is simple: operate at the highest value of M that the channel will support. Recall that the instantaneous symbol rate can be written as the following

$$R(t) = \frac{P_r(t, q)}{N_0 (E_s/N_0)_{req}} \tag{4.29}$$

For the following discussion, denote the power efficiency for M-ary QAM by

$(E_s/N_0)_M$, where $E_s = (\log_2 M)\, E_b$. Values of $(E_s/N_0)_M$ for M = 4, 8, 16, 32, and 64 are listed in Table 4.6.

Table 4.6 $(E_s/N_0)_{req}$ in dB for several values of P_b for M-ary QAM

Modulation	$P_b = 10^{-3}$	$P_b = 10^{-4}$	$P_b = 10^{-5}$	$P_b = 10^{-6}$
4-QAM (QPSK)	9.6	11.4	12.6	13.5
8-QAM	13.5	15.2	16.4	17.4
16-QAM	16.3	18.1	19.4	20.3
32-QAM	19.3	21.1	22.4	23.4
64-QAM	22.2	24.0	25.4	26.4

Realizing that the symbol rate is constant, we can rewrite (4.29) to get an expression for the signal-to-noise ratio per channel symbol as

$$(E_s/N_0) = \frac{P_r(t, q)}{N_0 R_s} \tag{4.30}$$

When the the right-hand side of (4.30) exceeds $(E_s/N_0)_M$, the modem changes modulation to M-ary QAM and operates at a bit rate of $(\log_2 M)R_s$ bits/s. Figure 4.10 demonstrates this operation graphically for an underdense trail with $q = 10^{13}$ e/m and a symbol rate of 1 kHz. Figure 4.11 demonstrates similar behavior for an overdense trail with $q = 10^{15}$ e/m and a symbol rate of 500 kHz. The operating thresholds of Figures 4.10 and 4.11 are those for a required maximum bit-error rate of 10^{-4} (see Table 4.6). Note that the underdense trail will not support 64-QAM and the overdense trail will support neither 32-QAM nor 64 QAM.

The adaptive QAM modem operates at or above a minimum SNR per bit to maintain reliable communications. Therefore, the *average* probability of bit error is always less than that given by $(E_s/N_0)_{req}$, and the subsequent performance predictions can be considered lower bounds on performance, rather than just estimates of performance.

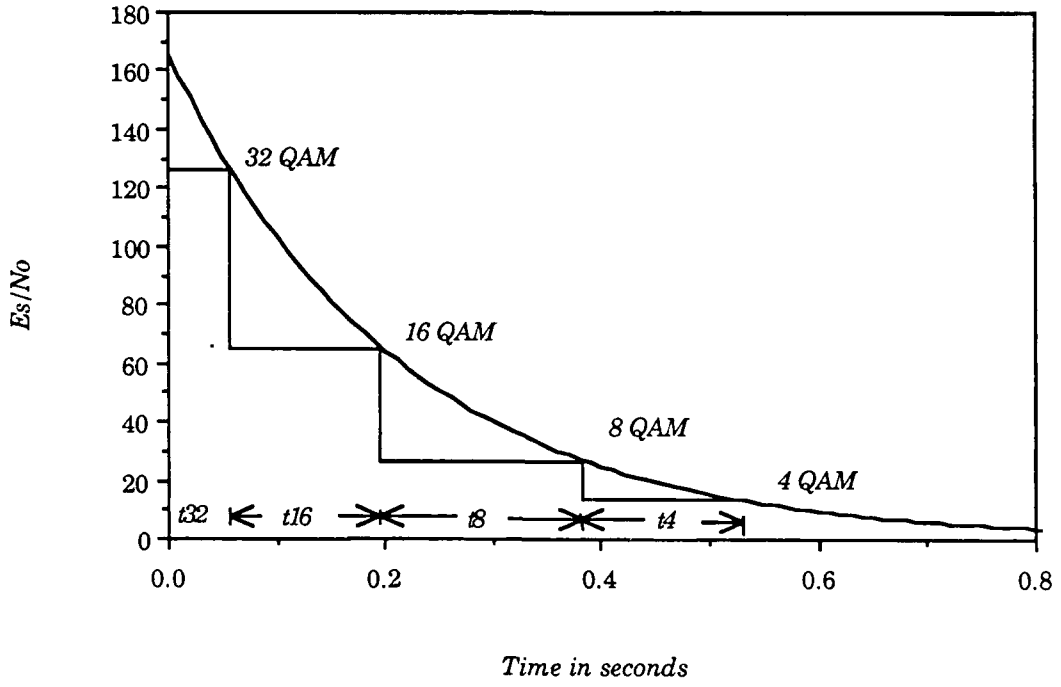

Figure 4.10 Operation of adaptive QAM on underdense trail
(P_T= 2000 watts, R_s = 1000 Hz, q = 10^{13} e/m)

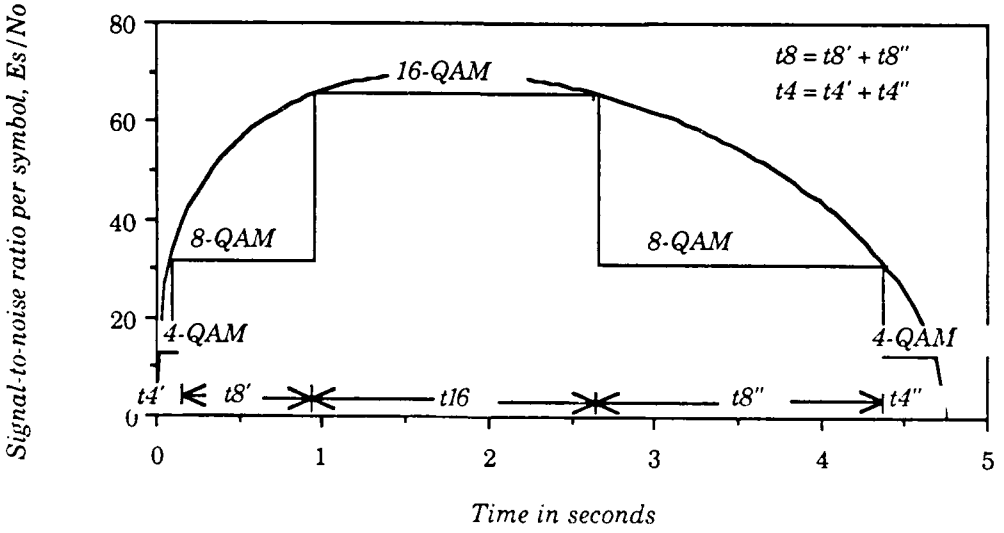

Figure 4.11 Operation of adaptive QAM on an overdense trail
(P_T = 2000 watts, R_s = 500 kHz, q = 10^{15} e/m)

On the surface, changing modulation with time may appear more complex than changing symbol rate, but in Subsections 4.4.4 and 4.4.5 we shall see that the adaptive QAM modem has definite advantages over adaptive-symbol-rate in implementation. One obvious advantage is that the adaptive QAM modem has only 5 information rates. In contrast, the theoretical adaptive-symbol-rate modem has an infinite number of information rates. We begin our investigation of the performance of adaptive QAM by examining the long run average bit rate.

4.4.1 Average bit rate, R_{bavg}. Let W(q) denote bits per meteor burst, a random variable and a function of electron line density, q. From Figures 4.10 and 4.11 we see that, in general, W(q) can be written as

$$W(q) = R_s\left[2\,t_4 + 3\,t_8 + 4\,t_{16} + 5\,t_{32} + 6\,t_{64}\right] \tag{4.31}$$

where t_M = the time that the modem operates at M-ary QAM for a given burst. Note that the total burst duration, T_d, is given by $T_d = t_4 + t_8 + t_{16} + t_{32} + t_{64}$. Since many trails will not support 64-QAM or even 32-QAM, we allow the possibility that $t_M = 0$ for some M.

The average bit rate can be written as

$$R_{bavg} = \int_Q W(q)\ f_Q(q)\, dq \tag{4.32}$$

where W(q) is given by (4.31). This expression is evaluated numerically with results tabulated in Table 4.7 for the link parameters of Chapter 2.

Comparing Tables 4.7 and 3.2, we see almost a three-fold improvement over adaptive-symbol-rate at R_s = 500 kHz.

Table 4.7 Average bit rate in bits/s for adaptive QAM, $P_T = 2000W$

R_S, kHz	underdense	overdense	total
1.0	11.1	5.0	16.1
5.0	20.3	24.6	44.9
10	24.9	48.7	73.6
50	32.9	221.8	254.7
100	31.8	402.5	254.7
500	12.0	1269	1281
1 000	1.0	1789	1790

The improvement factor for adaptive QAM over adaptive-symbol-rate is plotted in Figure 4.12 as a function of transmitter power. Note the improvement is significant, but is highly dependent on transmitter power for power levels below 3000 watts.

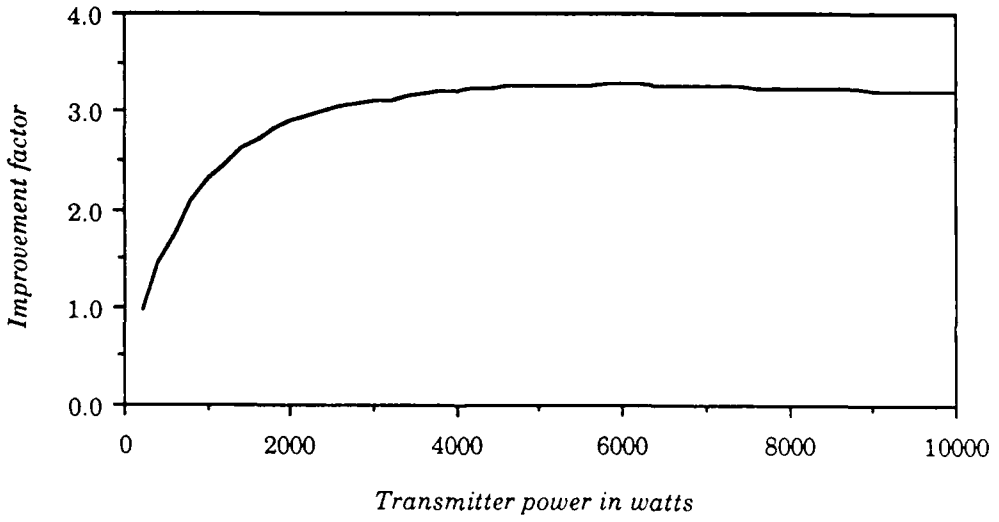

Figure 4.12 Improvement in average bit rate for adaptive QAM over adaptive-symbol-rate (R_{max} = 500 kHz)

4.4.2 Mean waiting time, T_{avg}. Recall from Section 3.2.3 of Chapter 3 that the Laplace transform of the mean waiting time is given by

$$\mathcal{L}\{ E[T_w] \} = \frac{1}{\lambda} \left[\frac{1}{s} + \frac{F(s)}{s\,[1 - F(s)]} \right] \tag{4.33}$$

where

$F(s)$ = the Laplace transform of the probability density function for the random variable W (= bits per meteor burst).

s = the argument of the Laplace transform with respect to N, the number of bits in the message to be transmitted. N is assumed known, not random.

λ = the meteor arrival rate (= rate of the Poisson process).

The first step in evaluating (4.33) for adaptive QAM is to derive an expression for the cumulative distribution function (CDF) for the number of bits per meteor burst, W. Denote the CDF for W by $F_W(x)$. The expression for $F_W(x)$ is derived in Appendix B and is given below

$$F_W(x) = 1 - K_{64} \exp\left\{ - \frac{x}{6R_s \tau} \right\}, \quad x \geq x_{64} \tag{4.34}$$

$$1 - K_{32} \exp\left\{ - \frac{x}{5R_s \tau} \right\}, \quad x_{32} \leq x < x_{64}$$

$$1 - K_{16} \exp\left\{ - \frac{x}{4R_s \tau} \right\}, \quad x_{16} \leq x < x_{32}$$

$$1 - K_8 \exp\left\{ - \frac{x}{3R_s \tau} \right\}, \quad x_8 \leq x < x_{16}$$

$$1 - \exp\left\{-\frac{x}{2R_s\tau}\right\}, \quad 0 \le x < x_8$$

where the constants K_M and x_M, M = 8, 16, 32, 64 are defined in Appendix B and τ (= t_c) is the mean burst duration in seconds. The function $F_W(x)$, given by (4.34), is plotted in Figure 4.13.

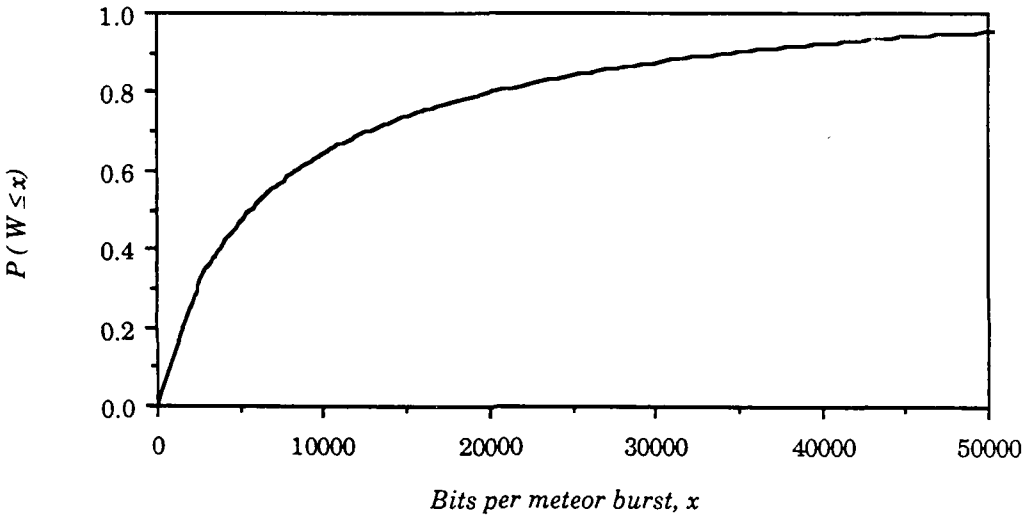

Figure 4.13 Cumulative distribution function for bits per burst, W, for adaptive QAM ($P_b = 10^{-4}$, R_s = 5900 Hz, τ = .58 s)

We can see from (4.34) that $F_W(x)$ is divided into 5 regions, each described by an exponential function with a different rate of decay. The CDF of (4.34) is continuous, but only piecewise differentiable. Therefore, the Laplace transform of the probability density function, denoted by F(s), will be quite intricate, involving polynomials and exponential functions of s. The corresponding expression for the Laplace transform of the mean waiting time, given by (4.33), is not tractable and possibly not invertible in closed form. To avoid this situation, we choose to approximate $F_W(x)$ by a sum of

three exponential functions with rates of decay given by the first, third and fifth terms of (4.34). A least-square linear approximation is derived in Appendix B and plotted in Figure 4.14.

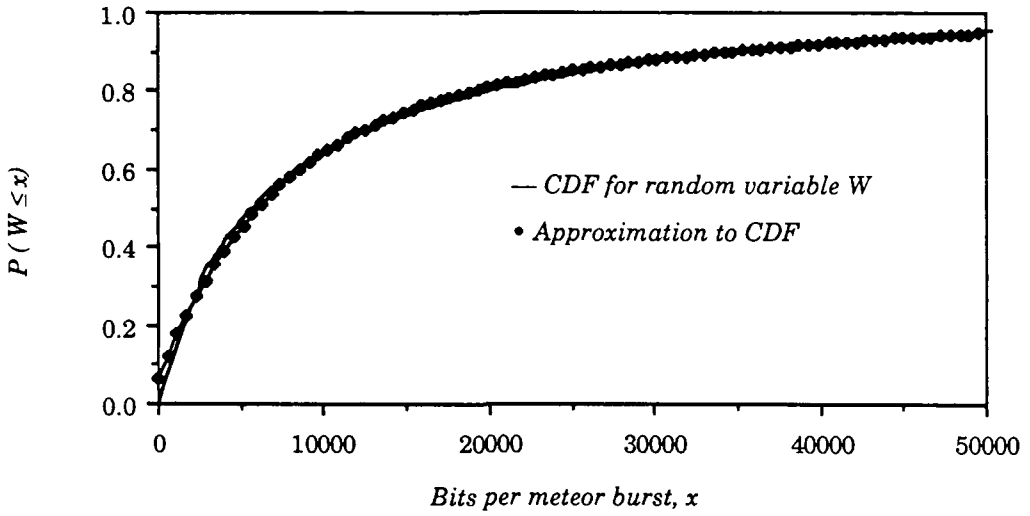

Figure 4.14 Approximate CDF for adaptive QAM
($P_b = 10^{-4}$, $R_s = 5900$ Hz, $\tau = .58$ s)

The approximate probability density function is just the first derivative of the approximate CDF and the Laplace transform of the approximate density (denoted by F(s)) is easily found for the sum of three exponential functions. When the Laplace transform of the density function is substituted into (4.33), we get the following expression

$$\mathcal{L}\{ E[T_w] \} = \frac{1}{\lambda}\left[\frac{A}{s^2} + \frac{B}{s} + \frac{Cs + D}{s^2 + d_2 s + d_1} \right] \qquad (4.35)$$

where A, B, C, D, d_2, and d_1 are constants defined in Appendix B. Consulting a table of Laplace transforms, (Fodor, 1965) the mean waiting time for $P_b = 10^{-4}$ is given by

$$E[T_w] \cong \frac{1}{\lambda}\left\{1.37 + \frac{N}{4.49\,R_s\,\tau} - \exp\left(-\frac{N}{3.64\,R_s\,\tau}\right)\right.$$
$$\left.\cdot\left[.37\cos\left(\frac{N}{7.40\,R_s\,\tau}\right) - .052\sin\left(\frac{N}{7.40\,R_s\,\tau}\right)\right]\right\} \quad (4.36)$$

where N is the message length in bits. For N = 10 000 bits and R_s = 3 000 Hz, the mean waiting time is 9.2 seconds.

Now that we have an approximate expression for the mean waiting time for the adaptive QAM modem, we should compare performance with the fixed-rate and the adaptive-symbol-rate modems.

We already have evidence that adaptive-symbol-rate outperforms adaptive QAM. For example, from Table 4.6 we see that to increase the bit rate by a factor of 3 (from QPSK to 64-QAM) the received power must increase by 12.6 dB ($P_b = 10^{-4}$). For adaptive-symbol rate, on the other hand, the instantaneous bit rate is directly proportional to received power and a three-fold increase in bit rate requires only a threefold (4.8 dB) increase in power. In the following discussion we shall present a more rigorous argument in favor of adaptive-symbol rate.

Recall that the CDF for W for the fixed-rate modem when operating with QPSK is given by the following

$$F_W(x) = 1 - \exp\left\{-\frac{x}{2\,R_s\,\tau}\right\}$$

The CDF for the adaptive-symbol-rate modem was found in Chapter 3 to be

$$F_W(x) = 1 - \frac{1}{\sqrt{\frac{2}{R_{min}\,\tau} + 1}}$$

where W is *symbols* per burst and R_{min} is the minimum symbol rate. When W is in bits and QPSK modulation is used, the CDF is given by

$$F_W(x) = 1 - \frac{1}{\sqrt{\frac{1}{R_{min}\,\tau} + 1}}$$

The cumulative distribution functions for these three modems are plotted in Figure 4.15 for $P_b = 10^{-4}$, $R_s = R_{min} = 5900$ Hz, and QPSK modulation.

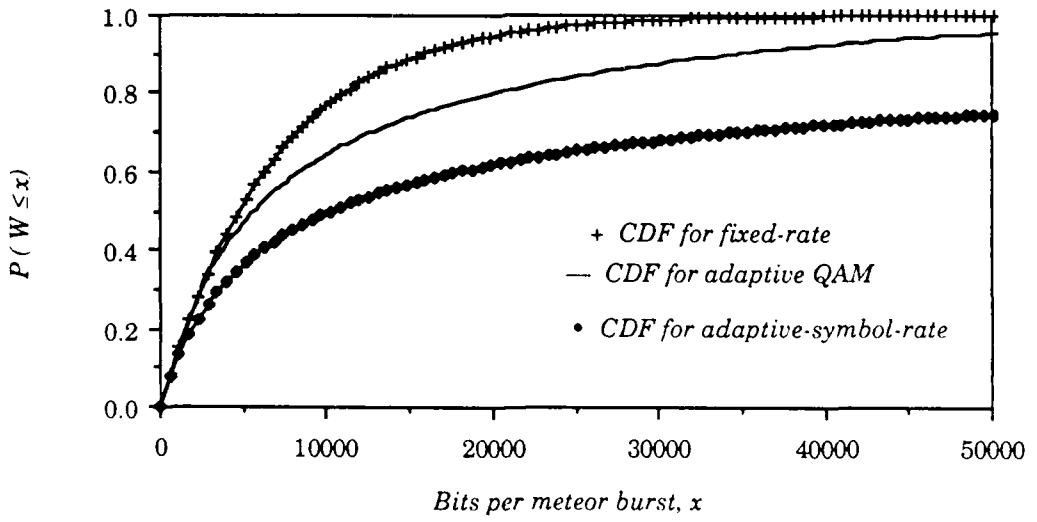

Figure 4.15 Cumulative distribution functions for three meteor-scatter modulation methods ($P_b = 10^{-4}$, $R_s = R_{min} = 5900$ Hz, and waveform modulation for fixed-rate and adaptive-symbol-rate = QPSK)

The most important feature of Figure 4.15 is that the CDF for adaptive-symbol rate is strictly less than the CDF of adaptive QAM for all values of x. Therefore, assuming that the symbol rate for adaptive QAM equals the minimum symbol rate for adaptive-symbol-rate (making the meteor arrival rate, λ, the same for both modems), the mean waiting time for adaptive-symbol rate will always be less than that for adaptive QAM.

The improvement factor for adaptive QAM over fixed-rate is defined as the ratio of the fixed-rate waiting time to the adaptive rate waiting time, i.e.

$$I = \frac{E[T_w]_{fixed}}{E[T_w]_{adaptive}}$$

From Chapter 3, we know that the optimal bit rate for the fixed-symbol-rate modem is given by N/τ and the mean waiting time when operating at this bit rate is given by

$$E[T_w] = \frac{2}{\lambda} \tag{4.37}$$

If we assume that the fixed-rate modem is operating with QPSK waveform modulation, then the optimal symbol rate is just $N/(2\tau)$. Furthermore, if the adaptive symbol rate modem operates at this same symbol rate, then the meteor arrival rate, λ, is the same for both modems and we can compute the improvement factor for adaptive QAM over fixed-rate as the ratio of (4.37) and (4.36), given by

$$E[T_w] \cong 2\left\{1.37 + \frac{N}{4.49\, R_s\, \tau} - \exp\left(-\frac{N}{3.64\, R_s\, \tau}\right) \cdot \left[.37 \cos\left(\frac{N}{7.40\, R_s\, \tau}\right) - .052 \sin\left(\frac{N}{7.40\, R_s\, \tau}\right)\right]\right\}^{-1} \tag{4.38}$$

Substituting in the value for symbol rate, $R_s = N/(2\tau)$, we get I = 1.205.

Although Equation 4.36 was derived assuming a bit-error rate of 10^{-4}, it is also an excellent approximation to mean waiting time for bit-error rates in the range $P_b = 10^{-3}$ to $P_b = 10^{-6}$, as noted in Appendix B. Further evidence to support this claim is given by the results of Table 4.8 where the improvement factor is computed for several values of bit-error rate. Note that the improvement factor is constant to two decimal places.

Table 4.8 Improvement in waiting time for adaptive QAM over fixed-rate

P_b	I
10^{-3}	1.203
10^{-4}	1.205
10^{-5}	1.202
10^{-6}	1.201

From Table 4.8, we see that the adaptive QAM modem offers a 20% improvement over the fixed-rate modem when operating at the optimal symbol rate for the fixed-rate modem. In Chapter 3, we derived a lower bound on improvement factor for adaptive-symbol-rate of 1.15. Since the adaptive-symbol-rate modem will always outperform adaptive QAM, we now have the following new, tighter bounds on the improvement factor for the adaptive-symbol-rate modem

$$1.2 \leq I \leq 2.0$$

To this point we have compared mean waiting time for the special case where both the adaptive QAM modem and the fixed-rate modem are operating at the same symbol rate. In Appendix B it is shown that the optimal symbol rate for adaptive QAM is approximately 0.3 (N) Hz where N is

the message length in bits. When both modems are operating at their respective optimal symbol rates, the improvement factor increases to 1.283, or 28.3%

When the message lengths are long compared to the symbol rate, the improvement factor increases as shown in Figure 4.16.

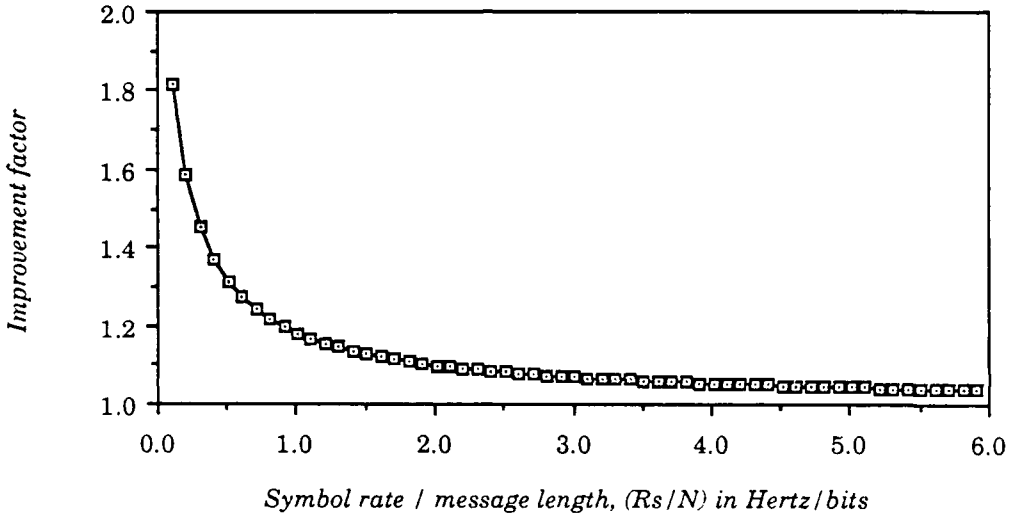

Figure 4.16 Improvement in mean waiting time for adaptive QAM

For very long messages, Figure 4.16 indicates that improvements on the order of 2.0 are expected (e.g. for $R_s/N = 0.1$, improvement factor is 1.81).

4.4.3 Optimal symbol rate. Figure 4.17 illustrates the behavior of average bit rate as a function of instantaneous symbol rate for adaptive QAM. As in the case of the fixed-rate modem, the optimal symbol rate appears to exceed the bandwidth limit of the channel. However, the optimal symbol rate is now approximately 3.5 MHz rather than 10 Mhz, so it is quite possible that for transmitter power levels below 2000 watts, the optimal symbol rate may be less than R_{max} = 500 kHz. In this case, the system designer should attempt

to operate at the optimal symbol rate rather than the maximum rate.

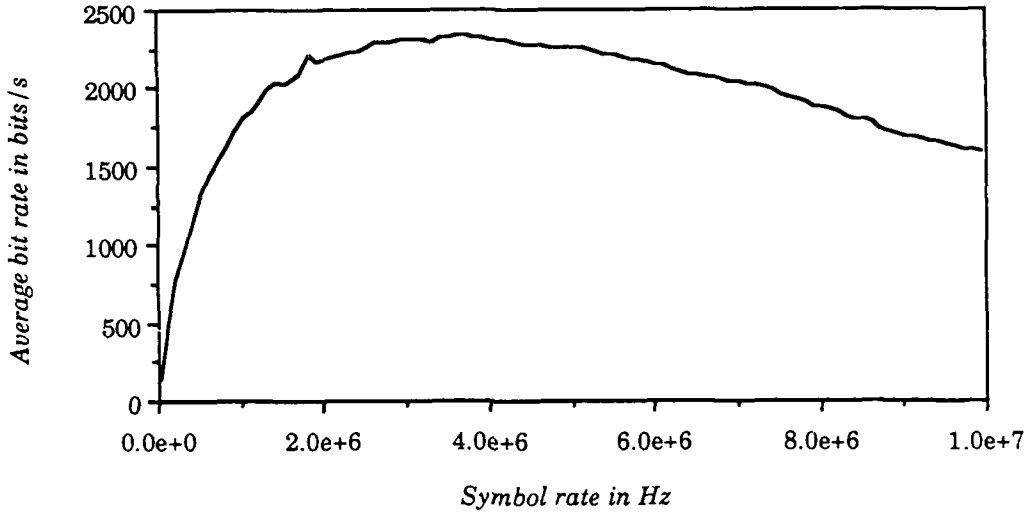

Figure 4.17 Average bit rate as a function of symbol rate for adaptive QAM

The symbol rate that minimizes the mean waiting time for adaptive QAM is approximated in Appendix B as $R_{sopt} \sim 0.3$ (N) Hz, where N is the length of the message in bits.

4.4.4 Signal constellation. To this point we have assumed idealized performance for adaptive QAM. Now we attempt to design an adaptive modem whose performance comes as close as possible to that of the idealized case.

The traditional quadrature amplitude modem of Figure 4.1 incorporates threshold detectors on the in-phase (I) and quadrature (Q) channels of the demodulator. These threshold detectors map the received data values $a_n' + jb_n'$ to the nearest (in terms of Euclidean distance) allowable data value, where the allowable values come from a set of order M. One possible realization of adaptive QAM would involve a demodulator with five threshold

detectors. The correct threshold detector would be chosen based on an estimate of the time-varying SNR at the receiver. Such an implementation is not cost efficient, however. The threshold detector is an analog device and modern-day analog devices tend to be more expensive than digital devices. For this reason, we choose to realize the adaptive information rate at the digital level of the modem and use a single threshold detector on each channel.

This type of design requires that the mapping of information bits to analog values, $a_n + jb_n$ be done in a manner that minimizes the complexity of the threshold detector and insures that demodulation errors result in the minimum possible number of bit errors. Such a mapping is the topic of this section.

An efficient signal constellation for adaptive QAM should accomplish the following:

- Incorporate decision regions identical to those for non-adaptive QAM, thus the symbol-error performance is unchanged.
- Minimize the number of distinct constellation points to reduce threshold detector complexity.
- Incorporate a Gray code, to minimize the probability of bit error.
- Place constellation points such that the average transmitted power is the same for all values of M.

Attempting to meet all four of the above requirements involves compromise

as seen by the signal constellation of Figure 4.18. This signal constellation holds 120 points; only four constellation points are co-located (4+8+16+32+64 = 124). One could design a constellation with fewer points, but incorporating fewer points makes it difficult to equalize average transmitted power and maintain the original decision regions.

The rectangular constellation for 8-ary QAM was abandoned in favor of one with better power efficiency.

The average power transmitted into a 1 ohm load for this constellation is given in Table 4.9.

Table 4.9 Average transmitted power in watts for adaptive QAM constellation

M	Average power
4	10.6
8	10.5
16	10.2
32	9.8
64	10.5

The signal constellation of Figure 4.18 incorporates 20 distinct amplitudes on the in-phase channel and 19 distinct amplitudes on the quadrature channel. Therefore, a digital-to-analog (D/A) converter should only require 5 bits to represent these amplitudes. It may be impossible to incorporate a Gray code with only 5 bits per channel, however, so the author suggests that 6-bit or higher D/A converters be used.

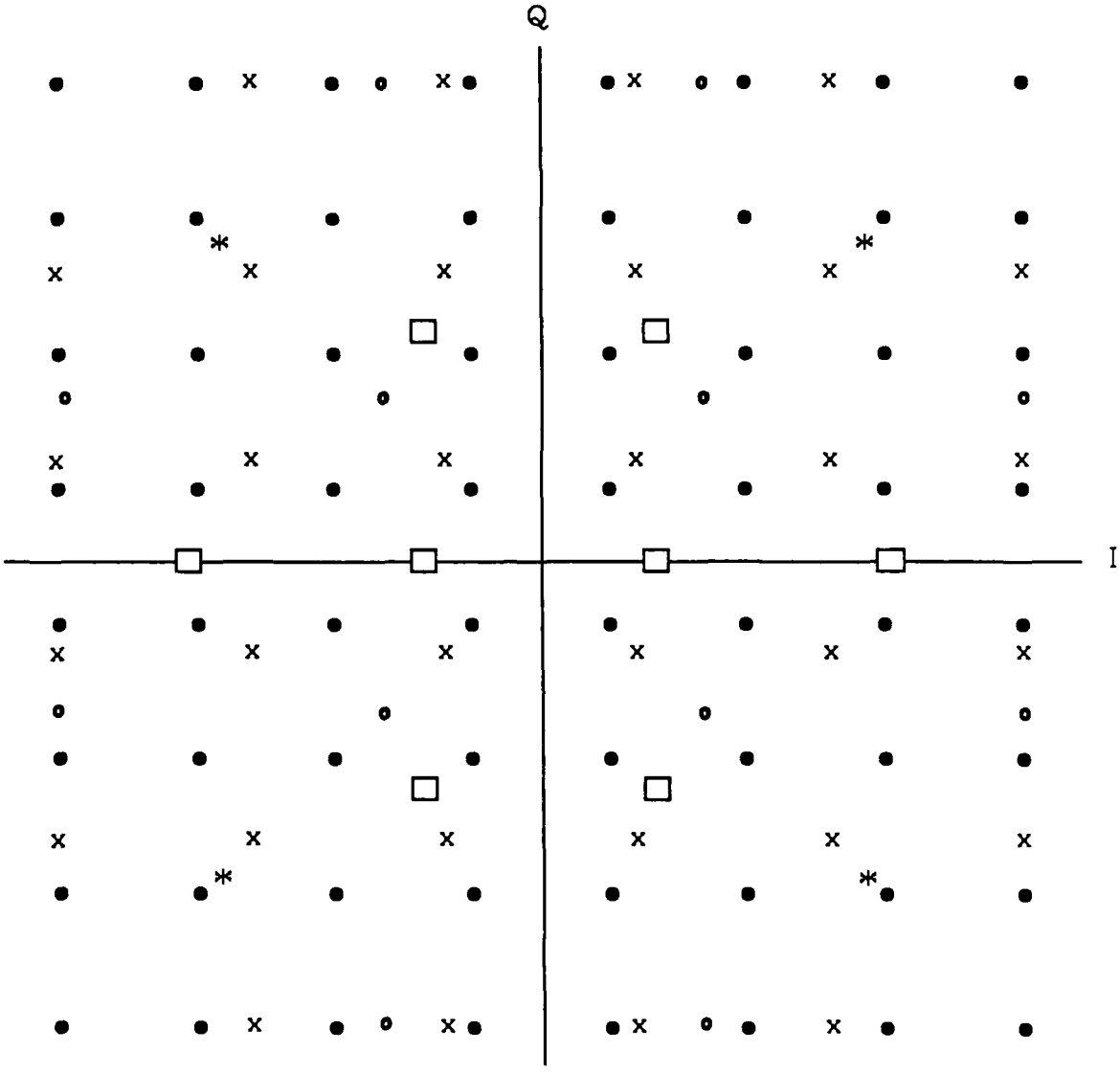

Legend

QPSK *
8-QAM □
16-QAM o
32-QAM x
64-QAM •
1 cm = 1 volt

Number of voltage levels on I axis = 20

Number of voltage levels on Q axis = 19

4 corners of 16-QAM are colocated with 64-QAM

Figure 4.18 Signal constellation for adaptive QAM

4.4.5 Modem block diagram. A modem block diagram is shown in Figure 4.19 that implements the design discussed thus far. A brief description of the operation of this modem follows. We assume a noiseless feedback path with zero delay is present.

The input to the modulator section (see Figure 4.19) is a stream of information bits traveling at some predetermined rate not to exceed the capacity of the data buffer. When a meteor trail of proper intensity and orientation is present, the receiver sends to the transmitter a message requesting information. This message includes the value of M (M = 4, 8, 16, 32, or 64) which is determined by an estimate of the signal-to-noise ratio, E_s/N_0. The data buffer sends $k=\log_2 M$ bits to the look-up-table encoder. The encoder takes the two inputs, (value of M and the k information bits) and maps them onto two 6-bit words (one for each channel of the modulator). This word length is chosen because we require at least 6 bits per channel to represent each of the constellation points with a Gray code. The digital-to-analog (D/A) converters map the 6-bit words onto 120 distinct constellation points in such a way that the probability of bit error at the receiver is minimized. The analog values, a_n and b_n from the I and Q channels, respectively, are quadrature modulated and transmitted over the channel.

At the receiver, the signal-to-noise ratio is estimated and an estimate of M is sent to three locations: the transmitter, the look-up-table decoder, and the rate changer. The received signal is demodulated and sent to the threshold detectors of the I and Q channels. The threshold detectors choose the nearest allowed values a_n' and b_n'. These values are sent to the look-up-table decoder where the inverse mapping of the encoder is performed. The output of the decoder is a k-bit word that is sent to the rate changer, which serves as a buffer.

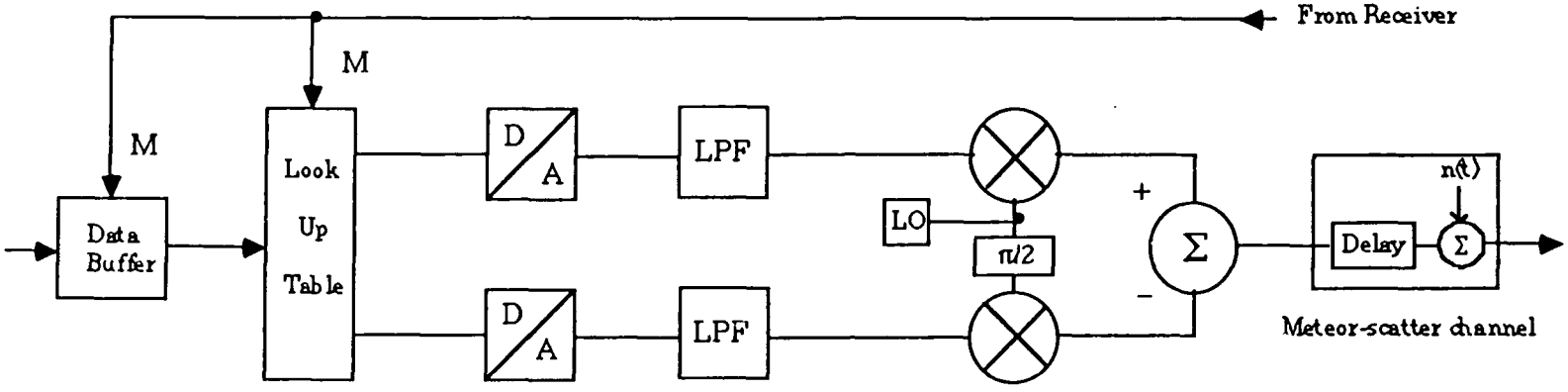

(a) Modulator section

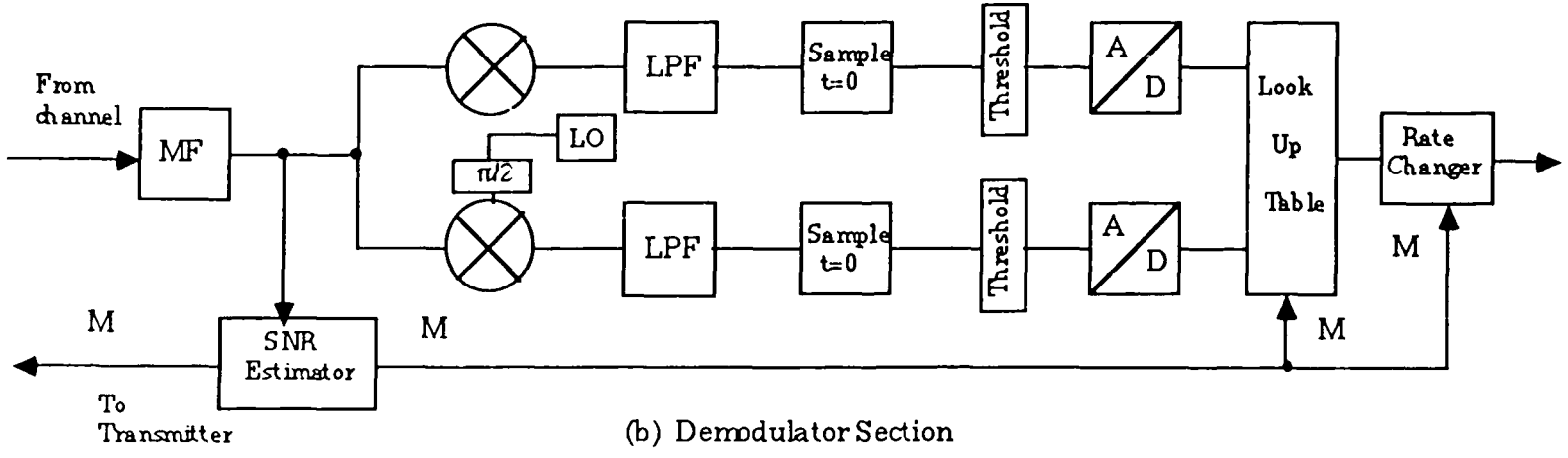

(b) Demodulator Section

Figure 4.19 Block diagram for adaptive QAM modem

Since the output of the encoder and the input to the decoder are always 6-bit words, regardless of the value of M, the modem operates at a fixed symbol rate, R_s, *and* a fixed bit rate. The information rate varies at the data buffer and the rate changer. Since all other components of the system operate at a fixed symbol rate and a fixed bit rate, synchronization and timing problems are minimized once the initial synchronization and timing are achieved. This feature of the modem, plus the fact that it requires only 5 information rates, makes this implementation of adaptive QAM quite feasible.

Chapter 5 - Error-Control Coding

In this chapter, we investigate the optimal use of Reed-Solomon (RS) codes on the meteor-scatter channel. These codes are examined on the basis of forward-error-correction (FEC) of random errors on an AWGN meteor-scatter channel. The burst characteristics of the channel make it possible to optimize coded performance in terms of an optimal code rate. A lower bound on optimal code rate for RS codes will be derived. Performance of the coded system will be investigated in terms of improvement in average bit rate, R_{bavg}, or mean waiting time, T_{avg}. Coded performance will be estimated for the three types of modems discussed thus far, namely fixed-rate, adaptive-symbol-rate, and adaptive QAM. Some familiarity with the theory of error-control coding is assumed. Excellent background information on this subject is found in the texts by Blahut (1983), and Lin and Costello (1983). The performance of Reed-Solomon codes is also treated in Berlekamp et al. (1987).

The topic of error-control coding for meteor-scatter communication has received some attention, yet much work remains to be done. The COMET system of the 1960's employed a crude form of error control called automatic-repeat-request (ARQ). Recent published research includes the work of Hampton (1985) and Milstein et al. (1987). Hampton's work includes the effect of the time-varying signal-to-noise ratio on the performance of a hybrid (ARQ and FEC) coding scheme. Milstein et al. produced an excellent paper on the performance of two packet communication protocols with RS codes for error correction. One rather obscure, but noteworthy, treatment of adaptive coding is the work of Rediske (1982). Rediske designed a coding scheme employing rate 1/N convolutional codes for use on Weitzen's adaptive modem. This work demonstrates that adaptive information rate can be achieved through error-correction coding rather than through adaptive

symbol rate or adaptive waveform modulation. Adaptive coding for meteor-scatter is one area that deserves more attention, as noted by Milstein et al. This chapter is concerned with traditional (not adaptive) coding techniques for meteor-scatter communications.

In many respects, this chapter is an extension of the work of Milstein et al. for non-packet communications and adaptive modulation (Milstein et al. considered only the fixed-rate modem). This author believes that the non-packet case is more general since the corresponding results apply to a wider class of communication systems.

Before examining the performance of RS codes, a brief introduction to their properties is in order.

5.1 Properties of Reed-Solomon Codes. Reed-Solomon codes are examples of non-binary linear block codes. Consider a message sequence of k symbols taken from a finite field, GF(q). A linear block code maps these k information symbols onto a codeword of n symbols such that the q^k codewords form a vector space over GF(q). For Reed-Solomon codes, q is almost always a power of 2 and the block length is normally $2^m - 1$. Reed-Solomon codes achieve the Singleton bound, meaning that the minimum distance $d_{min} = r + 1$, where r is the number of parity symbols ($r = n - k$). Codes that achieve the Singleton bound are called maximum-distance-separable (MDS) codes.

Codes with minimum distance, $d_{min} = 2t + 1$ can correct all patterns of t or fewer errors in any received n-tuple. Define the code rate, R, as $R = k/n$. Then the error-correcting capability of MDS codes can be written in terms of block length and code rate as

$$t = \frac{n - k}{2} = \frac{n(1 - R)}{2} \tag{5.1}$$

Reed-Solomon codes are good choices for meteor-scatter for the following reasons:

- Reed-Solomon codes are proven performers on AWGN channels.
- Since RS codes are MDS, they are efficient users of parity symbols and thus they are effective on channels that penalize increases in bit rate.
- Reed-Solomon codes can combat burst errors. On the meteor-scatter channel, burst errors would most likely occur in the presence of multipath fading, burst termination, interference, or jamming.
- RS codes are not perfect codes, so many n-tuples lie outside the ball of radius t that surrounds each codeword. Therefore, RS codes have a very low misdecode rate, meaning that the decoder will almost always recognize that such a received n-tuple cannot be properly decoded and flag it. Of course, some form of ARQ must be used to fully exploit this property. The error-rate of data that is both undecodable and not recognized as such is typically 5 orders of magnitude below the overall BER (Berlekamp et al., 1987).

A good error-control code will reduce the E_b/N_0 required to achieve reliable communication. The amount of this reduction is the traditional figure of merit for a coding scheme, called the *coding gain*, G_c. The usual method of determining coding gain is to plot the probability of bit error versus E_b/N_0 for the coded and the uncoded systems and read the difference at a specified error rate. For example, consider the plot of bit-error-rate for a (31,23) RS code with 32-ary FSK modulation found in Figure 5.1. In this case, the

coding gain is given by the difference in power efficiency (expressed in dB) for the coded and the uncoded systems. For a BER of 10^{-4}, the coding gain is found from figure 5.1 to be about 1.7 dB.

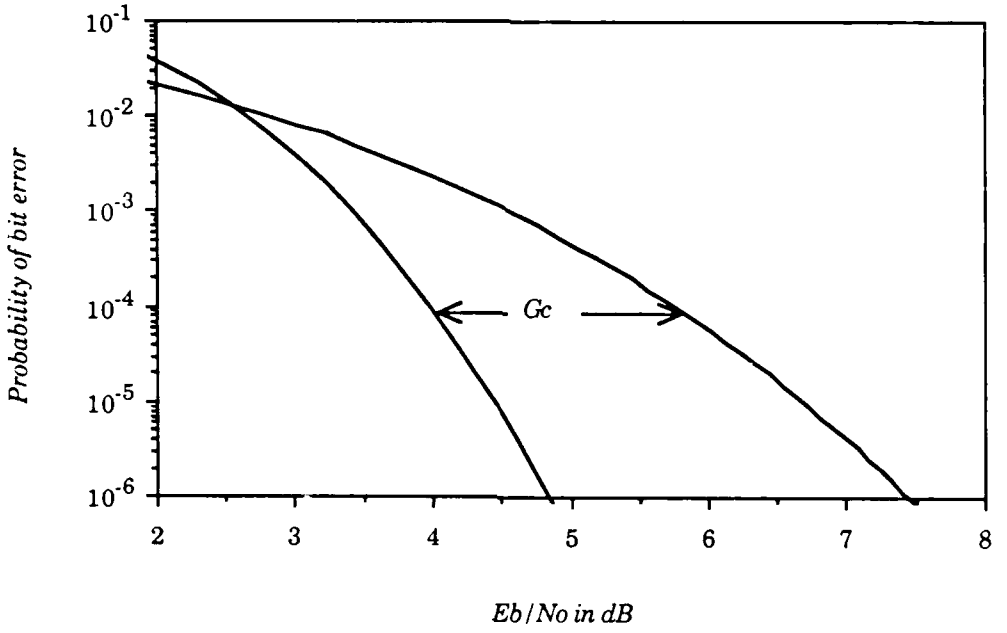

Figure 5.1 Coding gain for a (31, 23) Reed-Solomon code with 32-FSK modulation

The coding gain gives a measure of how much we can reduce transmitter power and maintain the same error performance. Thus, error-control can drive down hardware costs by allowing the use of less powerful (and less expensive) transmitter amplifiers.

5.2 Figure of Merit. Recall that our two performance measures are long run average bit rate, R_{bavg}, and mean message waiting time, T_{avg}. The figure of merit for a given coding scheme should reflect the improvement (if any) in either R_{bavg} or T_{avg}. The meteor-scatter channel exhibits the important property that even when the channel is modeled as strictly power-limited,

there is still a penalty for operating at a higher bit rate. This penalty is a decrease in the number of observed meteor trails per second, λ. In the discussion that follows, we shall attempt to derive appropriate figures of merit for a coding scheme on the meteor-scatter channel. The figure of merit will be a function of the code rate, R, and the coding gain, G_c. Consider first the figure of merit for R_{bavg}.

5.2.1 Figure of Merit for R_{bavg}. From Chapters 3 and 4 we know that the expression for R_{bavg} for the adaptive-symbol-rate modem is proportional to the inverse of $(E_b/N_0)_{req.}$ For a coded system, the instantaneous *information* bit rate, $R_I(t)$, is decreased in direct proportion to the code rate. A similar argument holds for adaptive QAM. Therefore, the figure of merit for a coded system with either adaptive modulation scheme should be the following

$$G_f = R\,G_c \tag{5.2}$$

For the fixed-rate modem, we can simplify matters by assuming that all trails are underdense. Making this assumption, the average bit rate is given by Equation 4.22 and the figure of merit is simply the square root of (5.2), i.e.

$$G_f = \sqrt{R\,G_c} \tag{5.3}$$

Note from Equations 5.2 and 5.3 that the same code will give a greater improvement in average bit rate for the adaptive modem than for the fixed-rate modem.

5.2.2 Figure of merit for T_{avg}. The mean waiting time for the fixed-rate modem operating at the optimal bit rate was found in chapter 3 to be $2/\lambda$ or equivalently

$$E\,[T_w]_{opt} = 20\sqrt{\frac{N(E_b/N_0)_{req}}{1.7\,G_R\,G_T\,P_T\,\tau}}\left(\frac{f}{37.5}\right)^{2.4} \qquad (5.4)$$

where all terms have been defined previously and the optimal bit rate is $R_b = N/\tau$. Now N denotes the *total* number of bits, i.e. information bits + parity bits. Since we wish to minimize the waiting time, we can see from (5.4) that the figure of merit should be simply

$$G_f = \sqrt{R\,G_c}$$

which is identical to (5.3). The adaptive-symbol-rate modem has mean waiting time proportional to $1/\lambda$, so we get the identical result. We assume the same for adaptive QAM, but we shall not prove it.

Summarizing, if one wishes to maximize the improvement in average bit rate or waiting time, one should maximize the product $G = RG_c$ as a function of code rate, R.

5.3 Optimal Code Rates. The objective of this section is to maximize the gain factor, G, as a function of code rate, R, provided that the maximum exists. The behavior of coding gain as a function of code rate for Reed-Solomon codes is not well documented, but the author has found that for RS codes used with BPSK and M–ary FSK, the coding gain peaks once at a value of code rate in the interval from 1/2 to 1.0. Since our goal is to maximize the product of code rate and coding gain, this behavior is consistent with the hypothesis that an optimal code rate exists.

By restricting waveform modulation to certain types, we can derive an expression for the optimal code rate for MDS codes used on the meteor-scatter

channel. This expression applies to systems operating with binary FSK and M-ary QAM to include BPSK and M-ary PSK. These modulation types all have bit-error-rate expressions in terms of either the complementary error function or the exponential function. These functions allow a straightforward derivation of asymptotic coding gain similar to that found in Clark and Cain (1981). Clark and Cain derive an expression for the asymptotic coding gain (as $E_b/N_0 \rightarrow \infty$) for a t-error correcting binary block code operating with BPSK modulation on a binary quantized channel. This expression is given by

$$G_a = R(t+1) \tag{5.5}$$

One can show that this expression also holds for M-ary QAM, M-ary PSK and binary FSK (both coherent and noncoherent) when used with t-error correcting Reed-Solomon codes. The reader should note that the coding gain predicted by (5.5) is only achieved in the limit as $E_b/N_0 \rightarrow \infty$. At modest signal-to-noise ratios, the actual gain may be considerably less. Equation 5.5 is useful because we want to maximize the product of code rate and coding gain i.e.

$$G = R\,G_a \approx R^2(t+1)$$

Substituting (5.1) into the above, we get the following

$$G = R^2\left[\frac{n}{2}(1-R)+1\right]$$

$$= \left(\frac{n}{2}+1\right)R^2 - \left(\frac{n}{2}\right)R^3$$

Differentiating and setting the result equal to zero yields

$$\frac{dG}{dR} = 2\left(\frac{n}{2}+1\right)R - \left(\frac{3n}{2}\right)R^2 = 0$$

Solving for R, we get R = 0, and R = 2/3 (1 + 2/n). We must check to see that the latter is in fact a maximum. The second derivative of G is given by

$$\frac{d^2G}{dR^2} = (n+2) - 3nR$$

Substituting R = 2/3 (1 + 2/n) into this expression yields

$$\frac{d^2G(R_{opt})}{dR^2} = -(n+2)$$

which is always less than 0. So this value of code rate is indeed a maximum and we can write the optimal code rate (as $E_b/N_0 \rightarrow \infty$) for $n \geq 5$ as the following

$$R_{opt} = \frac{2}{3}\left(1 + \frac{2}{n}\right) \tag{5.6}$$

We now make the assumption that coding gain, G_c, is a strictly non-decreasing function of E_b/N_0, a safe assumption since all good codes exhibit this behavior. If this is the case, then the optimal code rate is always greater than or equal to the value given by (5.6) and we can write bounds on the optimal code rate. Thus, the optimal code rate for MDS codes used on the meteor-scatter channel is bounded in the following way (for $n \geq 5$)

$$\frac{2}{3}\left(1 + \frac{2}{n}\right) \leq R_{opt} \leq 1 \tag{5.7}$$

Note that the lower bound on optimal code rate approaches 2/3 as $n \to \infty$. We shall see in the next section that for realistic signal-to-noise ratios, the optimal code rate is about 4/5. The lower bound of (5.7) should encourage system designers because it eliminates consideration of the low rate codes and the associated decoder complexity.

5.4 Performance Estimates. Since the weight distribution for Reed-Solomon codes is known, it is possible to derive exact expressions for the probability of incorrect decoding. Such expressions are found in Blahut (1983) and Michelson and Levesque (1985). For our purposes, a simple bound on decoding error will suffice. Assuming random errors on an AWGN channel, we can write an upper bound on the probabiltiy of decoding error for a t-error correctiong Reed-Solomon code of block length n symbols as

$$P_E \leq \sum_{j=t+1}^{n} \binom{n}{j} p_s^j \, (1 - p_s)^{n-j} \tag{5.8}$$

where p_s is the probability of code symbol error, which is dependent on the modulation type. We shall consider two implementations:

- Binary waveform modulation.
- M-ary waveform modulation matched to the RS code.

By "matched," we mean that the modulation symbol size in bits is the same as the RS code symbol size in bits. For example, 32-ary FSK is matched to a (31,23) 4-error correcting Reed-Solomon code. This type of coding scheme is convenient because the probability of code symbol error is simply the probability of modulation symbol error. For binary waveform modulation, the probability of symbol error equals the probability that we have 1 or more bit errors in a code symbol, i.e.

$$p_s = 1 - (1 - p)^k$$

where p = the probability of bit error for the binary modulation and k = the number of bits per code symbol. For RS codes, $k = \log_2 (n+1)$.

We can convert (5.8) into an approximate expression for the probability of symbol error by noting that a received n-tuple with more than t errors will almost always be undecodable and recognized as such. These n-tuples are routed around the decoder to avoid introducing additional errors. Based on this assumption, the probability of symbol error can be approximated by the following

$$P_s \cong \sum_{j=t+1}^{n} \frac{j}{n} \binom{n}{j} p_s^j (1 - p_s)^{n-j} \tag{5.9}$$

Finally, we convert this expression to a probability of bit error by assuming that when a code symbol is in error, each of the 2^k - 1 k-bit patterns are equally likely. (This is the same assumption we made in Chapter 4 for M-ary FSK.) This assumption leads to the following expression for probability of bit error

$$P_b \cong \frac{2^{k-1}}{2^k - 1} \sum_{j=t+1}^{n} \frac{j}{n} \binom{n}{j} p_s^j (1 - p_s)^{n-j} \tag{5.10}$$

Armed with this expression for the probability of bit error, we can evaluate the performance of RS codes on the meteor-scatter channel. Figure 5.2 demonstrates the behavior of the gain factor, $G = RG_c$, as a function of code rate for (31,k) Reed-Solomon codes. BPSK modulation is assumed. Note that the optimal code rate is approximately 0.8. The optimal code for $P_b = 10^{-4}$ is a (31,27) 2-error correcting RS code. For a bit-error rate of 10^{-6}, the optimal

code is a (31,25) 3-error correcting RS code. Note that the optimal code rate shifts toward the lower bound (approximately 2/3) as the power efficiency increases. This behavior was predicted in the previous section.

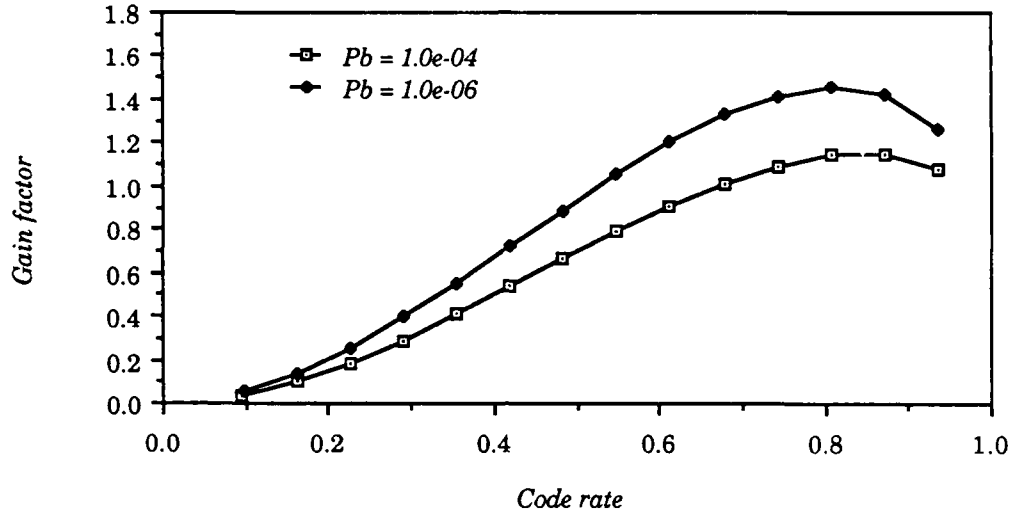

Figure 5.2 (31, k) Reed-Solomon codes with BPSK modulation

Figure 5.3 is the equivalent graph of figure 5.2, this time for 32-FSK modulation. Now we can see the behavior of the optimal code rate as a function of E_b/N_0. Note that once again, the optimal code for a required BER of 10^{-4} is the (31,27) 2-error correcting code, but for a required BER of 10^{-6}, the optimal code rate shifts toward the lower bound, making the optimal code a (31,25) 3-error correcting RS code.

From Figure 5.3 we see that for a required BER of 10^{-6}, the maximum gain is approximately 1.4. Recall that the figure of merit for the adaptive modems when evaluating average bit rate is simply the gain factor, $G = RG_c$. Therefore, the average bit rate for these modems would increase by a factor of 1.4. The figure of merit for the fixed-rate modem was found in section 5.2 to be the square root of G, so the improvement factor for this modem is 1.2. The figure of merit with respect to mean waiting time is the same for all systems

and is again the square root of G. So we can expect a reduction in mean waiting time by a factor of 1.2.

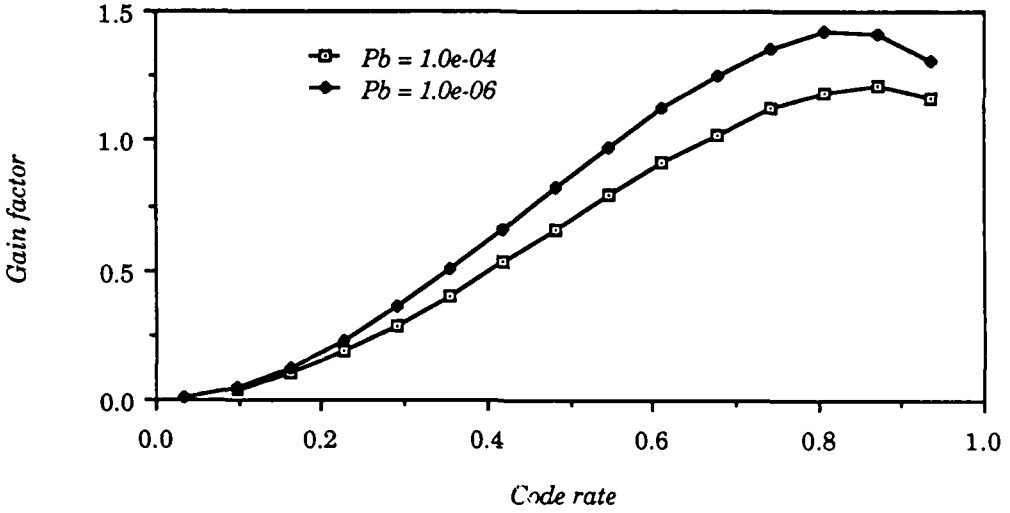

Figure 5.3 (31, k) RS codes with coherent 32-ary FSK

Figure 5.4 demonstrates the performance of (63, k) Reed-Solomon codes. Again, the optimal code rate is about .8 with the optimal codes being (63, 55) for a BER of 10^{-4} and (63, 53) for a BER of 10^{-6}.

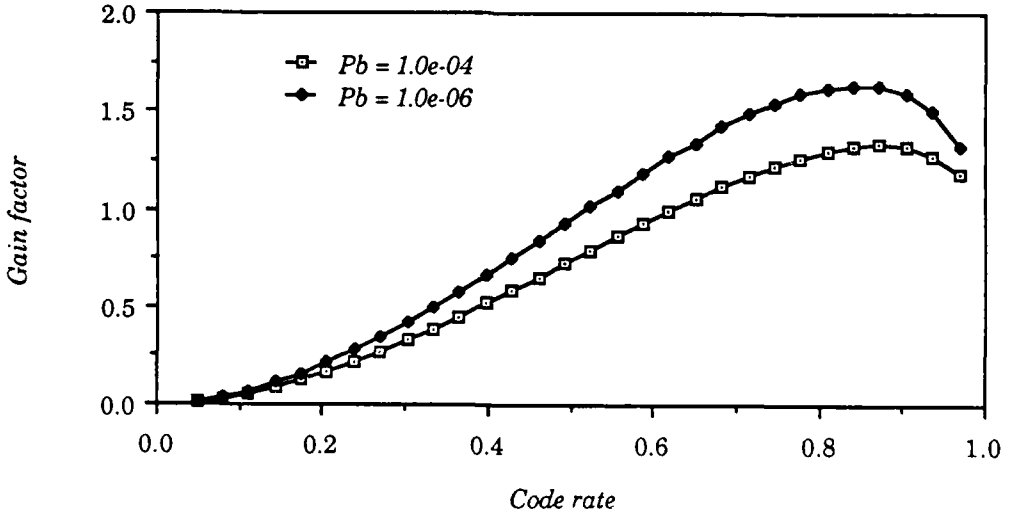

Figure 5.4 (63,k) RS codes with coherent 64-ary FSK

The performance results presented thus far indicate that Reed-Solomon codes can provide only modest improvements in average bit rate and mean waiting time. Because of the very low misdecode rate of Reed-Solomon codes, the inclusion of some type of ARQ may improve the coding gain and subsequently the gain factor.

Chapter 6 - Conclusion

6.1 Summary of Findings. The goal of this thesis is to improve the performance of digital communication systems on the meteor-scatter channel through the use of digital modulation and coding techniques. The main results fall conveniently into six categories: channel model, expressions for average bit rate, expressions for mean waiting time, optimal M-ary modulation, adaptive QAM, and Reed-Solomon codes. Following is a brief summary of the findings of this thesis, organized according to the aforementioned categories.

6.1.1 Channel model. The meteor-scatter channel exhibits several unique properties that should be exploited in digital signal design. These properties are described in detail in Chapter 2 where a channel model is derived. This channel model is based on the premise that meteor arrivals can be modeled as a Poisson process and the properties of the Poisson process are used extensively throughout the thesis.

Burst duration is found to have constant mean, independent of the link parameters. Thus, for a given modulation scheme, all variations in throughput are attributed to the meteor arrival rate, λ.

Channel noise is modeled as additive, white, and Gaussian distributed.

Multipath-induced intersymbol interference places a ceiling on channel symbol rate, effectively limiting the bandwidth of the channel. The maximum channel symbol rate is approximately 500 kHz.

6.1.2 Long run average bit rate. Recognizing that the process of transmitting messages on the meteor-scatter channel is a compound Poisson process, one can derive an expression for long run average bit rate. The general expression derived in Chapter 3 is given by

$$R_{bavg} = \lambda E[W] \tag{6.1}$$

$$= \lambda \int_Q W(q) f_Q(q) dq$$

where

λ is the meteor arrival rate
W is the number of bits per burst
q is electron line density
$f_Q(q)$ is the probability density function for electron line density

It is shown that this expression for average bit rate agrees in theory with one popular definition of throughput found in the literature. Equation 6.1, as evaluated in Chapter 3, is an approximation to the long run average bit rate since it assumes that all trails occur at a fixed point in the sky and that the electron line density, q, is upper-bounded by 10^{17} e/m.

Specific expressions are derived for the fixed-rate and the adaptive-symbol-rate modems. The symbol rate that maximizes the average bit rate for the fixed-rate modem will normally exceed the ceiling imposed by intersymbol interference.

The adaptive-symbol-rate modem offers a twenty-fold improvement in average bit rate when the channel is modeled as strictly power-limited. When the channel is modeled as bandwidth-limited, the improvement is reduced dramatically to about 25%.

6.1.3 Mean message waiting time. The mean message waiting time for a fixed-rate modem operating at a bit rate of R_b bits/s is derived in Chapter 3 and is given by

$$E[T_w] = \frac{1}{\lambda} + \frac{N}{\lambda \tau R_b} \tag{6.2}$$

where N is the message length in bits and τ (= .58 s) is the mean burst duration in seconds. The meteor arrival rate, λ, is a function of bit rate and it is shown that a unique bit rate exists that minimizes mean waiting time. This optimal bit rate is

$$R_{bopt} = \frac{N}{\tau} \tag{6.3}$$

Upper and lower bounds on the mean waiting time for the adaptive-symbol-rate modem are derived based on probabilistic arguments. These bounds are given by

$$\frac{1}{\lambda} \leq E[T_w] \leq \frac{1}{\lambda p} \tag{6.4}$$

where $p = P(W \geq N)$. When the adaptive symbol rate modem is operating at a minimum symbol rate, R_{min}, equal to the symbol rate given by (6.3), the improvement factor for adaptive-symbol-rate over fixed-rate is given by

$$\frac{2}{\sqrt{3}} \leq I \leq 2 \tag{6.5}$$

The work of Cox (1962) is used to derive an expression for the Laplace transform of the mean waiting time when the distribution for W is known

and the Laplace transform of the probability density function for W exists. This expression is given by

$$\mathcal{L}\{E[T_w]\} = \frac{1}{\lambda}\left[\frac{1}{s} + \frac{F(s)}{s[1 - F(s)]}\right] \tag{6.6}$$

where

F(s) = the Laplace transform of the probability density function for the random variable W.

s = the argument of the Laplace transform with respect to N, the message length in bits.

6.1.4 Optimal M-ary Modulation. When the meteor-scatter channel is modeled as strictly power-limited, the optimal M-ary modulation technique is M-ary FSK, $M \rightarrow \infty$. The power-limited model is valid when waiting time is the performance measure of interest. This model is not valid when the user wishes to maximize average bit rate. In this case, the channel must be modeled as bandwidth-limited and the optimal modulation is normally M–ary QAM. In general, the optimal modulation for the bandwidth-limited channel model is a function of the link parameters (especially transmitter power), and the particular bandwidth limitation.

When all trails are assumed underdense and the channel is bandwidth-limited, the optimal modulation for the fixed-rate modem is QPSK, independent of the link parameters.

6.1.5 Adaptive QAM. The adaptive-symbol-rate modem employing M-ary FSK ($M \rightarrow \infty$) uses the channel optimally, assuming that the channel is power-limited. The meteor scatter channel is bandwidth-limited, however, and for this type channel, adaptive-symbol-rate is not optimal.

An adaptive modulation scheme that out-performs adaptive-symbol-rate on a bandwidth-limited channel is adaptive QAM. The improvement in average bit rate over the adaptive-symbol-rate scheme is shown in Chapter 4 to be about three-fold for a bandwidth limit of R_{max} = 500 kHz.

In terms of mean waiting time, it is shown that adaptive-symbol-rate will always outperform adaptive QAM when QPSK modulation is used. Adaptive QAM offers an improvement in mean waiting time over the fixed-rate modem of about 28%. A suggested implementation of adaptive QAM is presented to include a signal constellation and a modem block diagram. This suggested implementation appears to be feasible using today's technology.

6.1.6 Reed-Solomon Codes. Reed-Solomon codes used for forward-error correction are shown to provide modest gains in average bit rate and modest reductions in mean waiting time.

An appropriate figure of merit is derived to measure the improvement in either average bit rate or mean waiting time. This figure of merit is given by

$$G = R\,G_c$$

where R = code rate and G_c = coding gain. The figure of merit for the fixed-rate modem and for all modems when waiting time is the performance measure of interest, is simply the square root of G. It is shown that a (31, 25) Reed-Solomon code offers gain in average bit rate of 40% for the two adaptive modulation schemes. The gain for the fixed-rate modem is about 20%. The improvement in mean waiting time is the same for all modulation schemes and is again 20%.

Bounds on optimal code rate for maximum-distance-separable (MDS) codes are derived in Chapter 5 and are given by

are derived in Chapter 5 and are given by

$$\frac{2}{3}\left(1+\frac{2}{n}\right) \leq R_{opt} \leq 1 \qquad (6.7)$$

where n is the block length of the code. Because of the very low misdecode rate of Reed-Solomon codes, some type of automatic-repeat-request (ARQ) may improve the coding gain and subsequently the gain factor, G.

6.2 Recommendations for Further Research.

6.2.1 Experimental confirmation of findings. Especially to verify strong dependence on overdense trails and strong effects of bandwidth ceiling. Both seem to contradict results published by Ostergaard et al. (1985).

6.2.2 Signal detection and estimation. Adaptive modems especially require fast and reliable estimate of channel SNR. This channel provides interesting application for signal estimation since we know much about how the received power behaves after trail formation. There are possible applications of linear prediction and other signal processing methods. Meteor arrivals are modeled as a Poisson random process and signal detection methods should exploit the properties of the Poisson process.

6.2.3 Variable rate codes. Achieve adaptive information rate through variable rate error-control codes. Some work has already been done in this area. See Rediske (1982).

6.2.4 Trellis codes for digital modulation. Trellis codes invented by Ungerboeck are in widespread use on bandwidth-limited digital radio channels. One possible adaptive implementation would use the same trellis for say, five QAM signal sets.

Appendix A - Expressions For Long Run Average Symbol Rate

A.1 Fixed-Symbol-Rate Modem. From Section 3.1.1 we have the following expression for long run average symbol rate for the fixed-rate modem

$$R_{avg} = \lambda \int_Q R_s \, T_d \, (q) \, f_Q(q) \, dq \qquad (A.1)$$

where

$$f_Q \, (q) \; = \frac{q_0}{q^2} \, , \; q \geq q_0$$

$T_d \, (q)$ = the burst duration as a function of electron line density, q

λ = the meteor arrival rate

The lower and upper limits of integration in (A.1) are q_0 and 10^{17} e/m, respectively. Assuming that $q_0 < 10^{14}$ e/m we can derive an expression for q_0 based on the underdense trail model. From Section 3.1.3 we have the instantaneous symbol rate as a function of time and electron line density as

$$R(t, q) = \frac{P_r \, (t, q)}{N_0 \, (E_s / N_0)_{req}} \qquad (A.2)$$

where

N_0 is the noise power spectral density

$(E_s/N_0)_{req}$ is the signal-to-noise ratio required to maintain an acceptable bit error rate (BER) for a particular modem

$P_r(t, q)$ is the received power as a function of time and electron line density

From Section 2.3 we have the following expression for $P_r(t, q)$ for underdense trails

$$P_r(t, q) = P_r(0,1)\ q^2\ \exp\left[\frac{-2t}{t_c}\right] \tag{A.3}$$

where

$$P_r(0,1) = \frac{P_T\ G_T\ G_r\ \sigma_e\ \lambda^3\ \exp -\left[\frac{8\pi^2 r_0^2}{\lambda^2 \sec^2\phi}\right]}{(4\pi)^3\ R_{CT}\ R_{CR}\ (R_{CT} + R_{CR})\ (1 - \sin^2\phi \cos^2\beta)}$$

$$t_c = \frac{\lambda^2 \sec^2\phi}{16\pi^2 D}$$

Let T_d = the duration of the burst in seconds. At the termination of an underdense burst the received power drops to the threshold value and the symbol rate is given by the following

$$R(t, q) = R_s = \frac{P_r(T_d, q)}{N_0\ (E_s / N_0)_{req}}$$

$$= \frac{P_r(0, q_0)}{N_0\ (E_s / N_0)_{req}}$$

$$= \frac{P_r(0,1)\ q_0^2}{N_0\ (E_s / N_0)_{req}}$$

Solving for q_0 yields

$$q_0 = \sqrt{\frac{R_s N_0 (E_s / N_0)_{req}}{P_r (0, 1)}} \tag{A.4}$$

A.1.1 Underdense Trails. From the preceding derivation of q_0, we have the received power at burst termination as

$$P_r (T_d, q) = P_r (0, q_0)$$

Or equivalently

$$P_r (0, 1)\, q^2 \exp\left[-\frac{2 T_d}{t_c} \right] = P_r (0, 1)\, q_0^2$$

Solving for burst duration, T_d, gives

$$T_d = t_c \ln\left[\frac{q}{q_0} \right] \tag{A.5}$$

Therefore, the expression for R_{avg} becomes

$$R_{avg} = \lambda R_s t_c \int_{q_0}^{10^{14}} \ln\left[\frac{q}{q_0} \right] \frac{q_0}{q^2}\, dq$$

Integrating by parts yields the following

$$R_{avg} = \frac{\lambda R_s t_c q_0}{10^{14}} \left[\frac{10^{14}}{q_0} - \ln\left(\frac{10^{14}}{q_0} \right) - 1 \right] \tag{A.6}$$

where q_0 is given by (A.4). If $q_0 << 10^{14}$, then R_{avg} is simply

$$R_{avg} \cong \lambda R_s t_c \tag{A.7}$$

Recognizing that the distribution for burst duration in symbols is exponential with mean $R_s \tau$ where $\tau = t_c$, then the above expression is equivalent to the following

$$R_{avg} = \lambda E [W]$$

where W in this case is the number of symbols/burst when all trails are assumed underdense.

A.1.2 Overdense trails. Recall from Section 2.3 of Chapter 2 that the received power from overdense trails is given by

$$P_r(t, q) = \frac{P_T G_T G_R \lambda^2 \left[\frac{(4Dt + r_0^2)}{\sec^2 \phi} \text{ Ln} \left(\frac{r_e \, q \, \lambda^2 \sec^2 \phi}{\pi^2 (4Dt + r_0^2)} \right) \right]^{1/2}}{32 \pi^2 R_{CR} R_{CT} (R_{CR} + R_{CT}) (1 - \cos^2 \beta \sin^2 \phi)} \qquad (A.8)$$

Or equivalently,

$$P_r(t, q) = P_r(0) \left[\frac{4Dt + r_0^2}{\sec^2 \phi} \text{ Ln} \left(\frac{r_e \, q \, \lambda^2 \sec^2 \phi}{\pi^2 (4Dt + r_0^2)} \right) \right] \qquad (A.9)$$

where

$$P_r(0) = \frac{P_T G_T G_R \lambda^2}{32 \pi^2 R_{CR} R_{CT} (R_{CR} + R_{CT}) (1 - \cos^2 \beta \sin^2 \phi)}$$

Note that $P_r(0)$ is only approximately equal to the received power at t = 0. The time varying symbol rate, R(t), (given by (A.2)) for overdense trails can be approximated by a triangle whose base has length t_{max} and whose altitude, or peak is R_{max} . See figure A.1.

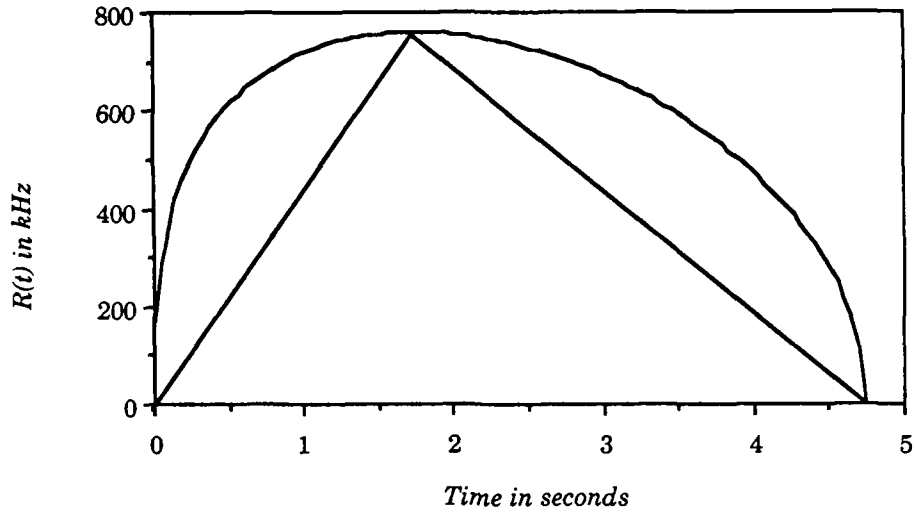

Figure A.1 Piecewise linear approximation to R(t) for overdense trails

Observe that $4Dt >> r_0^2$ for all but very small t. Making this approximation, it is straightforward to show that R_{max} and t_{max} are given by the following (Abel, 1986)

$$R_{max} = \left[\frac{P_r(0)}{N_0 (E_s / N_0)_{req}} \right] \left[\frac{r_e \, q \, \lambda^2}{\pi^2 \, e} \right]^{1/2} \tag{A.10}$$

$$t_{max} = \frac{r_e \, q \, \lambda^2 \sec^2 \phi}{4 \, \pi^2 \, D} \tag{A.11}$$

Based on our linear approximation to R(t), (see figure A.1) one can show quite easily that the burst duration, T_d, is simply a proportion of t_{max}

$$T_d = \left(1 - \frac{R_s}{R_{max}} \right) t_{max} \tag{A.12}$$

Thus the long run average symbol rate, R_{avg}, for overdense trails is given by

$$R_{avg} = \lambda \int_{10^{14}}^{10^{17}} R_s \left(1 - \frac{R_s}{R_{max}}\right) t_{max} \frac{q_0}{q^2} dq \qquad (A.13)$$

Let $R_{max} = A\, q^{1/2}$ and let $t_{max} = B\, q$ where the constants A and B are defined as follows

$$A = \left[\frac{P_r(0)}{N_0 (E_s / N_0)_{req}} \right] \left[\frac{r_e\, \lambda^2}{\pi^2 e} \right]^{1/2}$$

$$B = \frac{r_e\, \lambda^2 \sec^2 \phi}{4\, \pi^2 D}$$

Substituting these values into (A.13) results in

$$R_{avg} = \lambda\, R_s\, B\, q_0 \int_{10^{14}}^{10^{17}} \left(1 - \frac{R_s}{A\, q^{1/2}}\right) \frac{1}{q} dq$$

Straightforward integration yields

$$R_{avg} \cong \lambda\, R_s\, B\, q_0 \left[6.91 - \frac{2\, R_s}{A\, 10^7} \right] \qquad (A.14)$$

where the constants A and B are defined above. The expression for long run average symbol rate (for $q_0 << 10^{14}$ e/m) is found by adding (A.7) and (A.14)

$$R_{avg} \cong \lambda\, R_s\, t_c + \lambda\, R_s\, B\, q_0 \left[6.91 - \frac{2\, R_s}{A\, 10^7} \right] \qquad (A.15)$$

A.2 Adaptive-Symbol-Rate Modem. From Section 3.1.3 we have the following expression for R_{avg}

$$R_{avg} = \lambda \int_Q W(q)\, f_Q(q)\, dt\, dq \tag{A.16}$$

where $W(q) = \int_0^{T_d(q)} R(t, q)\, dt$ and R(t, q) is given by (A.2).

The threshold value for q is q_0 and is found by substituting R_{min} for R_s in (A.4)

$$q_0 = \sqrt{\frac{R_{min}\, N_0\, (E_s / N_0)_{req}}{P_r(0, 1)}}$$

A.2.1 Underdense trails. For underdense trails, the number of symbols/burst is given by

$$W(q) = \int_0^{T_d(q)} \frac{P_r(0, 1)\, q^2 \exp\left[-\frac{2t}{t_c} \right]}{N_0\, (E_s / N_0)_{req}}\, dt \tag{A.17}$$

where $T_d(q) = t_c \ln\left[\frac{q}{q_0} \right]$ = duration of underdense burst.

Straightforward integration of (A.17) yields the following

$$W(q) = \frac{P_r(0, 1)\, q^2}{N_0\, (E_s / N_0)_{req}}\, \frac{t_c}{2} \left[1 - \left(\frac{q_0}{q} \right)^2 \right] \tag{A.18}$$

Substituting (A.18) into (A.16) gives

$$R_{avg} = \lambda \int_{q_0}^{10^{14}} \frac{P_r(0,1)\, q^2}{N_0 (E_s / N_0)_{req}} \frac{t_c}{2} \left[1 - \left(\frac{q_0}{q} \right)^2 \right] \frac{q_0}{q^2}\, dq$$

Evaluating this integral results in the following expression

$$R_{avg} = \lambda \frac{P_r(0,1)\, t_c\, q_0}{2 \times 10^{14}\, N_0 (E_s / N_0)_{req}} \left[q_0^2 - 2 \times 10^{14}\, q_0 + 10^{28} \right] \qquad (A.19)$$

For $q_0 << 10^{14}$ this expression simplifies to the following

$$R_{avg} = \lambda \frac{P_r(0,1)\, t_c\, q_0\, 10^{14}}{2\, N_0 (E_s / N_0)_{req}} \qquad (A.20)$$

A.2.2 Overdense trails. In this case the number of symbols/burst is simply the area under the triangle in figure A.1. Thus we can write

$$W(q) = \int_0^{T(R_{min},\, q)} R(t, q)\, dt = \frac{R_{max}\, t_{max}}{2}$$

and R_{avg} is given by

$$R_{avg} = \lambda \int_{10^{14}}^{10^{17}} \frac{A\, q^{1/2}\, B\, q}{2} \frac{q_0}{q^2}\, dq$$

where the constants A and B were defined previously. We can simplify the integrand to give

$$R_{avg} = \lambda \int_{10^{14}}^{10^{17}} \frac{A\, B\, q_0}{2}\, q^{-1/2}\, dq$$

Evaluating this integral, we get the following result

$$R_{avg} = 3.06 \times 10^{8} \lambda A B q_0 \qquad (A.21)$$

combining (A.20) and (A.21), we get the following expression for the adaptive-symbol-rate modem

$$R_{avg} \equiv \lambda \frac{P_r(0,1)\, t_c\, q_0\, 10^{14}}{2 N_0 (E_s / N_0)_{req}} + 3.06 \times 10^{8} \lambda A B q_0 \qquad (A.22)$$

Appendix B - Mean Waiting Time For Adaptive QAM

Recall from Section 3.2.3 of Chapter 3 that the Laplace transform of the mean waiting time is given by

$$\mathcal{L}\{ E[T_w] \} = \frac{1}{\lambda}\left[\frac{1}{s} + \frac{F(s)}{s\,[1 - F(s)]} \right] \qquad \text{(B.1)}$$

where F(s) = the Laplace transform of the probability density function for the random variable W (= bits per meteor burst).

s = the argument of the Laplace transform with respect to N, the number of bits in the message to be transmitted. N is assumed known, not random.

λ = the meteor arrival rate (= rate of the Poisson process).

The first step in evaluating (B.1) for adaptive QAM is to derive an expression for the cumulative distribution function (CDF) for the number of bits per meteor burst. Let W represent this random variable and denote the CDF for W by $F_W(x)$.

B.1 CDF For Bits per Burst, W. As in Section 3.2 of Chapter 3, we make the following assumptions regarding the meteor-scatter channel:

- All trails are underdense.
- W is a continuous, rather than discrete, random variable.
- Overlapping trails (in time) are nonexistent.
- The W_m bits transmitted during the m^{th} meteor burst are sent in a time $\Delta t = 0$.

Recall that the instantaneous symbol rate can be written as the following

$$R(t) = \frac{P_r(t,q)}{N_0 (E_s/N_0)_{req}} \tag{B.2}$$

As in Chapter 4, we denote the power efficiency for M-ary QAM by $(E_s/N_0)_M$, where $E_s = (\log_2 M)\, E_b$. Values of $(E_s/N_0)_M$ for M = 4, 8, 16, 32, and 64 are listed in Table B.1.

Table B.1 $(E_s/N_0)_{req}$ in dB for several values of P_b for M-ary QAM

Modulation	$P_b = 10^{-3}$	$P_b = 10^{-4}$	$P_b = 10^{-5}$	$P_b = 10^{-6}$
4-QAM (QPSK)	9.6	11.4	12.6	13.5
8-QAM	13.5	15.2	16.4	17.4
16-QAM	16.3	18.1	19.4	20.3
32-QAM	19.3	21.1	22.4	23.4
64-QAM	22.2	24.0	25.4	26.4

Realizing that the symbol rate is constant, we can rewrite (B.2) to get an expression for the signal-to-noise ratio (SNR) per channel symbol as

$$E_s/N_0 = \frac{P_r(t,q)}{N_0 R_s} \tag{B.3}$$

When the the right-hand side of (B.3) exceeds $(E_s/N_0)_M$, the modem changes modulation to M-ary QAM and operates at a bit rate of $(\log_2 M)R_s$ bits/s.

The operation of adaptive QAM on a typical underdense trail is illustrated in Figure B.1.

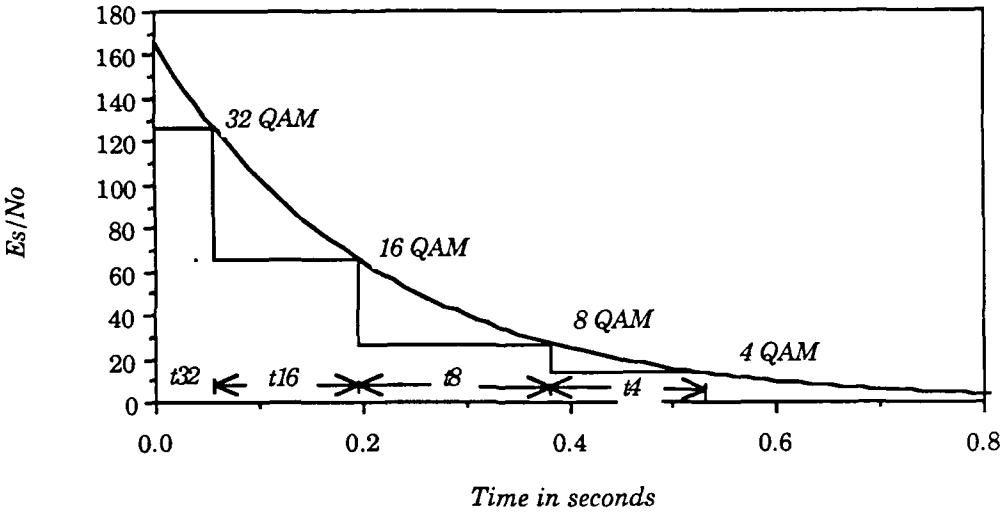

Figure B.1 Operation of adaptive QAM on an underdense trail
(P_T= 2000 watts, R_s = 1000 Hz, q = 10^{13} e/m)

From Figure B.1 we see that, in general, the number of bits per meteor burst, W, can be written as

$$W = R_s [\, 2\, t_4 + 3\, t_8 + 4\, t_{16} + 5\, t_{32} + 6\, t_{64} \,] \qquad (B.4)$$

where t_M = the time that the modem operates at M-ary QAM for a given burst. Note that the total burst duration, T_d, is given by $T_d = t_4 + t_8 + t_{16} + t_{32} + t_{64}$. Since many trails will not support 64-QAM or even 32-QAM, we allow the possibility that $t_M = 0$ for some M.

The initial (and maximum) bit rate for a given burst is determined by the initial signal-to-noise ratio per channel symbol which is a function of the electron line density, Q, a random variable. Let the minimum electron line density required to support M-ary QAM be given by q_M. For adaptive QAM, there are exactly five mutually exclusive events regarding the electron line density of observable meteor trails:

$$E_1 = \{ q_4 \le Q < q_8 \}$$
$$E_2 = \{ q_8 \le Q < q_{16} \}$$
$$E_3 = \{ q_{16} \le Q < q_{32} \}$$
$$E_4 = \{ q_{32} \le Q < q_{64} \}$$
$$E_5 = \{ Q \ge q_{64} \}$$

The probability that Q is less than q_4 is 0, so the union of these five events comprises the sample space.

The event $\{W \le x\}$ can be written as the union of five mutually exclusive events, $\{ \{W \le x\} \cap E_i \}$, i = 1, 2, 3, 4, 5. Therefore, the CDF for the random variable, W, can be written as the sum of the probabilities of these five mutually exclusive events, i.e.

$$F_W(x) = P(W \le x) = \sum_{i=1}^{5} P(W \le x, E_i) \qquad (B.5)$$

We must now find expressions for the probabilities: $P(W \le x, E_i)$, i = 1,2,3,4,5.

Consider first the case where E_5 has occurred, meaning that $Q \ge q_{64}$. We can use (B.4) to write the probability $P(W \le x, E_5)$ as the following

$$P(W \le x, E_5) = P(\mathcal{R}_s [2 t_4 + 3 t_8 + 4 t_{16} + 5 t_{32} + 6 t_{64}] \le x, Q \ge q_{64}) \qquad (B.6)$$

The burst duration for a fixed-rate modem operating with M-ary QAM can be written as a function of Q

$$T_d = t_c \ln\left[\frac{Q}{q_M} \right] \qquad (B.7)$$

where t_c is defined in Chapter 2.

We can use (B.7) to write the terms t_M , M = 4, 8, 16, 32, 64 for adaptive QAM in the following manner

$$t_{64} = t_c \ln\left[\frac{Q}{q_{64}}\right]$$

$$t_{32} = t_c \ln\left[\frac{Q}{q_{32}}\right] - t_c \ln\left[\frac{Q}{q_{64}}\right]$$

$$t_{16} = t_c \ln\left[\frac{Q}{q_{16}}\right] - t_c \ln\left[\frac{Q}{q_{32}}\right]$$

$$t_8 = t_c \ln\left[\frac{Q}{q_8}\right] - t_c \ln\left[\frac{Q}{q_{16}}\right]$$

$$t_4 = t_c \ln\left[\frac{Q}{q_4}\right] - t_c \ln\left[\frac{Q}{q_8}\right]$$

Realizing that the total burst duration is given by

$$T_d = t_c \ln\left[\frac{Q}{q_4}\right]$$

we see that the above expressions for t_M, M = 4,8,16,32, and 64 can be written in terms of T_d and logarithms of q_M. Furthermore, we recognize that q_M can be written as

$$q_M = \sqrt{\frac{R_s N_0 (E_s/N_0)_M}{P_r (0,1)}}$$

so the above expressions for t_M will be logarithms of the square root of the required SNR per channel symbol, $(E_s/N_0)_M$. Given this information, simple

algebraic manipulations yield the following expression for W

$$W = R_s\left[6T_d + \frac{t_c}{2}\ln\left\{\frac{(E_s/N_0)_4^4}{(E_s/N_0)_8\ (E_s/N_0)_{16}\,(E_s/N_0)_{32}\,(E_s/N_0)_{64}}\right\}\right] \qquad (B.8)$$

The probability $P(W \le x, E_5)$ can be written as

$$P\left(R_s\left[6T_d + \frac{t_c}{2}\ln\left\{\frac{(E_s/N_0)_4^4}{(E_s/N_0)_8\ (E_s/N_0)_{16}\,(E_s/N_0)_{32}\,(E_s/N_0)_{64}}\right\}\right] \le x,\ Q \ge q_{64}\right)$$

Since the burst duration, T_d, is exponentially distributed with mean $\tau = t_c$, and burst duration and electron line density are related by (B.7), we can write the above expression as the following

$$P\,(W \le x, E_5\,) = \sqrt{\frac{(E_s/N_0)_4}{(E_s/N_0)_{64}}} - K_{64}\ \exp\left\{-\frac{x}{6\,R_s\,t_c}\right\}$$

where

$$K_{64} = \left[\frac{(E_s/N_0)_4^4}{(E_s/N_0)_8\ (E_s/N_0)_{16}\,(E_s/N_0)_{32}\,(E_s/N_0)_{64}}\right]^{\frac{1}{12}}$$

Since the above expression was derived assuming that $Q \ge q_{64}$, the values of x must be restricted to $x \ge x_{64}$ where x_{64} is the number of bits per burst when $Q = q_{64}$. The burst duration for such a trail is given by

$$T_d = t_c \ln\left[\frac{q_{64}}{q_4}\right] = \frac{t_c}{2}\ln\left[\frac{(E_s/N_0)_{64}}{(E_s/N_0)_4}\right]$$

Substituting this value of burst duration into (B.8) yields

$$x_{64} = R_s\left[\frac{t_c}{2}\ln\left\{\frac{(E_s/N_0)_{64}^5}{(E_s/N_0)_4^2\,(E_s/N_0)_8\,(E_s/N_0)_{16}\,(E_s/N_0)_{32}}\right\}\right]$$

Similar expressions to the above can be derived for the events E_4, E_3, E_2, and E_1. These results can be substituted into our expression for the CDF of W yielding the following

$$F_W(x) = P(W \le x) = \sum_{i=1}^{5} P(W \le x, E_i) \qquad \text{(B.9)}$$

$$= 1 - K_{64}\exp\left\{-\frac{x}{6R_s t_c}\right\}, \quad x \ge x_{64}$$

$$1 - K_{32}\exp\left\{-\frac{x}{5R_s t_c}\right\}, \quad x_{32} \le x < x_{64}$$

$$1 - K_{16}\exp\left\{-\frac{x}{4R_s t_c}\right\}, \quad x_{16} \le x < x_{32}$$

$$1 - K_8\exp\left\{-\frac{x}{3R_s t_c}\right\}, \quad x_8 \le x < x_{16}$$

$$1 - \exp\left\{-\frac{x}{2R_s t_c}\right\}, \quad 0 \le x < x_8$$

where the constants K_M , M = 8, 16, 32, 64 are given by

$$K_{64} = \left[\frac{(E_s/N_0)_4^4}{(E_s/N_0)_8\ (E_s/N_0)_{16}\,(E_s/N_0)_{32}\,(E_s/N_0)_{64}}\right]^{\frac{1}{12}}$$

$$K_{32} = \left[\frac{(E_s/N_0)_4^3}{(E_s/N_0)_8 \ (E_s/N_0)_{16} \ (E_s/N_0)_{32}} \right]^{\frac{1}{10}}$$

$$K_{16} = \left[\frac{(E_s/N_0)_4^2}{(E_s/N_0)_8 \ (E_s/N_0)_{16}} \right]^{\frac{1}{8}}$$

$$K_8 = \left[\frac{(E_s/N_0)_4^2}{(E_s/N_0)_8} \right]^{\frac{1}{6}}$$

and the values of x_M are given by

$$x_{64} = R_s \left[\frac{t_c}{2} \ln \left\{ \frac{(E_s/N_0)_{64}^5}{(E_s/N_0)_4^2 \ (E_s/N_0)_8 \ (E_s/N_0)_{16} \ (E_s/N_0)_{32}} \right\} \right]$$

$$x_{32} = R_s \left[\frac{t_c}{2} \ln \left\{ \frac{(E_s/N_0)_{32}^4}{(E_s/N_0)_4^2 \ (E_s/N_0)_8 \ (E_s/N_0)_{16}} \right\} \right]$$

$$x_{16} = R_s \left[\frac{t_c}{2} \ln \left\{ \frac{(E_s/N_0)_{16}^3}{(E_s/N_0)_4^2 \ (E_s/N_0)_8} \right\} \right]$$

$$x_8 = R_s \left[\frac{t_c}{2} \ln \left\{ \frac{(E_s/N_0)_8^2}{(E_s/N_0)_4^2} \right\} \right]$$

Equation B.9 is plotted in Figure B.2 for R_s = 5900 Hz and $P_b = 10^{-4}$. Note that since the burst duration is independent of the link parameters, the CDF for

adaptive QAM is also independent of the the link parameters. The CDF is a function of symbol rate, mean burst duration, t_c, and ratios of $(E_s/N_0)_{req}$.

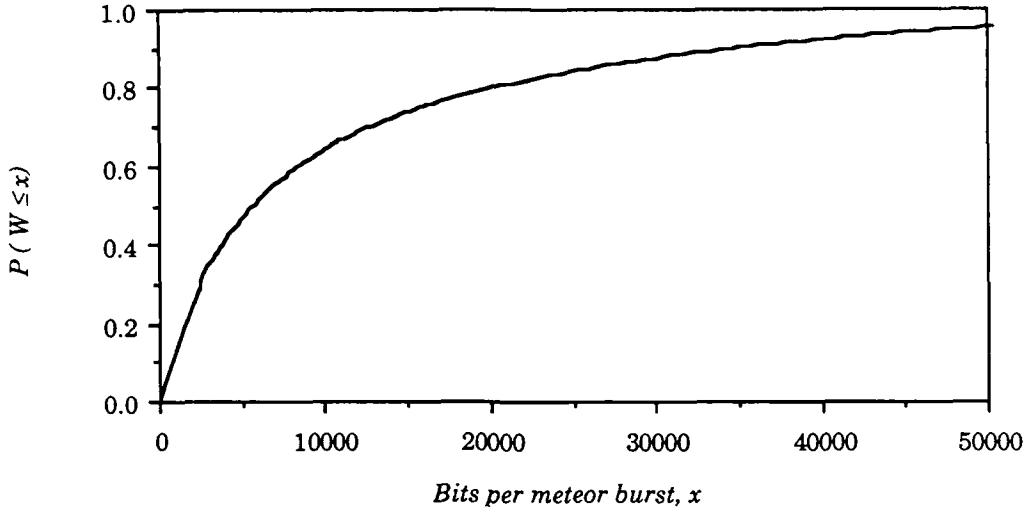

Figure B.2 Cumulative distribution function for bits per burst, W, for adaptive QAM ($P_b = 10^{-4}$, $R_s = 5900$ Hz, $t_c = .58$ s)

The distribution function of (B.9) is continuous, but only piecewise differentiable. Consequently, the Laplace transform of the probability density function (denoted by F(s)) involves polynomials of s and exponentials of s. A more tractable approach is to approximate (B.9) by a sum of three exponential functions and use this approximation to find an expression for mean waiting time. This is done in the next section.

B.2 Exponential Approximation. In this section we approximate the CDF for the number of bits per meteor burst by a linear approximation that minimizes the squared error. For the following discussion, the inner product of two vectors (functions) is given by

$$(\mathbf{x},\mathbf{y}) = \int_0^\infty x(t)\, y(t)\, dt$$

The approximation problem can be stated as follows: Find a_0, a_1, and a_2 such that

$$\int_0^\infty \left| [1 - F_W(x)] - \sum_{i=0}^{2} a_i \exp\left\{ - \frac{x}{2(1+i)\, R_s\, \tau} \right| ^2 dx \qquad \text{(B.10)}$$

is minimized. Let $\mathbf{s} = 1 - F_W(x)$, the function to be approximated. The basis is the set $\{\phi_0,\phi_1,\phi_2\}$ where

$$\phi_0 = \exp\left\{ - \frac{x}{2\, R_s\, t_c} \right\}$$

$$\phi_1 = \exp\left\{ - \frac{x}{4 R_s\, t_c} \right\}$$

$$\phi_2 = \exp\left\{ - \frac{x}{6 R_s\, t_c} \right\}$$

The error is minimized when the error vector is orthogonal to the subspace spanned by $\{\phi_0,\phi_1,\phi_2\}$. This orthogonality condition leads to the following matrix equation

$$\begin{bmatrix} (\mathbf{s}, \phi_0) \\ (\mathbf{s}, \phi_1) \\ (\mathbf{s}, \phi_2) \end{bmatrix} = \mathbf{G} \begin{bmatrix} a_0 \\ a_1 \\ a_2 \end{bmatrix}$$

where **G** is the Gram matrix given by

$$\mathbf{G} = \begin{bmatrix} (\phi_0, \phi_0) & (\phi_1, \phi_0) & (\phi_2, \phi_0) \\ (\phi_1, \phi_0) & (\phi_1, \phi_1) & (\phi_2, \phi_1) \\ (\phi_2, \phi_0) & (\phi_1, \phi_2) & (\phi_2, \phi_2) \end{bmatrix}$$

Straightforward integration yields the following matrix equation for $P_b = 10^{-4}$

$$R_s t_c \begin{bmatrix} 1.16 \\ 1.66 \\ 2.01 \end{bmatrix} = R_s t_c \begin{bmatrix} 1.00 & 1.33 & 1.50 \\ 1.33 & 2.00 & 2.40 \\ 1.50 & 2.40 & 3.00 \end{bmatrix} \begin{bmatrix} a_0 \\ a_1 \\ a_0 \end{bmatrix}$$

Solving the equation, we get $a_0 = 0.801$, $a_1 = -0.658$, and $a_2 = 0.795$. Thus, the exponential approximation to the CDF of W is given by

$$\hat{F}_W(x) = 1 - \left[.8 \exp\left\{ -\frac{x}{2 R_s t_c} \right\} - 0.66 \exp\left\{ -\frac{x}{4 R_s t_c} \right\} + 0.8 \exp\left\{ -\frac{x}{6 R_s t_c} \right\} \right] \quad \text{(B.11)}$$

Equation B.11 is plotted in Figure B.3 along with the original CDF.

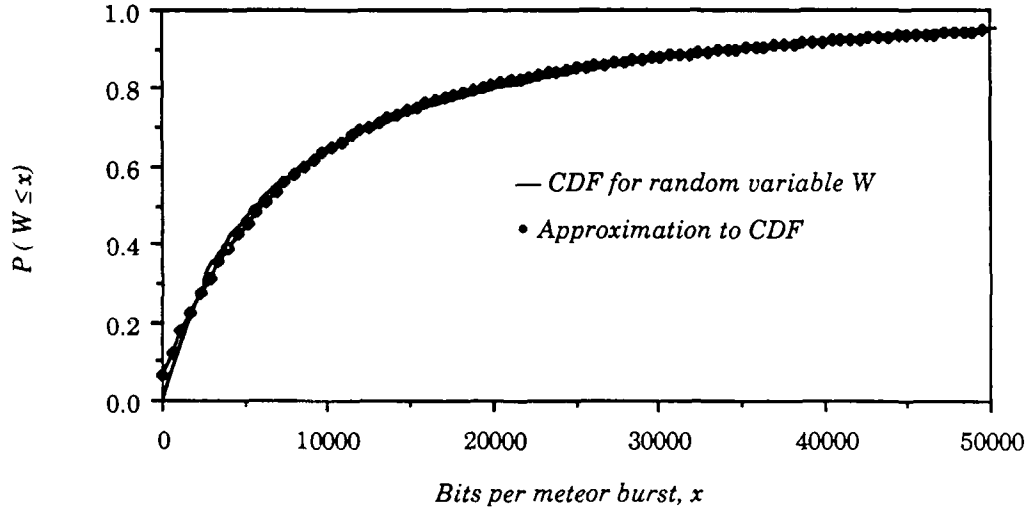

Figure B.3 Approximate CDF for adaptive QAM
($P_b = 10^{-4}$, $R_s = 5900$ Hz, $t_c = .58$ s)

B.3 Mean Waiting Time. The approximate probability density function for W is simply the first derivative of (B.11), given by

$$\hat{f}_W(x) = .8\,\lambda_2 \exp\{-\lambda_2 x\} - 0.66\,\lambda_4 \exp\{-\lambda_4 x\} + 0.8\,\lambda_6 \exp\{-\lambda_6 x\} \quad \text{(B.12)}$$

where $\lambda_2 = 1/(2\ t_c\ R_s)$, $\lambda_4 = 1/(4\ t_c\ R_s)$, and $\lambda_6 = 1/(6\ t_c\ R_s)$. The Laplace transform of (B.12) is given by

$$\hat{F}(s) = \mathcal{L}\{\hat{f}_W(x)\} = \int_0^\infty e^{-sx}\,\hat{f}_W(x)\,dx$$

This integral can be evaluated in a straightforward manner. The resulting expression is substituted into (B.1) yielding

$$\mathcal{L}\{E[T_w]\} = \frac{1}{\lambda}\left[\frac{1}{s} + \frac{c_2 s^2 + c_1 s + c_0}{s^2(s^2 + d_2 s + d_1)}\right] \quad \text{(B.13)}$$

where

$$c_2 = a_0\lambda_2 + a_1\lambda_4 + a_2\lambda_6$$

$$c_1 = (a_0 + a_1)\lambda_2\lambda_4 + (a_0 + a_2)\lambda_2\lambda_6 + (a_1 + a_2)\lambda_4\lambda_6$$

$$c_0 = \lambda_2\lambda_4\lambda_6$$

$$d_2 = (1-a_0)\lambda_2 + (1-a_1)\lambda_4 + (1-a_2)\lambda_6$$

$$d_1 = a_2\lambda_2\lambda_4 + a_1\lambda_2\lambda_6 + a_2\lambda_4\lambda_6$$

Partial fraction expansion of (B.13) yields

$$\mathcal{L}\{E[T_w]\} = \frac{1}{\lambda}\left[\frac{A}{s^2} + \frac{B}{s} + \frac{Cs + D}{s^2 + d_2 s + d_1}\right] \quad \text{(B.14)}$$

where

$$A = \frac{c_0}{d_1}$$

$$B = 1 + \frac{c_1}{d_1} - \frac{c_0 d_2}{d_1^2}$$

$$C = -\frac{c_1}{d_1} + \frac{c_0 d_2}{d_1^2}$$

$$D = c_2 - \frac{c_0}{d_1} - d_2\left(\frac{c_1}{d_1} - \frac{c_0 d_2}{d_1^2}\right)$$

Taking the inverse transform of (B.14) yields

$$E[T_w] \equiv \frac{1}{\lambda}\left\{ B + A N + \exp(g N)\left[C \cos(f N) + E \sin(f N)\right]\right\} \qquad (B.15)$$

where

$$E = \frac{D - C\left(\frac{d_2}{2}\right)}{\sqrt{d_1 - \left(\frac{d_2}{2}\right)^2}}$$

$$f = \sqrt{d_1 - \left(\frac{d_2}{2}\right)^2}$$

$$g = -\frac{d_2}{2}$$

For $P_b = 10^{-4}$, these constants can be written in terms of the symbol rate R_s and the mean burst duration, $\tau = t_c$. Doing so results in the following

$$E[T_w] \cong \frac{1}{\lambda}\left\{1.37 + \frac{N}{4.49\,R_s\,\tau} - \exp\left(-\frac{N}{3.64\,R_s\,\tau}\right)\right.$$
$$\left.\cdot\left[.37\cos\left(\frac{N}{7.40\,R_s\,\tau}\right) - .052\sin\left(\frac{N}{7.40\,R_s\,\tau}\right)\right]\right\} \quad \text{(B.16)}$$

Equation B.16 is also a reasonable approximation of mean waiting time for bit-error rates in the range 10^{-3} to 10^{-6}, not just for $P_b = 10^{-4}$. The bit-error rate curves for M-ary QAM in this range are almost parallel, and since the CDF of the random variable W is a function only of ratios of $(E_s/N_0)_M$, then the CDF does not vary with bit-error rate. The only term of (B.16) that will vary with P_b is the meteor arrival rate, λ, which is a function of $(E_s/N_0)_4$.

Equation (B.16) is plotted in Figure B.4 for $R_s = 5900$ Hz, and $\tau = .58$s. From Figure B.4, it appears that the optimal symbol rate is approximately $R_{sopt} = 0.3$ (N) Hz. The author has found that for other values of message length, N, the optimal symbol rate also equals approximately 0.3 (N).

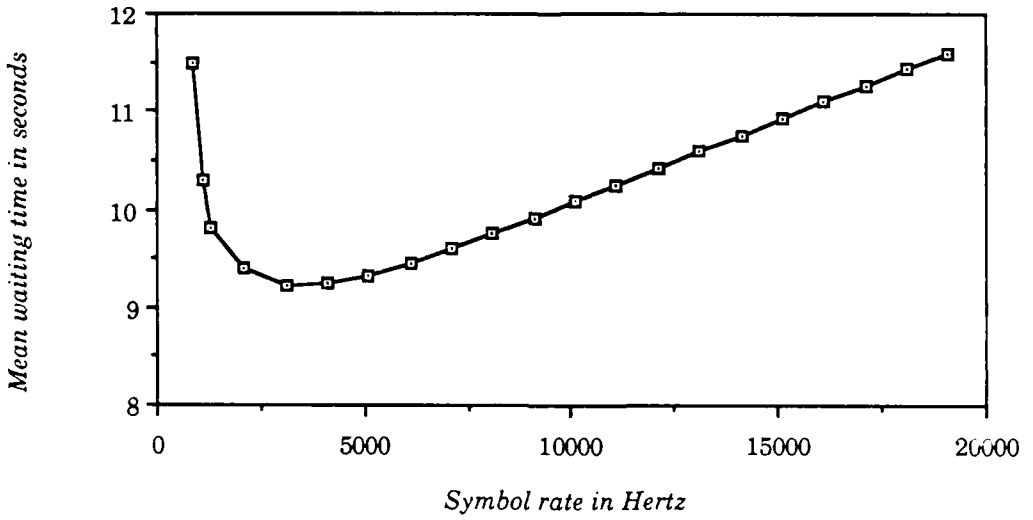

Figure B.4 Mean waiting time for adaptive QAM
($P_b = 10^{-4}$, N = 10 000 bits, $\tau = .58$ s)

References

Abel, M. W., "Meteor burst communications: bits per burst performance bounds," IEEE Transactions on Communications, vol. COM-34, September, pp. 927-936, 1986.

Bartholome, P. J. and Vogt, I.M., "COMET - A meteor burst system incorporating ARQ and diversity reception," IEEE Transactions on Communications Technology, vol. COM-16, pp. 268-278, April, 1968.

Berlekamp, E. R., Peile, R. E., and Pope, S. P., "The application of error control to communications," IEEE Communications Magazine, vol. 25, pp. 44-57, April, 1987.

Blahut, R. E., Theory and Practice of Error Control Codes. Reading, Massachusetts: Addison-Wesley Publishing Company, 1983.

Blahut, R. E., Digital Transmission of Information. Reading, Massachusetts: Addison-Wesley Publishing Company, (to be published in 1987).

Brown, D. W., "A comparison of the performance of the COMET meteor-burst system at 40 and 100 MHz," SHAPE Technical Center, The Hague, The Netherlands, TR-66, June, 1969.

Campbell, L. L. and Hines, C. O., "Bandwidth Considerations in a JANET system," Proceedings of the Institute of Radio Engineers, vol. 45, pp. 1658-1660, December, 1957.

Clark, C. C. and Cain, J. B., Error Correction Coding for Digital Communications. New York: Plenum Press, 1981.

Cox, D. R., Renewal Theory. New York: John Wiley and Sons, 1962.

Eshlemann, V. R., "Theory of radio reflection from electron ion clouds," IRE Transactions on Antennas and Propagation, January, 1955.

Fodor, G., Laplace Transforms in Engineering. Budapest: Publishing House of the Hungarian Academy of Sciences, 1965.

Hampton, J. R., "A meteor burst model with time-varying bit error rate," IEEE Military Communications Conference, Boston, Massachusetts, October 20 - 23, 1985.

Havens, D., "Covering and protocols for meteor burst communications," TELECOM, Memo Rep., ERDA, 1976.

Haykin, S. S., Communication Systems. New York: John Wiley and Sons, 1978.

Hines, C. O. and Forsythe, P.A., "The forward scattering of radio waves from overdense meteor trails," Canadian Journal of Physics, vol. 35, February, 1957

Kokjer, K. J. and Roberts, T. D., "Networked Meteor-Burst Data Communications," IEEE Communications Magazine, vol. 24, pp. 23-29, November, 1986.

Lee, P. J., "Computation of bit error rate of coherent M-ary PSK with Gray code bit mapping," IEEE Transactions on Communications, vol. COM-34, pp. 488-491, May, 1986.

Lin, S. and Costello, D. J., Error Control Coding: Fundamentals and Applications. Englewood Cliffs, NJ: Prentice-Hall, Inc., 1983.

Michelson, A. M. and Levesque, A. H., Error Control Techniques for Digital Communication. New York: John Wiley & Sons, 1985.

Milstein, L. B. et al., "Performance of meteor-burst communication channels," IEEE Journal on Selected Areas in Communications, vol. SAC-5, No. 2, pp. 146-153, February, 1987.

Nes, H., "Dimensioning technique for meteor burst communication systems," IEE Proceedings, vol. 132, Pt. F, No. 6, pp. 505-510, October, 1985.

Noguchi, T., Daido, Y., and Nossek, J. A., "Modulation techniques for microwave digital radio," IEEE Communications Magazine, vol. 24, pp. 21-30, October, 1986.

Oetting, J. D. "An analysis of meteor burst communications for military applications," IEEE Transactions on Communications, vol. COM-28, pp. 1591-1601, September, 1980.

Ostergaard, J. C. et al., "Characteristics of high latitude meteor scatter propagation parameters over the 45 - 104 MHz band," Advisory Group for Aerospace Research and Development, (paper reprinted from conference proceedings No. 382), 1985.

Proakis, J. G., Digital Communications, New York: McGraw-Hill, 1983.

Rediske, J. F., "Variable rate coding for meteor scatter communications," MS thesis, Wisconsin, Madison, WI, December, 1982.

Ross, S. M., A First Course in Probability. New York: MacMillan Publishing Company, 1984.

Ross, S. M., Introduction to Probability Models. Orlando, Florida: Academic Press, 1985.

Ungerboeck, G., "Trellis-coded modulation with redundant signal sets," IEEE Communications Magazine, vol. 25, pp. 5-21, February, 1987.

Villard, O. G. et al., "Some properties of oblique radio reflection from meteor ionization trails," Journal of Geophysical Research, vol. 61, pp. 233-249, 1956.

Weitzen, J. A., Grossi, M. D., and Birkemeier, W. P., "An estimate of the capacity of the meteor burst channel," IEEE Transactions on Communications, vol. COM-32, pp. 972-974, August, 1984.

Weitzen, J. A., Grossi, M. D., and Birkemeier, W. P., "High resolution multipath measurements of the meteor scatter channel," Radio Science, vol. 19, pp. 375-381, January-February, 1984.

Weitzen, J. A., "The feasibility of high speed digital communications on the meteor scatter channel," Ph.D. dissertation, University of Wisconsin, Madison, WI, June 1983.